William & Mary
CHARTERED 1693

W&M ScholarWorks

Dissertations, Theses, and Masters Projects

Theses, Dissertations, & Master Projects

Fall 2019

Impacts of Margalefidinium polykrikoides and Alexandrium monilatum on Oysters Cultured in Lower Chesapeake Bay

Clara L. Robison
Virginia Institute of Marine Science

Follow this and additional works at: https://scholarworks.wm.edu/etd

 Part of the Marine Biology Commons

Recommended Citation

Robison, Clara L., "Impacts of Margalefidinium polykrikoides and Alexandrium monilatum on Oysters Cultured in Lower Chesapeake Bay" (2019). *Dissertations, Theses, and Masters Projects.* Paper 1593092072.
https://doi.org/10.25773/d5vx-av73

This Thesis is brought to you for free and open access by the Theses, Dissertations, & Master Projects at W&M ScholarWorks. It has been accepted for inclusion in Dissertations, Theses, and Masters Projects by an authorized administrator of W&M ScholarWorks. For more information, please contact scholarworks@wm.edu.

Impacts of *Margalefidinium polykrikoides* and *Alexandrium monilatum* on Oysters Cultured in Lower Chesapeake Bay

A Thesis

Presented to

The Faculty of the School of Marine Science

The College of William & Mary

In Partial Fulfillment

of the Requirements for the Degree of

Master of Science

by

Clara L. Robison

August 2019

APPROVAL SHEET

This thesis is submitted in partial fulfillment of

the requirements for the degree of

Master of Science

_____

Clara L. Robison

Approved, by the Committee, August 2019

_____

Kimberly S. Reece, Ph.D.
Committee Co-Chairman/Co-Advisor

_____

Wolfgang K. Vogelbein, Ph.D.
Committee Co-Chairman/Co-Advisor

_____

Juliette L. Smith, Ph.D.

_____

Ryan B. Carnegie, Ph.D.

_____

Emily B. Rivest, Ph.D.

TABLE OF CONTENTS

Page

ACKNOWLEDGEMENTS

Writing a thesis is a labor of love, and it would never have been possible without the technical and moral support of so many people. First and foremost, I want to thank my advisors, Drs. Kim Reece and Wolf Vogelbein. Kim is more than an advisor – she also serves as my second mother and mother and mentor to the entire Virginia Institute of Marine Science (VIMS) Aquatic Health Science Department (AHS). Thank you for your brilliance and your 24/7 support and guidance. This project revolved around two lengthy field seasons, and Wolf spent countless hours with me in the field – driving the boat, providing technical expertise, and making dad jokes.

For the past three years, the Reece Lab has provided me with so much support. In particular, I want to thank Gail Scott, lab supervisor extraordinaire, for both her technical expertise and unfaltering emotional support. Not only was Gail in the field almost as often as I was, but she never said no to lunch with me either! Accomplished algal culturist Bill Jones, or Dr. Dino, examined every single one of my water samples and provided a wealth of knowledge about phytoplankton and harmful algal bloom dynamics. Thank you to Dr. Hamish Small for always making me laugh and for your help in the field. Finally, thank you to Alanna MacIntyre and Corinne Audemard, both for your help and your warm encouragement.

I also received so much support from my committee members Drs. Juliette Smith, Ryan Carnegie, and Emily Rivest. Juliette taught me everything I could ever want to know about toxin dynamics, Ryan provided a rounded perspective on oyster health and stressors, and Emily helped me understand more about oyster physiology. Although not on my committee, Dr. Willy Reay offered truly invaluable technical support by providing all the continuous water quality data at all

sites both summers. Thank you to him and the rest of the Chesapeake Bay National Estuarine Research Reserve team.

Thank you also to Laura Whitefleet-Smith, Melanie Kolacy, and Rita Crockett for the help and guidance with oyster histology. Rita's long-term perspective on local oyster histology was truly invaluable.

I owe eternal gratitude to all of our collaborators in the oyster aquaculture industry, including Mobjack Bay Seafood Company, Big Island Oyster Company, and Chessie Seafood and Aquafarms. The incredibly kind and hard-working people at these companies generously shared their knowledge and, in some cases, their gear and leases, to help with this field study. I want to especially thank Tommy Leggett, owner of Chessie Seafood and Aquafarms. Not only did he serve as my Virginia Sea Grant (VASG) Outreach Mentor, but he also quickly became one of my closest friends in Virginia. He taught me nearly everything I know about oyster aquaculture – from building gear to growing oysters to delivering the product to customers. He also gave me a hands-on perspective of the ecology and history of the Chesapeake Bay that I could never have learned in a textbook.

This project was heavy in terms of lab and field work, and I truly could not have done it alone. In addition to others I have already mentioned, I want to thank technician Corey Corrick for his assistance in the lab and field and technician Kristen Vogelbein for her work in the lab. I also want to acknowledge my many wonderful volunteers, including Virginia Summer Residential Governor's Academy student Anna Song and VIMS graduate students Sam Askin and Ann Ropp.

Even after all the data is collected, the work is hardly done. I want to give a huge thank you to Dr. Rob Latour for spending hours discussing the various ways to analyze my data

statistically, even though he was not even on my committee. Thank you for your patience and for generously sharing your time and knowledge.

I also want to thank my funding sources, the VIMS Office of Academic Studies, the National Oceanic and Atmospheric Administration's National Ocean Service (for travel support), and VASG. I was so surprised and so honored to receive a VASG Fellowship as a first-year graduate student. The VASG community has provided me not only with financial support, but also science communication and networking opportunities, as well as hands-on preparation for my future career. I want to give special thanks to Fellowship and Research Program Coordinator, Dr. Sam Lake, for always being available for advice, guidance, and a friendly chat.

They say it takes a village to raise a child, and it certainly takes a village to support a graduate student. I want to give a warm thank you to the larger VIMS community. I especially want to thank AHS Financial Officer, Mike Ivey, both for his financial help, and for his kindness and amazing sense of humor. Thank you also to Linda Schaffner, Cathy Cake, and Jen Hay for administrative support.

Last but certainly not least, I want to thank my family. I am the person I am today due in large part to my two greatest female role models and supporters – my mother and my sister, Mary and Rachel Robison.

LIST OF TABLES

LIST OF FIGURES

ABSTRACT

Harmful algal blooms (HABs) are expanding globally and are anticipated to continue increasing with climate change. Two dinoflagellate species, *Margalefidinium polykrikoides* and *Alexandrium monilatum*, form extensive and dense blooms most summers in the lower Chesapeake Bay. *Alexandrium monilatum*, which produces the toxin goniodomin A, tends to bloom soon after *M. polykrikoides*, for which a toxin has not yet been identified. Previous laboratory studies and a more limited number of field studies indicate mortality and pathology in multiple shellfish species associated with exposure to *M. polykrikoides* and *A. monilatum*. However, the impacts of sequential exposure to both HAB species on marine organisms in the natural environment are less well understood.

Local aquaculturists grow oysters under a variety of conditions that may be differentially impacted by HAB exposure. No extensive and controlled studies have been carried out in lower Chesapeake Bay assessing impacts of sequential exposure to *M. polykrikoides* and *A. monilatum* blooms on oysters cultured using different aquaculture strategies. The two main objectives of this study were to: 1) investigate *M. polykrikoides* and *A. monilatum* as a potential threat to cultured oysters, and 2) inform mitigation strategies to minimize HAB impacts based on current grow-out methods. To address these objectives, oysters were grown in 2017 and 2018 at sites characterized by differing water energetics and HAB dynamics. At all sites during both summers, oysters were grown intertidally and subtidally, and in 2018 were also grown in floating cages at one site. Water quality parameters were monitored, including cell concentrations of *M. polykrikoides, A. monilatum*, and two other local HAB species known to negatively impact oysters, *Karlodinium veneficum* and *Prorocentrum minimum*, along with oyster health and survival.

Blooms of *M. polykrikoides* and *A. monilatum* occurred at the study sites, but not the reference site, in summer 2017 with cell concentrations that were lower than those quantified in some previous years. In summer 2018, neither species bloomed, providing the opportunity to assess oysters during both a bloom and a non-bloom year. Overall oyster mortality in both summers was relatively low compared to mortality often seen associated with other oyster stressors such as disease. Results indicated oyster health and survival were more impacted by factors indirectly related to HABs, specifically location factors (i.e. site and placement location), temperature, and DO. In both summers, mortality was significantly higher for intertidal oysters, compared to subtidal oysters, suggesting intertidal placement may incur stress in summer. It is unknown whether this intertidal stress may be further compounded during more HAB-intensive years.

The results of this study suggest *M. polykrikoides* and *A. monilatum* had little impact on the health and survival of oysters cultured in the lower Chesapeake Bay in the summers of 2017 and 2018. More than one year of bloom data is likely necessary, however, to fully evaluate the impacts of *M. polykrikoides* and *A. monilatum* as potential stressors to cultured oysters in the context of inter-annual variability and the expanding distribution of these two HABs in the Chesapeake Bay.

Impacts of *Margalefidinium polykrikoides* and *Alexandrium monilatum* on Oysters Cultured in Lower Chesapeake Bay

INTRODUCTION

Harmful Algal Blooms in the Chesapeake Bay

Harmful algal blooms (HABs) occur when photosynthetic unicellular phytoplankton proliferate rapidly to densities that can cause adverse impacts on the aquatic environment and humans who consume bloom-exposed seafood (Sellner et al. 2003). Reports of HABs and their impacts have increased in frequency and distribution in recent decades (Hallegraeff 1993) and are predicted to increase further with ongoing climate change (Hallegraeff 2010, Glibert et al. 2014). Environmental factors, such as temperature, salinity, and irradiance (Kim et al. 2004, Juhl 2005), as well as biological factors, such as algal life stage (Brosnahan et al. 2015), can influence algal growth and potential bloom formation. Some HAB species form resting cysts, and factors such as irradiance, oxygen, and sediment resuspension can facilitate excystment (Anderson et al. 1987, Keafer et al. 1992, Anderson et al. 2005), which can drive bloom formation.

HABs can negatively impact the aquatic environment by reducing light penetration to benthic plants, clogging the gills of finfish and shellfish, and lowering the concentration of dissolved oxygen (DO) (Sellner et al. 2003). When blooms die, the algal organic matter sinks to the benthos and is broken down by heterotrophic bacteria. Bacterial metabolism lowers DO, which can create hypoxic or anoxic “dead zones” detrimental to marine life. In addition, some HAB-forming species are toxigenic, producing compounds that can directly harm aquatic organisms and may bioaccumulate in shellfish and finfish, posing health risks to higher trophic level consumers, including humans (Shumway 1990, Wang 2008). Some toxins can be aerosolized when cells lyse, potentiating respiratory impacts on terrestrial organisms. Thus,

animals can be exposed to toxins directly through physical contact with the aquatic environment or air, and indirectly through the consumption of intoxicated organisms.

HAB-related illnesses that affect higher vertebrates include ciguatera fish poisoning, amnesic shellfish poisoning, azaspiracid shellfish poisoning, diarrhetic shellfish poisoning, neurotoxic shellfish poisoning, and paralytic shellfish poisoning. Most of these illnesses result from the consumption of fish or shellfish intoxicated by HAB toxins (Van Dolah 2000; Backer & McGillicuddy, Jr. 2006). Marine HABs are primarily caused by eukaryotic dinoflagellates or diatoms, which may produce hepatotoxins or, more commonly, neurotoxins (Wang 2008). Most dinoflagellates and diatoms with the ability to form harmful blooms and produce toxins are present at low concentrations in the marine environment throughout the year (Wang 2008).

To date, at least 37 harmful algal species have been reported in Chesapeake Bay (Marshall et al. 2008), including several species known to produce toxins associated with higher vertebrate poisonings around the country and world. According to the Virginia Department of Health (VDH), no human poisonings have been reported following the consumption of seafood grown in the Chesapeake Bay in association with HABs or their toxins. However, research indicates that the frequency and extent of HABs are increasing in the Chesapeake Bay (Li et al. 2015), and ongoing HAB monitoring is critical.

HAB monitoring in the lower Chesapeake Bay is a collaborative and multi-pronged effort. In a National Aeronautics and Space Administration (NASA) Digital Earth Virtual Environment and Learning Outreach Project pilot study, satellite imagery collected by NASA hyperspectral sensors mounted on planes was used in conjunction with concurrent Chlorophyll *a* (Chl *a*) data to develop an algorithm to map blooms of *Alexandrium monilatum,* based on the idea that Chl *a* levels might serve as a proxy for algal cell biomass (Lubkin et al. 2017). The

National Oceanic and Atmospheric Administration (NOAA) Satellite Remote Sensing Group also contributes satellite data by producing images almost daily during the late summer bloom season. Water samples are collected by sources including, but not limited to, the Virginia Institute of Marine Science (VIMS), Old Dominion University, VDH, the Virginia Marine Resources Commission, the Chesapeake Bay National Estuarine Research Reserve System (CBNERRS), the Virginia Department of Environmental Quality (DEQ), private citizens, and oyster growers. The ongoing Lower York River Estuary Dataflow project, funded by the National Science Foundation, also collects regular and systematic water and sediment samples in the York River from West Point to the mouth. In the Reece Lab at VIMS, algal cells are quantified and identified both via light microscopy and using quantitative polymerase chain reaction (qPCR) targeting the DNA of particular HAB species that have historically bloomed in the lower Chesapeake Bay. These cell concentration data are documented in annual reports that have been submitted to VDH from 2007 to 2017 and these data are deposited in the Center for Disease Control (CDC) HAB Database.

Two HAB-forming species of dinoflagellates, *Margalefidinium* (formerly *Cochlodinium*) *polykrikoides* and *Alexandrium monilatum*, form extensive blooms in lower Chesapeake Bay almost annually. Blooms of *M. polykrikoides* are usually initiated in mid- to late July, and usually transition within one to two weeks to *A. monilatum* blooms in most years. The mechanism or cause of this bloom progression is unknown. Both species form chains, although chains of *A. monilatum* tend to be much longer (up to approximately 80 cells) than those of *M. polykrikoides* (up to 4-6 cells) as expressed in lower Chesapeake Bay (W. M. Jones, VIMS, pers. comm.). Both species form resting cysts that can settle in benthic sediments (Mulholland et al. 2009, Pease 2016).

Margalefidinium polykrikoides has bloomed along the coasts of North America and East Asia for decades, with bloom reports increasing since the 1990s (Kudela & Gobler 2012). In the Peconic Estuary and Shinnecock Bay, New York, USA, bloom densities exceeded 1×10^6 cells mL^{-1}, and Chl *a* levels exceeded 100 µg L^{-1} (Gobler et al. 2008). Blooms in North America appear to be ichthyotoxic (Whyte et al. 2001, Gobler et al. 2008), although a toxin has not been characterized for this species. *Margalefidinium polykrikoides* has bloomed in the York River for over 50 years (MacKiernan 1968). In 2015 and 2016, cell concentrations in the York River quantified using pPCR exceeded 2×10^4 cells mL^{-1} and 6×10^4 cells mL^{-1}, respectively (Reece 2016-2017 VDH Reports). Although blooms in the lower Chesapeake Bay are not typically associated with mass mortality events of finfish or shellfish, blooms have been increasing in frequency, cell density, and spatial distribution over the past several decades (Marshall et al. 2005; Scott & Reece 2018), raising questions about impacts to the local ecosystem.

Bloom concentrations of *M. polykrikoides* have been associated with adverse impacts to finfish and shellfish in the laboratory. Gobler et al. (2008) observed 100% mortality of multiple fish species, including larval *Cyprinodon variegatus*, adult *Fundulus majalis*, and adult *Menidia menidia*, and 80% mortality of adult *Fundulus heteroclitus*, exposed to NY bloom water consisting of $>5 \times 10^4$ cells mL^{-1} of *M. polykrikoides* for 24 hr. Microscopic examination of fishes revealed significant damage to respiratory epithelia and focal fusion of gill lamellae. Elevated levels of mortality, as well as inflammation and damage in the gill and digestive tissues, were observed in juvenile bay scallops (*Arcopecten irradians*; ~11 mm) and eastern oysters (*Crassostrea virginica*; ~21 mm) exposed in the laboratory to bloom water containing $\sim 5 \times 10^4$ cells mL^{-1} of *M. polykrikoides* for 9 days (Gobler et al. 2008). Specifically, scallop

mortality reached 67%, while oyster mortality peaked at 16%, both of which exceeded mortality of control animals not exposed to *M. polykrikoides* cells. Surviving scallops exhibited significantly slower growth rates following *M. polykrikoides* exposure (Gobler et al. 2008).

Alexandrium monilatum has long been associated with finfish kills in Florida (Howell 1953) and finfish and invertebrate kills in the Gulf of Mexico (Connell & Cross 1950, Wardle et al. 1975, Perry et al. 1979). *Alexandrium monilatum* was first reported in Chesapeake Bay in the 1940s (Morse 1947) and again in the 1960s (MacKiernan 1968). It was not until 2007, however, that *A. monilatum* re-emerged locally and began blooming almost annually in lower Chesapeake Bay, with maximum cell concentrations typically occurring in late August to early September (Marshall & Egerton 2009, 2013). Blooms tend to be observed first in the York River (Dauer et al. 2010). Since 2007, blooms have generally increased in spatial distribution, density, and duration in the lower Chesapeake Bay (Marshall et al. 2008; Marshall & Egerton 2009, 2013; Dauer et al. 2010; Scott & Reece 2018). Local York River bloom concentrations quantified using qPCR surpassed 2×10^5 cells mL^{-1} in 2015 and 1×10^5 cells mL^{-1} in 2016 (Reece 2016 VDH Report). Sediment data collected by Pease (2016) document cysts of *A. monilatum* in the benthos of the lower York River, although it is unknown whether these excyst to seed future blooms.

Blooms of *A. monilatum* may be affiliated with toxic impacts to shellfish in the lower Chesapeake Bay. In 2007, veined rapa whelks (*Rapana venosa*; shell lengths 34-165 mm; n>200) held in flow-through tanks experienced total mortality during the peak of the 2007 *A. monilatum* bloom in the York River (Harding et al. 2009). A water sample collected near the tank intake on 9/7/07 contained around 4×10^4 *A. monilatum* cells mL^{-1} (Reece 2008 VDH Report), and all whelks were dead by 9/10/07. Oysters and northern quahogs (*Mercenaria mercenaria*) held in the same tanks experienced 0% mortality (Harding et al. 2009). In 2015,

mild erosion of mantle epithelium was observed in adult oysters planted in the York River during the peak of an *A. monilatum* bloom (Pease 2016). Also in 2015, VIMS scientists received several reports from local oyster farm owners describing unusually high oyster mortality concurrent with the *A. monilatum* bloom that year (K. Reece, VIMS, pers. comm.). However, the exact cause(s) of the elevated mortality and pathology found in these studies and reports is unknown.

Alexandrium monilatum in Chesapeake Bay produces the toxin goniodomin A (GDA) (Hsia et al. 2006), which has been implicated in a range of cellular-level effects. Research by Bass et al. (1983) and Bass & Kuvshinoff (1983) demonstrated hemolytic and neurotoxic effects, respectively, associated with exposure to GDA isolated from *Goniaulax monilata* (Howell 1953), which was renamed *A. monilatum* by Balech (1985). GDA produced by other algal species has also been associated with cellular-level effects, including antibiotic (Sharma et al. 1968) and antifungal properties (Murakami et al. 1988). Murakami et al. (1988) reported that GDA disrupted the cell division of sea urchin eggs. Abe et al. (2002) found that GDA inhibits angiogenesis in aortic endothelial cells, in part by interfering with actin reorganization. Other research has indicated GDA is associated with an alteration in actin structure, disrupting the interaction between actin and myosin (Furukawa et al. 1993, Hsia et al. 2006, Espiña et al. 2016). Based on analyses of a Gulf Coast *A. monilatum* isolate by Hsia et al. (2006), GDA has a molecular weight of 768 Da. It is unknown whether GDA crosses through cell membranes to induce a toxic effect.

GDA and *A. monilatum* cells have also been implicated in a range of whole-organism effects in both terrestrial and marine organisms in the laboratory. Crude extract exposure from *A. monilatum* has been associated with toxicity to a range of organisms, including cockroaches (Clemons et al. 1980), frogs (Bass & Kuvshinoff 1983), and mice (Erker et al. 1985). Laboratory

studies found that finfish and marine invertebrates, including oysters, exhibited significant mortality following exposure to living *A. monilatum* cells and purified GDA (Gates & Wilson 1960, Aldrich et al. 1967, Sievers 1969, May et al. 2010, Reece et al. 2016, Pease 2016). Toxicity bioassays have resulted in dose-dependent gill erosion and mortality of adult oysters exposed to live York River-isolated *A. monilatum* cells after 96 hours (Pease 2016). However, it is unknown whether toxic impacts are related to toxin accumulation within these organisms.

As of yet, no rigorous bioaccumulation or depuration study has been carried out in the laboratory for GDA. In 2018, Krock et al. described a method for quantifying GDA and the analogue goniodomin B (GDB), isolated from 17 strains of *A. pseudogonyaulax*, using LC-MS/MS. All 17 strains produced GDA (5-35 pg cell^{-1}), and many strains also contained GDB (0.01-0.07 pg cell^{-1}). Research by Espiña et al. (2016) on rat hepatocytes suggested that GDB was less toxic than GDA. GDA was first isolated and purified from local York River *A. monilatum* by Drs. Thomas and Connie Harris at VIMS (Harris et al. In review). Concentrations of GDA ranging from 0.02-8.39 µg g^{-1} were detected in the foot tissue of whelks that died during the 2007 York River *A. monilatum* bloom (Harding et al. 2009). Many bivalve mollusc species are filter feeders that use gills to concentrate algal particles for consumption, and toxins often concentrate in the siphon, gills, and digestive gland of shellfish (Halstead & Shantz 1984). However, it is unknown whether GDA bioaccumulates in bivalve tissues and, if so, where it concentrates.

Evaluating toxin exposure in bivalve species is made more complicated due to feeding inhibition. May et al. (2010) demonstrated reduced feeding of several bivalve species, including *C. virginica*, in response to *A. monilatum* exposure, and Hégaret et al. (2007) observed that *C. virginica* ceased feeding in the presence of toxigenic *A. fundyense* and two other toxigenic non-

Alexandrium species. Recent laboratory challenges of adult oysters by Pease (2016) suggest that while *C. virginica* will feed on York River-isolated *A. monilatum,* oysters may remain closed for long periods and feeding can be inhibited at higher cell concentrations. Thus, oysters have the potential to experience not only nutritional and oxidative stress resulting from feeding inhibition, but also toxin exposure when feeding and otherwise interacting with *Alexandrium* cells. However, it is currently unknown whether GDA bioaccumulates in oysters.

In the lower Chesapeake Bay, pathology and mortality of marine life have been reported more frequently during *A. monilatum* blooms than those of *M. polykrikoides,* and it is possible these adverse effects may be due in part to sequential exposure to both species. However, no extensive studies have been carried out in the lower Chesapeake Bay assessing the impacts of sequential *M. polykrikoides* and *A. monilatum* blooms on oysters cultured throughout the bloom season.

Oysters in the Chesapeake Bay

The eastern oyster (*Crassostrea virginica*; Gmelin 1791) has long played a critical ecologic and economic role in Chesapeake Bay (Wilberg et al. 2013). Oyster reefs provide habitat structure for a diverse community of organisms (Peterson et al. 2003), reduce turbidity through filtration (Haven & Morales-Alamo 1970), enhance nutrient cycling (Dame & Libes 1993), and facilitate energy transfer between benthic and pelagic food webs (Baird & Ulanowicz 1989). Over the past century, oyster abundance in Chesapeake Bay has been reduced to less than 1% of historic levels (Newell 1988), due to several factors including overfishing and habitat destruction (Rothschild et al. 1994, Mackenzie 2007). Emergence of multinucleated sphere unknown (MSX) disease in 1959 (Wood & Andrews 1962) and the intensification of dermo

disease in the 1980s (Burreson & Andrews 1988) also contributed to oyster decline. These diseases are caused by the oyster parasites *Haplosporidium nelsoni* and *Perkinsus marinus*, respectively.

Recently, Chesapeake Bay oyster stocks have begun to recover due in part to fishing restrictions, restoration, and disease adaptation (Carnegie & Burreson 2011, Schulte 2017). In the lower Chesapeake Bay, oyster abundance has also been bolstered by the rapidly developing aquaculture industry that primarily utilizes fast-growing, disease-resistant triploid (3N) oyster strains (Hudson & Murray 2016). The 2017 farm gate value of Virginia shellfish aquaculture was $53.4 million, and of that, oysters represented over $15 million (Hudson 2018). Continued efforts to restore oyster populations are critical to the health of coastal ecosystems like the Chesapeake Bay (Beck et al. 2011). Not only does aquaculture contribute to the local economy and create new jobs, but also harvesting farmed oysters may shift some of the demand away from wild populations, enhancing recovery of these populations. In addition to their economic value, cultured oysters provide many of the same ecosystem services as wild oysters, including water filtration and nutrient cycling.

Significance of HAB-Oyster Dynamics to Aquaculture

HABs represent a potential threat to the aquaculture industry, and members of the lower Chesapeake Bay oyster aquaculture industry have expressed concern regarding the potential impacts of HABs on cultured oysters. Blooms can be associated with lethal and sub-lethal effects in wild and farmed animals, as well as reduced marketability of seafood products (Shumway 1990, Landsberg 2002). HABs have the potential to adversely impact oysters through multiple mechanisms. Oysters are herbivorous filter feeders and feed on phytoplankton for their nutrition.

This feeding method and diet make oysters more likely to consume HAB species and to experience feeding disruption via gill clogging. In the presence of certain species of toxigenic algae, some shellfish may practice avoidance behaviors, including reduced valve gape and clearance rate (Hégaret et al. 2007, May et al. 2010), burrowing, siphon retraction, and shell clapping (Gainey & Shumway 1988, Bricelj et al. 1990, Mons et al. 1998). May et al. (2010) demonstrated reduced feeding of several bivalve species, including *C. virginica*, in response to *A. monilatum* exposure. These feeding avoidance behaviors may incur metabolic costs. For instance, when shellfish species like oysters close their valves, feeding and respiration are inhibited.

Many aspects of oyster aquaculture might influence the potential effects of HABs on oysters. Firstly, aquaculturists grow oysters of different families and ploidies and deploy oysters of different sizes. The majority of the local industry uses triploid (3N) animals bred for fast growth and disease resistance (Hudson 2018). The minimum oyster deployment size is at least partially limited by the mesh size of the bags oysters are placed in at the time of deployment, and many growers initially deploy spat oysters (shell height between 5-10 mm) in bags with a mesh size of ~ 0.6 cm for grow-out to marketable size (A. T. Leggett, Jr., Chessie Seafood and Aquafarms, pers. comm.). Smaller oysters are likely to have more limited energy reserves relative to larger, older oysters and as a result may not be able to cease feeding to avoid bloom exposure for as long as larger oysters. Physiological stress to oysters may be further compounded in intertidal locations, where animals are already subject to stress associated with lower DO and shorter feeding times (Crosby et al. 1991, Roegner & Mann 1995, Bishop & Peterson 2006).

Toxicity bioassays by Mulholland et al. (2009) demonstrated 20% mortality of juvenile (~ 21 mm) *C. virginica* exposed to ~10^3 *M. polykrikoides* cells mL^{-1} for 72 hr. In contrast, May

et al. (2010) reported 0% mortality of two size classes of *C. virginica* (~29 mm and ~70 mm) exposed to 5.5×10^2 cells mL^{-1} of toxic *A. monilatum* for 24 hr. Bioassays at VIMS indicated both *M. polykrikoides* and *A. monilatum* exposure are associated with larval oyster mortality, but mortality of oyster spat (2-3 mm) only occurred during exposure to *A. monilatum*, not *M. polykrikoides* (Reece et al. 2016). Specifically, mortality of diploid and triploid spat oysters exposed to up to 4,000 *M. polykrikoides* cells mL^{-1} was 0% after 120 hr. Triploid spat experienced 80% mortality following exposure to 800 *A. monilatum* cells mL^{-1}, and 100% mortality after being exposed to 2,000-8,000 *A. monilatum* cells mL^{-1} for 72 hr.

Deployment location is another aspect of oyster culture that might affect the potential for HAB impacts on oysters. For instance, the relative water energy conditions and flushing rates of grow-out locations are relevant in terms of HAB impacts on oysters and aquaculture production. In the lower Chesapeake Bay, oyster aquaculture is conducted in both shallow low-energy, slow-flushing systems (e.g. tidal creeks), as well as deeper, high-energy rapidly-flushing systems (e.g. the York River mainstem). Fast-flowing water replenishes DO, removes wastes, and increases food availability to oysters (Wilson-Ormond et al. 1997). However, fast-flowing water also promotes the growth of other filter-feeding organisms, such as tunicates and barnacles, which compete with oysters for food and can reduce oyster marketability, particularly for the half-shell market. In terms of bloom impacts, fast-flowing water and shorter flushing times promote bloom dispersal and patchiness, which may reduce the time that oysters are exposed to blooms. In quickly flushing bodies of water, algal cells may be removed from the system at a rate that equals or exceeds the doubling time of the species; this could inhibit cells from reaching high enough concentrations to form a bloom (Roelke & Pierce 2011).

Placement of oyster bags and cages within the grow-out site is another factor that may affect potential HAB impacts on oysters. Much of the local Virginia oyster aquaculture industry grows animals in mesh bags in mesh cages placed on the sediment surface (Hudson 2018). When submerged, these animals may directly experience hypoxia and anoxia resulting from HAB decomposition in the benthos. Industry members sometimes deploy oyster cages intertidally, where oysters are periodically exposed to air at low tide, or subtidally, where oysters are always covered by water. Many local aquaculturists favor intertidal oyster deployment with the resultant periodic aerial exposure to reduce biofouling on oysters and gear (Leggett, Jr., pers. comm.). However, intertidal oysters may experience stress due to significant changes in temperature and DO, as well as reduced feeding times, compared to subtidal oysters (Crosby et al. 1991, Roegner & Mann 1995, Bishop & Peterson 2006).

VIMS scientists received several anecdotal reports from local oyster farm owners in 2015 describing unusually high oyster mortality concurrent with the *A. monilatum* bloom that year (Reece, pers. comm.). One grower reported >50% mortality of his oysters cultured intertidally in the Perrin River, a low energy tributary branching off the York River in the lower Chesapeake Bay during the 2015 *A. monilatum* bloom. The cause of these mortality events is uncertain. In response to the 2015 grower reports, a NOAA-funded Event Response study was carried out during the 2016 *A. monilatum* bloom. Higher cumulative mortality (13.6%) was observed for oysters grown intertidally in the Perrin River, compared to oysters grown subtidally at the same site (3.6%), as well as intertidally and subtidally at both a high energy site in the York River where an *A. monilatum* bloom occurred (4.0% and 2.9%, respectively) and a low energy site where a bloom did not occur (4.0% and 6.3%, respectively) (Reece et al., unpublished data).

These reports suggest oysters may be more impacted by HABs when cultured intertidally in low-energy environments.

Some growers deploy oysters at the water surface in floating bags, a strategy that may also be associated with costs and benefits. These mesh bags, referred to as "cages," are attached to a long-line, holding the oysters just below surface at all times. This method allows oysters ready access to food and DO. However, in the event of a HAB accumulating at the surface, floating oysters may receive higher and more consistent exposure to an on-going bloom, contributing to environmental stress. Griffith et al. (2018) found that first-year scallops (approximately 6 mm) cultured at the surface experienced significantly higher mortality (75-100%), compared to those deployed at depth, during a 1-2 week bloom of *M. polykrikoides* of $>1.5\times10^4$ cells mL^{-1}. However, two size classes (approximately 5 and 32 mm) of juvenile diploid oysters cultured at the surface and at depth did not experience elevated mortality related to the bloom.

Additional research is necessary to evaluate the impacts of sequential *M. polykrikoides* and *A. monilatum* blooms on oysters cultured using different strategies in the lower Chesapeake Bay throughout the bloom season.

Purpose and Objectives

Understanding the effects of emerging, potential stressors, such as HABs, on Chesapeake Bay oysters is critical to the continued success of the aquaculture industry. As HABs increase locally in terms of density, duration, and distribution, it may be necessary for aquaculture industry personnel to modify grow-out procedures at certain times to optimize oyster production. Clear trade-offs exist between different approaches to oyster grow-out as it is currently practiced,

and every method and hydrodynamic profile is associated with certain benefits, as well as potential costs. Emerging HABs may further complicate the optimization of grow-out procedures in the lower Chesapeake Bay.

The two main objectives of this study were to 1) investigate *M. polykrikoides* and *A. monilatum* as a potential threat to cultured oysters in the lower Chesapeake Bay, and 2) inform mitigation strategies to minimize HAB impacts based on current grow-out methods used by the local oyster aquaculture industry. To address these questions, oysters were grown at multiple sites characterized by a range of water energetic and HAB dynamics in the summers of 2017 and 2018. Oysters were grown intertidally and subtidally at all sites in both summers and were also grown in floating cages at one site in 2018. Water quality parameters, including cell concentrations of *M. polykrikoides*, *A. monilatum*, as well as those of two other HAB species known to negatively impact oysters, *Karlodinium veneficum* and *Prorocentrum minimum*, were measured along with assessment of oyster health and survival.

METHODS

Field Study Overview

Oysters were cultured in summers 2017 and 2018 at multiple sites in the lower Chesapeake Bay characterized by a range of water energetic and HAB dynamics. Independent variables investigated included oyster size at the time of blooms of *M. polykrikoides* and *A. monilatum*, oyster deployment site (high vs. low water energy and the presence or absence of HABs), placement location (intertidal, subtidal, and floating at the surface), water quality parameters not directly associated with HABs (temperature, salinity, pH, and DO), and water quality parameters more directly associated with HABs (Chl *a* and *M. polykrikoides*, *A. monilatum, K. veneficum*, and *P. minimum* cell concentrations). Oyster health and survival were also monitored.

Oysters

Triploid seed oysters (1-2 mm) were purchased from Oyster Seed Holdings in Gwynn, VA and grown in a land-based upweller system circulating water from the Perrin River, a tributary branching off the York River, until they reached deployment size (>5 mm). In a land-based upweller, the amount of water flowing through the system is limited, which in turn limits oyster food delivery and waste removal. In contrast, oysters tend to experience greater water flow in the natural environment and, therefore, grow more quickly (Leggett, Jr., pers. comm.). Thus, it was anticipated that oysters deployed in the natural environment a month earlier would be larger at the time of *M. polykrikoides* and *A. monilatum* blooms compared to those grown in the upweller system for an additional month preceding bloom onset. In 2017, two sets of oyster spat (5-10 mm) were deployed one month apart (6/1/17-6/2/17 and 7/5/17-7/6/17, respectively)

in an attempt to evaluate HAB impacts to juvenile oysters of different size classes (**Fig. 1**). In 2018, oysters were deployed only once, from 6/20/18-6/21/18 (**Fig. 2**). At the time of deployments in both summers, oysters were placed in bags with a mesh size of approximately 5 mm; when the majority of oysters in a bag reached a sufficient size, the animals were transferred to bags with a mesh size of approximately 10 mm to facilitate more efficient water flow.

Oyster Deployment Sites

In the summers of 2017 and 2018, oysters were grown at multiple sites in the lower Chesapeake Bay characterized by different water energetics and HAB dynamics. The Chesapeake Bay is an estuary located on the East Coast of the United States that exchanges water with the Atlantic Ocean via an inlet located in the southern portion. The York River is a subestuary of Chesapeake Bay, located near the mouth. In summers 2017 and 2018, oysters were deployed at multiple sites in the lower Chesapeake Bay prior to the dates of the typical onset of local blooms of *M. polykrikoides* and *A. monilatum* – i.e. mid-late July to early September. In 2017, oysters were deployed in the Perrin, York, and Ware Rivers, and in 2018, an additional site was added near Big Island in Guinea, VA proximal to the mouth of the York River (**Fig. 3**). Blooms of the HAB species *M. polykrikoides* and *A. monilatum* have been observed in the Perrin and York Rivers and near Big Island, while blooms of these species have not been observed at the upriver site in the Ware River, the reference location. The Perrin River, a small tributary off the north shore of the York River near its mouth, site was characterized by low water energy. The York River site, located on the north shore of the river near the mouth, was characterized by high water energy (**Table 1)**. The site near Big Island and the site in the Ware River were both

characterized by intermediate water energy. Due to the fact oysters were in some cases grown on the leases belonging to collaborating oyster farm owners, the exact GPS locations of the sites are not disclosed out of sensitivity to the industry members.

The relative flushing rate for each site was based on data from the VA DEQ Coastal Geospatial and Educational Mapping System (GEMS) website (www.coastalgems.org) and a report by Herman et al. (2007). In the report, tidal flushing in water bodies along the Virginia coastal zone was categorized as quick, intermediate, or slow based on factors including residence time and mean water depth. The relative energy condition, or "relative wave energy," for each site was determined according to the nautical mileage of the average fetch exposure of the site (Hardaway et al. 1984). Substrate was characterized by Dr. William Reay (CBNERRS) at all sites based on field-collected sediment cores.

Oyster Placement at Sites

In the summers of 2017 and 2018, oysters were deployed in both intertidal and subtidal bottom cages at all sites. Intertidal and subtidal cages were approximately 7 m apart in the Perrin River, 100 m apart in the York River, 20 m apart at the Big Island site, and 50 m apart at the Ware River site. Intertidal cages were positioned closer to shore in an effort to obtain around 20% aerial exposure of oysters, and subtidal cages were positioned farther from shore to obtain 0% aerial exposure of oysters.

Oysters were grown in three individual mesh bags in each cage to provide pseudo-replication (n=3). A floating cage treatment was included at the Big Island site in 2018 to compare to oysters grown in bottom cages. Floating oysters were grown in three individual mesh bags, referred to as "cages," attached immediately adjacent to each other on a long-line, to create

pseudo-replicates (n=3). Throughout this thesis, "placement" refers to the location oysters were grown within a site – i.e. intertidal, subtidal, or surface deployment.

Water Quality Monitoring

Throughout oyster deployments in 2017 and 2018, water quality was monitored in an effort to characterize the independent variables impacting oyster health and survival. Water quality data (temperature, salinity, pH, DO, and Chl *a*) were monitored in two ways in both summers. These data were monitored *in situ* using a hand-held YSI multi-parameter meter (Xylem, Inc.) held as close to each cage (intertidal, subtidal, and floating) as possible at each site. Measurements were taken biweekly (every two weeks) at the time of oyster sampling and weekly during the time blooms of *M. polykrikoides* and *A. monilatum* typically occur – i.e. mid-late July to early September. The YSI was calibrated at least monthly by CBNERRS staff using standard protocols.

Water quality was also monitored near-continuously next to the subtidal cages at all sites throughout both summers by Reay and CBNERRS. A YSI 6600 series multi-parameter water quality sonde was deployed at depth and took *in situ* measurements every 15 min of water quality parameters, including temperature (resolution: 0.01°C, accuracy: ± 0.15°C), specific conductance (0.001 mS cm^{-1}, ± 0.5% of reading), pH (0.01 SU, ± 0.2 SU), % DO saturation (0.1%, ± 1% of reading), turbidity (1 NTU, ± 0.2% of reading), and Chl *a* fluorescence (~0.1 µg L^{-1}, 0.1% of RFU). Water depth (0.001 m; ± 0.01 m) was also measured, and the non-vented pressure sensor was corrected for atmospheric pressure changes during the deployment period. Salinity (0.01, ± 1% of reading) and DO (0.01 mg L^{-1}, ± 1% of reading) were calculated based on the relevant measured quantities.

Sondes were positioned next to the subtidal cages approximately 25 cm above the sediment in fixed PVC milled to maximize water circulation around the sensors. YSI instruments were configured and calibrated according to standard protocols by Reay and other members of the CBNERRS staff. To minimize biofouling, the sonde equipment was cleaned and monitored in short intervals (~1 week), self-cleaning optical sensors were implemented, and anti-fouling materials were used wherever possible. Quality assurance/quality control (QA/QC) was performed on all data by Reay. QA/QC identified time gaps, exceedance of sensor tolerances, out of water conditions, and single point spike conditions. During sonde deployments and retrievals, water samples were collected and analyzed for Chl *a* to facilitate post-adjustment of sonde Chl *a* fluorescence data to correct for phaeophytin according to Lorenzen (1967).

HAB Sampling

HAB species were monitored at all sites throughout summers 2017 and 2018. Water samples were collected biweekly at the time of oyster sampling and weekly during the time blooms of *M. polykrikoides* and *A. monilatum* typically occur – i.e. mid-late July to early September. At each sampling time, two 100-mL water samples, one for visual identification and quantification of algal species using light microscopy and the other for the identification and quantification of HAB species using qPCR, were collected at the surface as close to each cage (intertidal, subtidal, and floating) as possible at all sites.

Visual identification and enumeration of algal cells, including *M. polykrikoides* and *A. monilatum* as well as other algal species present, was performed by William M. Jones III in the Reece Laboratory at VIMS. Following analyses using light microscopy, 3 mL of one of the 100-mL samples were preserved with Lugol's iodine solution (Lugol's; Fisher Scientific) in an

approximately 0.05:1 Lugol's to sample dilution. The second 100-mL sample was vacuum filtered onto a 3-µm polycarbonate membrane filter, and filters were stored in 5-mL tubes at -20°C until DNA was extracted for qPCR. If the sample was particularly dense, a smaller volume (e.g. 25-50 mL) was filtered for DNA extraction and the subsequent qPCR cell concentration was adjusted accordingly.

In this thesis, a bloom was defined as a cell concentration ≥500 cells mL^{-1} of the relevant species. A bloom period at a particular site was defined as the period between which the first and last samples containing ≥500 cells mL^{-1} were collected during the sampling season. Chl *a* data collected by the data sondes every 15 min at all sites were anticipated to serve as a high frequency proxy for HAB cell concentrations in light of the more limited number of water samples used for the direct enumeration of HAB cells.

DNA Extraction

DNA was extracted from filters using the QIAamp Fast DNA Stool Mini kit (Qiagen) according to manufacturer's instructions with some modifications. After adding InhibitEX Buffer, tubes were placed in a 95°C water bath for 5 min. Samples were vortexed for 15 s following cell lysis. Rather than centrifuging the sample and using only 200 µL of the lysate, as per the manufacturer's instructions, the entire sample was retained and carried through the extraction protocol. The reagent volumes were increased in the subsequent steps to maintain a ratio of sample to reagent consistent with that in the manufacturer's instructions. Following cell lysis, 1 mL of Buffer AL was added to each 5-mL tube, and samples were vortexed for 15 s. Then, 75 µL of Proteinase K was added to each tube, and samples were vortexed for another 15 s. Samples were then incubated in a 70°C water bath for 10 min. Following incubation, 1 mL

of 100% ethanol was added to each sample, and tubes were vortexed. The lysate was then applied to the QIAmp mini-spin DNA extraction column with silica resin in 600-µL increments and centrifuged at full speed (>20,000 xg). After most of the sample was applied to the column, sterile forceps were used to pull up the filter and clip it under the lid of the 5-mL tube. Samples were then centrifuged for 1 min at 1000 rpm to remove any remaining sample from the filter. The remaining volume was transferred onto the column and centrifuged at full speed for 1 min. Columns were then transferred into clean collection tubes, and Buffers AW1 and AW2 were added to each column. Columns were then placed in Axygen tubes (Corning, Incorporated), and 100 µL ATE Buffer was placed on top of each column and incubated for 1 min at room temperature. Samples were centrifuged at full speed for 1 min, and the eluted DNA was stored at -20°C until qPCR was performed.

Development of Positive Control Material

Positive control material for the standard curve was developed using clonal cultures of *M. polykrikoides* and *A. monilatum*, both in the log growth phase. The *M. polykrikoides* isolate was originally obtained from a 2005 York River bloom, and the *A. monilatum* isolate was originally obtained from a 2007 York River bloom. Cell concentrations were determined using light microscopy. The concentrations were used to determine the appropriate volume of culture to filter onto a 3-µm polycarbonate membrane filter to represent a 100-mL sample with approximately 1,500 cells mL^{-1} for *M. polykrikoides* and 10,000 cells mL^{-1} for *A. monilatum*. Filters were then stored at -20°C until DNA extractions (as described above) were performed. The extracted DNA was used to generate the standard curves used in the qPCR analyses below.

Quantitative Real-time PCR

qPCR reactions were performed on all water samples for the identification and quantification of *M. polykrikoides* and *A. monilatum*, as well as two common toxigenic HAB species, *K. veneficum* and *P. minimum*. qPCR reactions were performed using the TaqMan Fast Advanced Master Mix (Thermo Fisher Scientific) in accordance with the manufacturer's instructions using primers and probes targeting the small subunit (SSU) ribosomal RNA gene, the large subunit (LSU) ribosomal RNA gene, or the internal transcribed spacer region (ITS) for each species (Eurofins MWG Operon).

The forward and reverse primer and probe sequences (5'-3') used for *M. polykrikoides* reactions were as follows (Reece, unpublished data):

Cpoly 730F: TCTTTCCGACCCGTCTTGAA

Cpoly 875R: CCATCTTTCGGGTCCTAGCA

CpLSU_828PR: FAM-TTGCGAGACGTTTGAGTGTG-MGBNFQ

The forward and reverse primer and probe sequences (5'-3') used for *A. monilatum* were as follows (Vandersea et al. 2017):

Amon2_500F: TGAAAGGTAAGGTGCCTGTG

Amon2_658R: GCAGAAACATGTTGCCAAAG

Amon2_523PR: FAM-TGCAAGCACAAGCAACCCAGC-QSY7

The forward and reverse primer and probe sequences (5'-3') used for *K. veneficum* were as follows (VA DEQ 2014):

KvITS_242F: TTCGTTGTGTAGTTGTTGACTCG

KvITS_328R: TGCTGACCTAACTTCATGTCTTG

Kv_266PR: FAM-AGCCTGCTCCAGCTCACGACTCCT-TAMRA

The forward and reverse primer and probe sequences (5'-3') used for *P. minimum* were as follows (Handy et al. 2008):

Pmin 200F: TGTGTTTATTAGTTACAGAACCAGC

Pmin 525R: AATTCTACTCATTCCAATTACAAGACAAT

Pmin PR: FAM-CCGCCTGGTCCTTTGGTGATTCATAATAAC-MGBNFQ

An internal control (IAC) was run on one assay for each sample to check for inhibition. The forward and reverse primer and probe sequences (5'-3') used for the IAC were as follows (Nordstrom et al. 2007):

IAC_F: GACATCGATATGGGTGCCG

IAC_R: CGAGACGATGCAGCCATTC

IAC_cy5PR: Cy5-TCTCATGCGTCTCCCTGGTGAATGTG-BHQ2a

The final volume of each qPCR reaction was 10 µL made up of the following: 4 mg mL^{-1} bovine serum albumin (BSA), 1.0X TaqMan Fast Advanced Master Mix (diluted from the original 5X solution included in the kit), 0.9 µM of the forward primer, 0.9 µM of the reverse primer, 0.10 µM of the species probe, and 1 µl of template DNA. For assays in which the IAC was run, the 10-µL final volume also included final concentrations of 0.08 µM of the IAC forward primer, 0.08 µM of the IAC reverse primer, 0.15 µM of the IAC probe, and 1 µl of a 1:1000 dilution of the IAC DNA (Bio-Gx product #760-0001). In all cases, nuclease-free H_2O was used to bring the reaction volume up to 10 µL when necessary. Amplifications were performed in accordance with the kit manufacturer's instructions, including initial denaturation at 95°C for 20 s, followed by 40 cycles of denaturing at 94°C for 3 s, and annealing/extension at 60°C for 30 s.

Each plate included a standard curve, consisting of seven ten-fold serial dilutions of the positive control material. The limits of detection are based on the standard curve ranges from the maximum cell concentration for each species, typically 1.5×10^{3} cells mL^{-1} to 1.5×10^{-3} cells mL^{-1} for *M. polykrikoides* and 1×10^{4} cells mL^{-1} to 0.02 cells mL^{-1} for *A. monilatum, K. veneficum*, and *P. minimum*. All samples were run in duplicate using a 7500 Fast Real-Time PCR System (Applied Biosystems). The system software determined the threshold cycle values, and the values for cells mL^{-1} were interpolated for each reaction based on the standard curve.

Six Dependent Oyster Variables

At regular intervals, oysters were monitored for six dependent variables, referred to in this thesis at the "dependent oyster variables." The dependent oyster variables included interval

mortality, cumulative mortality, shell height, growth rate, condition index (CI), and histopathology. These variables were chosen to help quantify oyster survival and health during the bloom season.

1. *Interval Mortality*

Interval oyster mortality was quantified for each of the three bags at each placement location (intertidal, subtidal, and surface) biweekly, and dead oysters were removed. Gaping oysters unresponsive to touch, as well as empty whole or half-shells, were considered dead. A half-shell discovered in the bag without a matching half-shell was considered as a whole (n=1) dead oyster.

Interval mortality was calculated according to the following equation, in which T_x refers to the time of sampling:

$$\text{IM} = \frac{Dead\ oysters\ in\ the\ bag\ at\ T_x}{Total\ oysters\ in\ the\ bag\ at\ T_x}$$

These data were calculated as a ratio and must be multiplied by 100 to be considered as a percent value.

2. *Cumulative Mortality*

Cumulative oyster mortality was also calculated biweekly for each of the three bags at each placement location (intertidal, subtidal, and surface) according to the following equation, in which T_0 is the time when oysters were deployed and T_x refers to the time of sampling:

$$\mathrm{CM} = \frac{Total\ dead\ oysters\ from\ T_0\ until\ T_x}{Total\ oysters\ in\ bag\ at\ T_0}$$

These data were calculated as a ratio and must be multiplied by 100 to be considered as a percent value.

3. Shell Height

Concurrent with mortality quantification, a random sample of live oysters (n=25) from each of the three bags at each placement location (intertidal, subtidal, and surface) was measured using calipers. Shell height was considered as the maximum length from hinge to bill.

4. *Growth Rate*

Using the oyster shell height measurements, interval oyster growth rate was calculated in mm day^{-1} for each of the three bags at each placement location (intertidal, subtidal, and surface) according to the following equation, in which T_f refers to the last day of the sampling interval and T_i refers to the first day of the sampling interval:

$$\mathrm{GR} = \frac{\left(Average\ shell\ height\ at\ T_f - \ Average\ shell\ height\ at\ T_i\right)}{T_f - \ T_i}$$

5. Condition Index

CI is one metric for assessing oyster health, in which the ratio between oyster tissue, or viscera, and oyster shell is quantified. A random sample of live oysters (n=3) was collected from each of the three bags at each placement location (intertidal, subtidal, and surface) approximately

once a month for CI determination. Oysters were shucked, and all tissue was removed. Shells and tissue were dried separately in individual pans in a drying oven and subsequently weighed. A CI was then calculated for each oyster according to the following equation (Walne & Mann 1975, Rainer & Mann 1992):

$$\mathrm{CI} = \frac{(Dry\ viscera\ weight \times 100)}{Dry\ shell\ weight}$$

6. Histopathology

Histopathology is another metric for assessing oyster health, in which tissues are examined for the presence of pathogens and pathology. A random sample of live oysters (n=3) was collected from each of the three bags at each placement location (intertidal, subtidal, and surface) for routine paraffin histology approximately once a month in 2017 and 2018. Much of the histological preparation was done by the VIMS Shellfish Pathology Lab. Oyster tissues were fixed with Davidson's solution (Shaw & Battle 1957) and processed using standard methods, with 6-µm transverse sections that included gills, mantle, and organs of the visceral mass stained with hematoxylin and eosin (H&E) and evaluated using light microscopy (100-400X). The sections were examined for any signs of infection or disease, including infection and tissue disruption caused by the major pathogens *P. marinus* and *H. nelsoni*. Attention was also paid to the potential presence of dinoflagellates possibly associated with blooms, including *A. monilatum*-like cells. For the 207 total samples from 2017 and 2018, prevalence data is reported for gill erosion, hemocytosis in the gills and mantle, and *P. marinus* and *H. nelsoni*.

Data Analysis: Graphs

Results were analyzed in two consecutive ways. First, the raw data from individual years were graphed. Cell concentrations of *M. polykrikoides* and *A. monilatum*, as determined by qPCR, were graphed alongside Chl *a* values to provide a visual idea of how well Chl *a* concentration served as a proxy for HAB concentration. Oyster data were also graphed to aid in the visualization of the relative differences in five of the six dependent oyster variables (interval mortality, cumulative mortality, shell height, growth rate, and CI) and to guide subsequent modeling efforts. Histopathology data were not graphed due to the low prevalence of pathogens and pathology. In all graphs, error bars represent the 95% confidence intervals. Confidence intervals were calculated using the three pseudo-replicate bags associated with each placement location (intertidal, subtidal, and surface). In terms of the graphs, significant differences between treatments within years were defined as non-overlapping confidence intervals.

Data Analysis: Modeling Overview

Following a visual analysis of the raw data using the graphs, general linear models (McCullagh & Nelder 1989) were designed using R version 3.5.1 software (www.r-project.org) to investigate more deeply the independent variables (site, placement location, temperature, HAB concentration, etc.) that influenced differences in five of the dependent oyster variables – interval mortality, cumulative mortality, shell height, growth rate, and CI. Surface/floating cage data were not included in the modeling, as surface cages were only utilized at the Big Island, and only in 2018, when blooms were not observed at any of the experimental sites; intertidal and subtidal bottom cage data from Big Island were included in 2018 modeling, however. Due to limited sampling for CI in 2018 (oysters were only sampled for CI twice in 2018), CI data were only

modeled for 2017. Histopathology data from 2017 and 2018 were not included in statistical analyses due to the low prevalence of pathogens and pathology in both summers. A link function designates the relationship between the expected value of the response variable and the explanatory variables. This function must be differentiable and monotonic.

Because blooms of *M. polykrikoides* and *A. monilatum* only occurred at the study sites in 2017, data from 2017 and 2018 were modeled separately. For each of the two years, dependent oyster variables were evaluated for the assumption of normality and log transformed if transformation made data appear more normal. All independent variables were then analyzed for collinearity. The units of all continuous independent variables (temperature, salinity, HAB concentration, etc.) were then standardized to facilitate ease of comparison. A suite of models was then created for each of the dependent oyster variables, and the most supported model was selected and used for analysis.

Model Development: Independent Variables

Independent variables considered during model development included site, placement location, temperature, salinity, pH, DO, Chl *a*, *A. monilatum* concentration, and *M. polykrikoides* concentration. All models utilized water quality data based on the measurements collected using the hand-held YSI concurrent with oyster monitoring (e.g. for mortality and shell height quantification). The relationship between intertidal YSI data and subtidal YSI data was modeled and used to generate predicted values for intertidal water quality data, allowing YSI and sonde data to be compared directly. The resultant water quality data represent data collected at the time of oyster monitoring/sampling. Because HAB concentrations were never quantified more than

once a week, all HAB data used in the model were taken at the time of oyster sampling. Models utilized HAB cell concentrations determined via qPCR.

The units of all continuous covariates (temperature, salinity, pH, DO, Chl *a*, *A. monilatum* concentration, and *M. polykrikoides* concentration) were standardized to place all explanatory variables on the same scale to facilitate comparisons. The independent variables were investigated for collinearity by comparing the calculated variance inflation factors (VIFs). In cases of collinearity between two independent variables, one of the two variables was removed from the relevant models.

The independent variables were grouped into three different categories. The first category was referred to as "HAB factors," or factors directly related to HABs (*A. monilatum*, *M. polykrikoides*, and Chl *a* concentrations). The second category was referred to as "non-HAB factors," or factors not directly related to HABs (temperature, salinity, pH, and DO). The final category was labeled "location factors," or factors related to oyster aquaculture methods (site and placement location). The intertidal and subtidal bottom cage placement location data were used from all sites both years. However, surface/floating cage data were not included in the models, as surface cages were only included at one site, and only in 2018, when blooms were not observed at any of the experimental sites.

Model Development: Dependent Variables

Dependent variables investigated using modeling included 2017 and 2018 interval mortality, cumulative mortality, shell height, and growth rate data, as well as 2017 CI data. CI data from 2018 were not modeled due to low sample size. Histopathology data were not included in statistical analyses due to the low prevalence of pathogens and pathology in both summers.

Due to notable differences in water quality between the two summers, including HAB occurrence, data from 2017 and 2018 were modeled separately. As mentioned above, the three pseudo-replicate bags were used for statistical comparisons between treatments within each year for the graphs. However, the models were created using a more rigorous definition of replication, pooling the three bags within a placement location (intertidal and subtidal) and considering the cage itself as the unit of replication. After a cursory investigation of the raw 2017 data revealed only an approximately 15 mm difference in oyster shell height between the two deployments by the time of bloom onset, data from the two deployments were combined for the 2017 statistical analyses. Thus, oyster size class was not evaluated as an independent variable in either year.

Diagnostic plots (Normal Q-Q and Residuals vs. Fitted) were used to assess the variance estimation and the assumption of normality for each of the dependent oyster variables in 2017 and 2018. When appropriate, the data sets were log transformed to make the data appear more normal. For data sets that benefited from log transformation but contained zeros, a constant of 0.1 was added to all values in the data set to permit log transformation. Preliminary model exploration for 2017 oyster data supported the assumption of normality for the cumulative mortality, shell height, and growth rate data sets. Diagnostic plots supported the assumption of log normality for the 2017 interval mortality and CI data sets, and these data were log transformed. Preliminary model exploration for 2018 oyster data supported the assumption of normality for the shell height and growth rate data sets. Diagnostic plots supported the assumption of log normality for the 2018 interval mortality and cumulative mortality data sets, and these data were log transformed.

Model Development

The purpose of this thesis was to investigate the impacts of HABs in the context of oyster aquaculture. To address the biological hypothesis that oysters would be impacted by HAB factors and location factors, a suite of models was created for each of the five 2017 dependent oyster variables (interval mortality, cumulative mortality, shell height, growth rate, and CI) considered and for each of the four 2018 dependent oyster variables (interval mortality, cumulative mortality, shell height, and growth rate) considered. Each model in the suite of models contained a different combination of the independent variables. Due to the fact that the potential impacts of HABs were being assessed within the context of oyster aquaculture, the two location factors (site and placement location) were included in all models created for each of the 2017 and 2018 dependent oyster variables.

In 2017, a suite of four models was created for each of the five dependent oyster variables considered. In addition to the location factors, the first model contained non-HAB factors and HAB factors. The second model contained the location factors and only the non-HAB factors. The third model contained the location factors, the non-HAB factors, and added Chl *a* back in; this model was included in case Chl *a* did not serve as an effective a proxy for HAB concentration as anticipated. Finally, the fourth model contained the location factors and the HAB factors only. For 2017 data, the suite of models created for each of the five dependent oyster variables (interval mortality, cumulative mortality, shell height, growth rate, and CI) were as follows:

1. Dependent oyster variable ~ location factors + non-HAB factors + HAB factors
2. Dependent oyster variable ~ location factors + non-HAB factors
3. Dependent oyster variable ~ location factors + non-HAB factors + Chl *a*
4. Dependent oyster variable ~ location factors + HAB factors

For 2018 data, the suite of models created for each of the four dependent oyster variables (interval mortality, cumulative mortality, shell height, and growth rate) did not include concentrations of *A. monilatum* and *M. polykrikoides*, as blooms were not detected at any of the sites. Instead the suite of models sought to evaluate in particular the importance of Chl *a* in relation to the other water quality parameters and contained the following two models:

1. Dependent oyster variable ~ location factors + non-HAB factors + Chl *a*
2. Dependent oyster variable ~ location factors + non-HAB factors

Model Selection

Fits of the potential models within each suite were evaluated based on diagnostic plots, including the Normal Q-Q and Residuals vs. Fitted. Model selection was achieved using Akaike's Information Criterion (AIC), which balances model complexity with model fit (Akaike 1973). The model with the lowest ΔAIC is that which receives the most empirical support. Based on these investigations, one model was selected to evaluate each of the dependent oyster variables from 2017 and 2018. A linear regression table was then generated for each selected model, and the relative explanatory power of each independent variable included in the model was investigated based on its parameter estimate, standard error, and the traditional measure of statistical significance, the p-value.

When operating under the AIC mode of inference, the model with the most empirical support – i.e. the lowest ΔAIC – in a suite of models is that which retains the covariates that best explain the response variable, compared to the other models in the suite. Thus, the parameters

retained in the selected model are thought to be associated to some degree with the response variable. However, when considering the output table of the selected model, it is also important to consider the magnitude of the parameter estimate for each covariate compared to that of its standard error. A high standard error in relation to a parameter estimate can indicate that the estimate is a less accurate representation of the true population mean. High standard error can be caused by low sample size. In contrast, a parameter estimate that is at least one order of magnitude greater than its corresponding standard error indicates that the independent variable in question has a strong relationship with the dependent variable being investigated by the model. The direction of the estimate (positive or negative) indicates whether the relationship between the independent and dependent variables is direct or inverse.

Consider an example linear regression table generated for 2017 interval oyster mortality data, in which site, placement location, temperature, salinity, pH, and DO are evaluated as predictor variables (**Table 2**). The table provides a parameter estimate for each independent variable included in the model and the standard error for that estimate. Oyster mortality was inversely related to pH, meaning that mortality was higher at lower pH values. Two of the independent variables considered in these models are categorical variables with different levels. First, site is a categorical variable with multiple levels. In 2017, site contained three different levels – the Perrin River (PR, in the figure), York River (YR, in the figure), and Ware River sites; in 2018, site contains four levels – the Perrin River, York River, Ware River, and Big Island sites. In both years, placement location was a categorical variable containing two levels – intertidal and subtidal (ST, in the figure). In a linear regression table, the first row is the "intercept," which collapses the first level of each categorical variable. For all models evaluated in this thesis, the intercept represented the intertidal placement location and the Ware site, the

reference location where blooms of *M. polykrikoides* and *A. monilatum* have not typically been reported. Thus, the direction of all subsequent parameter estimates for all categorical variables represents a comparison with the intercept – i.e. the intertidal placement location at the Ware River site. For example, **Table 2** data indicate oyster mortality was higher in the York River compared to the Ware River, and mortality was higher for oysters placed in subtidal locations compared to oysters placed in intertidal locations.

To simplify evaluation of the model outputs, the traditional measure of significance, the p-value, was also considered for each independent variable. The significance codes for the p-values in the linear regression tables were as follows:

$p < 0.001$ ***
$p < 0.01$ **
$p < 0.05$ *

RESULTS

Considering 2017 and 2018 data were both graphed and modeled independently, the results summarize 2017 data first, followed by 2018 data.

2017

Water Quality Monitoring

Based on summary statistics of water quality data collected near-continuously next to the subtidal cages in the summer of 2017, average temperature was slightly lower at the York River site compared to the Perrin and Ware River sites, while average salinity was the lowest at the Ware River site (**Table 3**). Average pH, DO, and Chl *a* levels were similar across sites in 2017. The highest average DO, and the widest range of DO measurements, were observed at the York River site, the highest energy site. Average subtidal Chl *a* levels were highest at the Ware River site (12.9 µg L^{-1}), the reference location. However, the ranges of Chl *a* values were much wider, and the maxima were much higher, at the Perrin and York River sites. Chl *a* levels ranged from 0.3-461.9 µg L^{-1} next to the subtidal cages in the Perrin River, from 0.2-483.9 µg L^{-1} next to the subtidal cages in the York River, and from 0.1-106.7 µg L^{-1} next to the subtidal cages in the Ware River.

HAB Species Sampling

All water samples collected in 2017 were analyzed both visually and via qPCR; however, all cell concentration data reported in this section were quantified by qPCR. Based on an analysis of correlation using Pearson's correlation coefficient, neither *M. polykrikoides* nor *A. monilatum* concentrations, quantified by qPCR, were strongly correlated with Chl *a*.

At the Perrin River site, the low-energy HAB-endemic location, the maximum *M. polykrikoides* concentration detected from weekly HAB sampling next to the intertidal cages was 421 cells mL^{-1} on 7/31/17. The maximum concentration measured next to the subtidal cages was 431 cells mL^{-1} on 8/15/17 (**Fig. 4A**). In this thesis, a bloom was defined as a cell concentration ≥500 cells mL^{-1} of the relevant species. A bloom period at a particular site was defined as the period between which the first and last samples containing ≥500 cells mL^{-1} were collected during the sampling season. Based on these definitions, when intertidal and subtidal HAB collection data were pooled, a *M. polykrikoides* bloom was not detected at the Perrin River site in 2017.

The maximum *A. monilatum* concentration detected from weekly HAB sampling next to the intertidal cages at the Perrin River site was 319 cells mL^{-1} on 8/15/17. The maximum concentration measured next to the subtidal cages was 3,425 cells mL^{-1} on 8/28/17 (**Fig. 4A**). When intertidal and subtidal HAB collection data were pooled, an *A. monilatum* bloom was detected on only one day, 8/28/17, at the Perrin River site in 2017.

Samples from the Perrin River site never contained >25 cells mL^{-1} of *K. veneficum*, and *P. minimum* concentrations remained below 10 cells mL^{-1}, except on 10/4/17, when both the intertidal and subtidal samples contained between 300-400 cells mL^{-1} of *P. minimum*.

At the York River site, the high-energy HAB-endemic location, the maximum *M. polykrikoides* concentration detected from weekly HAB sampling next to the intertidal cages was 375 cells mL^{-1} on 8/8/17. The maximum concentration measured next to the subtidal cages was 16,842 cells mL^{-1} on 7/27/17 (**Fig. 4B**). When intertidal and subtidal HAB collection data were pooled, a *M. polykrikoides* bloom was detected on only one day, 7/27/17, at the York River site. However, a sample collected on 8/8/17 in the channel of the York River offshore of the sampling site contained 116,580 *M. polykrikoides* cells mL^{-1} (Reece et al., unpublished data).

The maximum *A. monilatum* concentration detected from weekly HAB sampling next to the intertidal cages at the York River site was 92,529 cells mL^{-1} on 8/22/17. The maximum concentration measured next to the subtidal cages was 69,051 cells mL^{-1} on 8/22/17 (**Fig. 4B**). When intertidal and subtidal HAB collection data were pooled, an *A. monilatum* bloom was detected from 8/22/17-9/4/17, a period of approximately two weeks at the York River site.

Concentrations of *K. veneficum* never exceeded 1 cell mL^{-1} in samples collected at the York River site in 2017, and *P. minimum* concentrations remained below 70 cells mL^{-1}.

Blooms of *M. polykrikoides* were not detected at the Ware River site, the intermediate-energy reference location, in 2017. *Margalefidinium polykrikoides* concentrations detected from weekly HAB sampling next to the intertidal cages never exceeded 1 cell mL^{-1}. The maximum concentration measured next to the subtidal cages was 4 cells mL^{-1} on 7/24/17 (**Fig. 4C**).

Blooms of *A. monilatum* also were not detected at the Ware River site in 2017. The maximum *A. monilatum* concentration detected from weekly HAB sampling next to the intertidal cages was 36 cells mL^{-1} on 8/23/17. The maximum concentration measured next to the subtidal cages was 65 cells mL^{-1} on 9/5/17 (**Fig. 4C**).

Concentrations of *K. veneficum* never exceeded 60 cells mL^{-1} in samples from the Ware River site, and *P. minimum* concentrations never exceeded 70 cells mL^{-1}.

Interval Oyster Mortality

Based on the graphs of the interval oyster mortality data for the June and July deployments in 2017, interval mortality (calculated as the ratio of dead oysters to the total number of oysters in the bag at the time of sampling) never exceeded 0.04, or 4% (**Figs. 5, 6**).

Model selection for 2017 interval mortality data favored the generalized linear model containing site (Perrin River, York River, and Ware River), placement location (intertidal and subtidal), temperature, salinity, pH, and DO (**Table 4**). Based on this model, interval oyster mortality was significantly higher at the Perrin River site, compared to the Ware River site, the reference location ($p<0.05$) (**Table 5**). A significant, direct relationship was also found between interval mortality and temperature ($p<0.001$).

Cumulative Oyster Mortality

Based on the graphs of the cumulative oyster mortality data for the June and July deployments in 2017, cumulative mortality (calculated as the ratio of the total number of oysters that had died up to the time of sampling to the original number of oysters deployed in the bag) never exceeded 0.12, or 12% (**Figs. 7, 8**). Cumulative oyster mortality was relatively higher at the two HAB-endemic sites compared to cumulative mortality in the Ware River, the reference location. Mortality of intertidal oysters deployed in the June was significantly higher in the Perrin River compared to mortality in the Ware River intertidal in early and late August (**Fig. 7**). (As described in the Methods, significance for the graphs was determined by the 95% confidence intervals, which were calculated using the three pseudo-replicate bags at each placement location.) Mortality of intertidal and subtidal oysters deployed in June at both HAB-endemic sites was significantly higher than intertidal mortality in the Ware River in early and late September (**Fig. 7**). Mortality of intertidal oysters deployed in July in the York River was significantly higher than mortality of intertidal oysters in the Ware River in late September (**Fig. 8**).

Model selection for 2017 cumulative mortality data favored the generalized linear model containing site (Perrin River, York River, and Ware River), placement location (intertidal and subtidal), temperature, salinity, pH, and DO (**Table 4**). Based on this model, cumulative oyster mortality was significantly higher at the Perrin River site, compared to the Ware River site, the reference location ($p<0.001$) (**Table 5**). Cumulative mortality was significantly lower for oysters grown subtidally compared to those grown intertidally ($p<0.05$). A significant, inverse relationship was also found between cumulative mortality and temperature ($p<0.001$).

Oyster Shell Height

Based on the graphs of the oyster shell height data for the June and July deployments in 2017, by the end of the sampling season, the oysters deployed one month later reached similar sizes (~50-60mm) as the oysters deployed earlier in the summer (~55-65 mm) (**Figs. 9, 10**). For oysters deployed in June 2017, shell height was significantly larger for oysters deployed intertidally at the Ware River site, the reference location, compared to those deployed in the two HAB-endemic locations, in early and late August (**Fig. 9**). For oysters deployed in July 2017, shell height was larger for oysters deployed both intertidally and subtidally at the Ware River site, compared to oysters deployed at both placement locations at the two HAB-endemic sites, beginning in early August and continuing throughout the rest of the sampling season (**Fig. 10**).

Model selection for 2017 shell height data favored the generalized linear model containing site (Perrin River, York River, and Ware River), placement location (intertidal and subtidal), temperature, salinity, pH, and DO (**Table 4**). Because oysters from the two deployments were similar heights around the time peak concentrations of *M. polykrikoides* and *A. monilatum* occurred at the Perrin and York River sites, shell height data for the two

deployments at all sites were pooled for modeling. Based on this model, oyster shell height was significantly smaller at the York River site, compared to the Ware River site, the reference location ($p<0.05$) (**Table 5**). A significant, inverse relationship was found between shell height and temperature ($p<0.001$).

Oyster Growth Rate

Based on the graphs of the oyster growth rate data for the June and July deployments in 2017, intertidal and subtidal growth rate was significantly slower at the York River site in early August, following the peak concentration of *M. polykrikoides* (16,842 cells mL^{-1} next to the subtidal cage on 7/27/17) at that site, compared to both placement locations at the Ware River site, where blooms of *M. polykrikoides* and *A. monilatum* were not detected (**Figs. 11, 12**).

Model selection for 2017 growth rate data favored the generalized linear model containing site (Perrin River, York River, and Ware River), placement location (intertidal and subtidal), temperature, salinity, pH, DO, Chl *a*, *M. polykrikoides* concentration, and *A. monilatum* concentration (**Table 4**). Based on this model, oyster growth rate was significantly faster at higher temperatures ($p<0.01$) and at lower DOs, ($p<0.05$) (**Table 5**). A significant, direct relationship was found between oyster growth rate and *M. polykrikoides* concentration ($p<0.01$).

Oyster Condition Index

Based on the graphs of CI data for the June and July deployments in 2017, CI was significantly higher for oysters grown intertidally at the York River site, the high-energy HAB-endemic location, compared to those grown subtidally at the same site and at both placement locations at the other two sites, in late August (**Figs. 13, 14**).

Model selection for 2017 condition index data favored the generalized linear model containing site (Perrin River, York River, and Ware River), placement location (intertidal and subtidal), temperature, salinity, pH, DO, and Chl *a* (**Table 4**). Based on this model, CI was significantly higher at higher temperatures ($p<0.01$) (**Table 5**).

Oyster Histopathology

Based on histology data, oysters did not show considerable adverse health impacts in 2017, and as such, these data were not graphed or modeled. Of the oysters collected throughout the summer of 2017 (n=126), no oysters displayed notable gill erosion or significant loss of epithelial structure, and <1% exhibited hemocytosis in the gills or mantle. In terms of pathogens, 7.9% of oysters contained an unidentified microsporidian species, commonly associated with erosion, in the gut epithelium. No *H. nelsoni* infections were identified, and only 2.4% of oysters were infected with *P. marinus* cells. All *P. marinus* infections (n=3) were rare, consisting of <10 cells. No other significant pathology or pathogens were observed in oysters collected in 2017.

2018

Water Quality Monitoring

Based on summary statistics of water quality data collected near-continuously next to the subtidal cages in the summer of 2018, average temperature was slightly lower at the York River and Big Island sites compared to the Perrin and Ware River sites (**Table 6**). Average salinity was lowest at the Ware River site, the reference location, and the minimum salinity was also lowest at

this site (7.2) compared to the minima at the other sites (minima ranged from 9.1-11.8). Near-continuous salinity data collected next to the subtidal cage at the Ware River site in 2018 indicated a rapid decrease in salinity beginning on 7/25/17 and a gradual return to early-summer levels throughout the rest of the summer (**Fig. 15**). Average pH and DO were similar across sites in 2018. The highest average DO, and the widest range of DO measurements, were observed at the York River site, the highest energy location. Average subtidal Chl *a* was highest at the Ware River site (15.1 µg L^{-1}), the reference location, and concentrations ranged from 1.9-68.1 µg L^{-1}. The average Chl *a* was similar at the Big Island site (9.5 µg L^{-1}), and concentrations ranged from 1.2-72.8 µg L^{-1}. The Chl *a* range was widest in the York River, with concentrations ranging from 0.1-115.1 µg L^{-1}. Average Chl *a* was lowest in the Perrin River (8.9 µg L^{-1}), and the range was the narrowest, from 7.8-10.2 µg L^{-1}.

HAB Species Sampling

All water samples collected in 2018 were analyzed both visually and via qPCR; however, all cell concentration data reported in this section were quantified by qPCR.

At the Perrin River site, the low-energy HAB-endemic location, neither *M. polykrikoides* nor *A. monilatum* concentrations reached 1 cell mL^{-1} in water samples collected weekly next to the intertidal and subtidal cages in 2018 (**Fig. 16A**). Concentrations of *K. veneficum* were less than 500 cells mL^{-1} in all samples, except on 7/8/18, when the intertidal and subtidal samples contained between 900-1000 *K. veneficum* cells mL^{-1}. Concentrations of *P. minimum* were less than 500 cells mL^{-1} in all samples collected intertidally, and below 300 cells mL^{-1} in all samples collected subtidally.

At the York River site, the high-energy HAB-endemic location, neither *M. polykrikoides* nor *A. monilatum* concentrations reached 1 cell mL^{-1} in water samples collected weekly next to the intertidal and subtidal cages in 2018 (**Fig. 16B**). Concentrations of *K. veneficum* were less than 70 cells mL^{-1} in all samples, except on 8/13/18, when the intertidal and subtidal samples both contained between 90-200 *K. veneficum* cells mL^{-1}. Concentrations of *P. minimum* were less than 50 cells mL^{-1} in all samples collected intertidally and subtidally.

At the Big Island site, the intermediate-energy HAB-endemic location, neither *M. polykrikoides* nor *A. monilatum* concentrations reached 1 cell mL^{-1} in water samples collected weekly next to the floating, intertidal, or subtidal cages in 2018 (**Fig. 16C**). Concentrations of *K. veneficum* peaked at 185 cells mL^{-1} next to the floating cages on 9/6/18, but otherwise concentrations were <100 cells mL^{-1}. Concentrations of *K. veneficum* never exceeded 60 cells mL^{-1} in intertidal samples and remained below 300 cells mL^{-1} in subtidal samples. Concentrations of *P. minimum* were less than 200 cells mL^{-1} in all samples collected next to the floating cages. Concentrations of *P. minimum* were less than 100 cells mL^{-1} in all samples collected intertidally, and the maximum concentration quantified in a subtidal sample was 133 *P. minimum* cells mL^{-1} on 10/1/18.

At the Ware River site, the intermediate-energy reference location, neither *M. polykrikoides* nor *A. monilatum* concentrations reached 1 cell mL^{-1} in water samples collected weekly next to the intertidal or subtidal cages in 2018 (**Fig. 16D**). Concentrations of *K. veneficum* peaked in intertidal samples at 852 cells mL^{-1} on 9/27/18, but otherwise concentrations were <300 cells mL^{-1}. Concentrations of *K. veneficum* peaked in subtidal samples at 758 cells mL^{-1} on 9/27/18, but otherwise remained <600 cells mL^{-1}. Concentrations of *P. minimum* were <300 cells mL^{-1} in intertidal and subtidal samples.

Interval Oyster Mortality

Based on the graph of the interval oyster mortality data from 2018, interval mortality never exceeded 0.12, or 12% (**Fig. 17**). Interval oyster mortality was highest for oysters grown intertidally at the Ware River site, the reference location, compared to the other placement locations and sites. This difference was significant, based on the 95% confidence intervals, at the sampling time in mid-July, preceding the rapid drop in salinity in the Ware River beginning on 7/25/18 (**Fig. 15**).

Model selection for 2018 interval mortality data favored the generalized linear model containing site (Perrin River, York River, Big Island, and Ware River), placement location (intertidal and subtidal), temperature, salinity, pH, and DO (**Table 7**). As stated in the Methods section, floating cage data were not included in the modeling, as these data were only collected at one site. Based on this model, interval oyster mortality was significantly lower at the Big Island site ($p<0.05$) and the Perrin River site ($p<0.01$), compared to the Ware River site, the reference location (**Table 8**). Interval mortality was significantly lower for oysters grown subtidally compared to those grown intertidally ($p<0.01$). A significant, inverse relationship was also found between interval mortality and DO ($p<0.01$).

Cumulative Oyster Mortality

Based on the graph of the cumulative oyster mortality data from 2018, cumulative mortality remained <0.15, or 15%, throughout the sampling season at all sites and placement locations other than the Ware River intertidal (**Fig. 18**). At the mid-July sampling time preceding the rapid drop in salinity in the Ware River beginning on 7/25/18 (**Fig. 15**), cumulative mortality was significantly higher for oysters grown intertidally at the Ware River site, relative to the other

placement locations at the Ware and other sites. Cumulative mortality continued to be highest at this location throughout the rest of the sampling season, reaching 0.26, or 26%, at the end of the sampling season.

Model selection for 2018 cumulative mortality data favored the generalized linear model containing site (Perrin River, York River, Big Island, and Ware River), placement location (intertidal and subtidal), temperature, salinity, pH, and DO (**Table 7**). Based on this model, cumulative oyster mortality was significantly lower at the Big Island site ($p<0.01$), the York River site ($p<0.001$), and the Perrin River site ($p<0.001$), compared to the Ware River site, the reference location (**Table 8**). Cumulative mortality was significantly lower for oysters grown subtidally compared to those grown intertidally ($p<0.001$). A significant, inverse relationship was also found between cumulative mortality and temperature ($p<0.05$).

Shell Height

Based on the graph of the oyster shell height data from 2018, floating cage oysters were significantly larger than oysters at the other placement locations and sites beginning in mid-August and continuing throughout the majority of the sampling season (**Fig. 19**).

Model selection for 2018 shell height data favored the generalized linear model containing site (Perrin River, York River, Big Island, and Ware River), placement location (intertidal and subtidal), temperature, salinity, pH, and DO (**Table 7**). Based on this model, oyster shell height was significantly smaller at the York River site, compared to the Ware River site, the reference location ($p<0.05$) (**Table 8**). A significant, inverse relationship was also found between shell height and both temperature ($p<0.001$) and DO ($p<0.001$).

Oyster Growth Rate

Few patterns are apparent in the graph of oyster growth rate data from 2018 (**Fig. 20**). However, in early August, floating cage oysters grew significantly faster than oysters deployed at all other placement locations and sites, except for the York River subtidal.

Model selection for 2018 growth rate data favored the generalized linear model containing site (Perrin River, York River, Big Island, and Ware River), placement location (intertidal and subtidal), temperature, salinity, pH, and DO (**Table 7**). However, based on the p-values, none of the independent variables were significantly related to oyster growth rate (**Table 8**).

Oyster Condition Index

Based on the graph of oyster CI data from 2018, CI was significantly higher for oysters grown intertidally at the York River site, the high-energy HAB-endemic location, at the late August sampling point (**Fig. 21**).

As stated in the Methods, CI data from 2018 were not modeled due to low sample size.

Oyster Histopathology

Based on histology data, oysters did not show considerable adverse health impacts in 2018, and as such, these data were not graphed or modeled. Of the oysters collected throughout the summer of 2018 (n=81), 1.2% displayed notable gill erosion, and 4.9% exhibited hemocytosis in the gills or mantle. In terms of pathogens, 2.5% of oysters contained an unidentified microsporidian species in the gut epithelium. No *H. nelsoni* or *P. marinus* infections

were identified, and no other significant pathology or pathogens were observed in oysters collected in 2018.

DISCUSSION

Reports of HABs and their impacts are expanding globally (Hallegraeff 1993, 2010; Glibert et al. 2014), including in the Chesapeake Bay (Li et al. 2015). *Margalefidinium polykrikoides* and *Alexandrium monilatum* form sequential blooms most summers in the lower Chesapeake Bay, and both species are generally increasing in terms of bloom density, distribution, and duration in the region (Marshall et al. 2005; Marshall et al. 2008; Marshall & Egerton 2009, 2013; Dauer et al. 2010; Scott & Reece 2018). Both species have been associated with mortality and pathology in finfish and shellfish, including oysters, in laboratory settings (Gobler et al. 2008, Harding et al. 2009, May et al. 2010, Pease 2016, Reece et al. 2016), and several studies suggest that blooms of *M. polykrikoides* and *A. monilatum* may be associated with adverse impacts to shellfish cultured on the east coast of the U.S. (Pease 2016, 2016 NOAA Event Response study by Reece et al., unpublished data; Griffith et al. 2018). However, the potential impacts of sequential blooms of *M. polykrikoides* and *A. monilatum* to shellfish in the lower Chesapeake Bay are not well understood, particularly in the context of the oyster aquaculture industry.

The two main objectives of this study were to 1) investigate *M. polykrikoides* and *A. monilatum* as a potential threat to cultured oysters in the lower Chesapeake Bay, and 2) inform mitigation strategies to minimize HAB impacts based on current grow-out methods used by local oyster culturists. To address the first objective, oysters were grown at HAB-endemic sites characterized by high and low energies in 2017 in the York and the Perrin Rivers, respectively. In 2018, the intermediate-energy HAB-endemic site near Big Island was added. In both years, the intermediate-energy site in the Ware River was used as a reference; the HABs that were the

focus of this study are not typically observed at that site in the Ware River. Oysters were grown both intertidally and subtidally at all sites in summers 2017 and 2018 and were also grown in cages floating just below the surface at the Big Island site in 2018. Water quality parameters were monitored, including cell concentrations of *M. polykrikoides*, *A. monilatum*, and two other local HAB species known to negatively impact oysters, *Karlodinium veneficum* and *Prorocentrum minimum*, along with oyster health and survival.

Blooms of *M. polykrikoides* and *A. monilatum* were only detected in 2017, and then only at the HAB-endemic sites. *Margalefidinium polykrikoides* was not detected at bloom levels (i.e. <500 cells mL^{-1}) at the low-energy site in the Perrin River, and a bloom concentration of *A. monilatum* (i.e. 3,425 cells mL^{-1}) was detected on only one day. Higher cell concentrations were observed at the high-energy site in the York River with a maximum *M. polykrikoides* concentration of 16,842 cells mL^{-1} and a maximum *A. monilatum* concentration of 92,529 cells mL^{-1}. A bloom concentration of *M. polykrikoides* was detected on only one day at the York River site, whereas *A. monilatum* cell concentrations were above bloom levels for approximately two weeks. However, with the patchiness of blooms and intermittent water sampling that may have missed some bloom peaks, it is challenging to determine how long during those two weeks oysters were actually exposed to HAB cells. It was not possible to use the Chl *a* data collected near-continuously at all sites to approximate the timing of the blooms, as no correlation was found between these data and concentrations of either *M. polykrikoides* or *A. monilatum*.

The lack of correlation between Chl *a* and either *M. polykrikoides* or *A. monilatum* may have been related to limited water sampling during blooms and/or the biology of the HAB species. Compared to the Chl *a* data, which was collected every 15 min at all sites, water samples

were never collected more than once a week in 2017. This relatively small number of water samples containing non-zero HAB cell concentrations provided limited data with which to accurately characterize a potential relationship with Chl *a*. Another potential reason for the lack of correlation is the mode of nutrient acquisition utilized by the algal cells at different times. Many dinoflagellate species are mixotrophic (Jeong et al. 2004, Burkholder et al. 2008, Anderson et al. 2012), and at times when algal cells are relying more on heterotrophy, Chl *a* may be a less reliable proxy for cell density.

Based on modeling of the 2017 data, oyster health and survival were impacted more by factors not directly related to HABs, specifically location factors (site and placement location), temperature, and DO. Overall mortality was never high (interval mortality <4% and cumulative mortality <12%) compared to mortality levels that are often observed in association with other oyster stressors, such as the oyster parasite *P. marinus*, which was reported in a study by Ford & Smolowitz (2007) to be associated with 60-80% mortality of field animals. These results are similar to those found by Griffith et al. (2018), when two size classes of cultured diploid oysters (approximately 5 and 32 mm) were exposed to a 1-2 week bloom of *M. polykrikoides* $>1.5\times10^4$ cells mL^{-1} in eastern Long Island, NY. In contrast to first-year scallops (approximately 6 mm), neither size class of oysters experienced a significant increase in mortality following exposure to the bloom.

Although overall oyster mortality levels were not high in 2017, the relative differences between the different sites and treatments are still informative. Cumulative mortality was significantly higher for oysters grown intertidally. Intertidal oysters may experience stress related to fluctuating environmental conditions, including intermittent aerial exposure, limited feeding times, and high summer temperatures (Roegner & Mann 1995, Bishop & Peterson 2006). It is

unknown whether the physiological stress related to intertidal planting may be further compounded during HAB-intensive years.

Impacts of *M. polykrikoides* and *A. monilatum* on oysters may differ based on the cell concentrations of the blooms in different years. Cell concentration data collected by the Reece Lab at VIMS in the lower Chesapeake Bay in previous years allows maximum cell concentrations and bloom dates to be compared between years; these data are documented in annual reports submitted to VDH from 2007-2017 and deposited in the CDC HAB Database. The findings in this thesis indicate that *M. polykrikoides* and *A. monilatum* had minimal adverse impacts on experimental oysters in 2017. However, *M. polykrikoides* and *A. monilatum* concentrations never exceeded 431 cells mL^{-1} and 3,425 cells mL^{-1}, respectively, at the Perrin River site, in water samples collected for this study. In 2015, when VIMS scientists received an anecdotal report of >50% mortality of intertidal oysters at the Perrin River site, the maximum concentration of *A. monilatum* detected in a water sample at that site was 25,006 cells mL^{-1}, and a water sample collected at the mouth of the Perrin River contained 75,600 *A. monilatum* cells mL^{-1}. No bloom of *M. polykrikoides* was detected in the Perrin River in 2015. In 2016, when the NOAA-funded Event Response study found slightly elevated mortality of intertidal oysters (13.6%) grown at the Perrin River site compared to other depths and sites (2016 NOAA Event Response study by Reece et al., unpublished data), no *M. polykrikoides* bloom was detected. However, the maximum *A. monilatum* concentration measured at that site in 2016 was 7,772 cells mL^{-1}, over twice as high as the maximum concentration detected in 2017. In 2017, the maximum concentrations of *M. polykrikoides* and *A. monilatum* detected at the York River site were 16,842 cells mL^{-1} and 92,529 cells mL^{-1}, respectively. In 2015, the maximum *M. polykrikoides* concentration detected in the York River was 22,600 cells mL^{-1}, and the maximum

concentration of *A. monilatum* detected was 220,100 cells mL^{-1}. When interpreting the biological impacts of *M. polykrikoides* and *A. monilatum* on oyster health, it is important to consider the cell concentrations of the two species, as well as the bloom durations and locations. It is possible, but unknown whether, the minimal oyster health impacts seen in 2017 were related to lower bloom concentrations.

Characterizing the toxic impacts of HABs to oysters can be more challenging in the field compared to in controlled laboratory experiments. In laboratory bioassays, oysters can be exposed to specific cell concentrations for specific time periods. In contrast, natural blooms tend to be patchy and fluctuate in terms of cell density. This may be especially true in high-energy systems, such as the York River, where fast-flowing water can contribute to the dispersal of algal cells, reducing oyster exposure to HAB species. Blooms may occur at one location for hours, days, or weeks, making high-frequency monitoring of cell concentrations challenging. Previous research also suggests both *M. polykrikoides* and *A. monilatum* vertically migrate in the water column (Park et al. 2001, Pease 2016, Griffith et al. 2018), which could impact the time oysters deployed at the surface and at depth are exposed to HAB cells. Oyster feeding behavior is another important consideration when evaluating HAB impacts. Previous laboratory studies have reported feeding inhibition of oysters in the presence of toxigenic algal species (Hégaret et al. 2007), including *A. monilatum* (May et al. 2010). Feeding inhibition could induce respiratory and oxidative stress; however, it could also reduce oyster exposure to toxins produced by HABs. Future field studies might collect oyster samples for the quantification of GDA, the toxin produced by *A. monilatum*, to help characterize oyster exposure to *A. monilatum* and its toxin.

It is possible there is a time lag between the occurrence of HABs and the observation of toxic impacts in oysters. In this study, measurements of the oyster dependent variables (e.g.

mortality, growth rate, and CI) were modeled with water quality variables (e.g. temperature, salinity, and HAB cell concentrations) collected at the time of oyster sampling. Thus, the models evaluated the relationship between oyster health and survival and concurrent measures of water quality. This method of modeling might fail to capture delayed expression of adverse health impacts of HABs to oysters. For instance, modeling of the 2017 data indicated that growth rate was higher at higher concentrations of *M. polykrikoides*. However, the graphs of growth rate data show a significant decrease in oyster growth rate at the York River site in early August 2017, following the peak concentration of *M. polykrikoides* (16,842 cells mL^{-1} on 7/27/17). Griffith et al. (2018) found that cultured first-year oysters (diploid; approximately 5 mm) that survived a 1-2 week bloom of *M. polykrikoides* of $>1.5\times10^4$ cells mL^{-1} exhibited significantly slower growth rates following the bloom. However, second-year oysters (diploid; approximately 32 mm) did not display reductions in growth. Future modeling efforts might explore the possibility of delayed impacts to triploid juvenile oysters following sequential exposure to both *M. polykrikoides* and A. *monilatum* by building in a lag between measures of water quality and those of oyster health and survival.

The conclusions related to 2017 data may be somewhat limited given the relatively low number of water samples collected during the blooms. For example, in this study, the 2017 oyster interval mortality data set is comprised of 160 observations; each observation represents the average interval mortality calculated for the three bags at a particular placement location at a particular site at a particular time. HAB concentration data were collected for each of these oyster observations. However, of the 160 water samples collected, only 58 samples (~36%) contained a non-zero concentration of *A. monilatum*, and only eight samples (5%) contained a bloom concentration of *A. monilatum*. The ratio of the number of bloom concentrations of both

M. polykrikoides and *A. monilatum* to the total number of observations is similar for the rest of the data sets, including cumulative oyster mortality, shell height, growth rate, and CI. These may be insufficient data with which to accurately characterize a relationship between two variables – i.e. blooms of *M. polykrikoides* and *A. monilatum* and metrics of oyster health.

In 2018, blooms of neither *M. polykrikoides* nor *A. monilatum* were detected at any of the four sites, providing the opportunity to assess oyster health and survival during both a bloom and a non-bloom year. Heavy rainfall during summer 2018 resulted in high water flow in the York River region with retention times often less than 2 days (M. Brush, VIMS, pers. comm.). Salinity in summer 2018 was significantly lower (± 2 SD) than the long-term annual cycle, based on almost 30 years of water quality data (CBNERRS and Chesapeake Bay Program data analyzed by Brush). These environmental conditions likely did not favor bloom formation for *M. polykrikoides* and *A. monilatum*. These species typically bloom at higher salinities (i.e. >18-20) than those observed in the York River Region in 2018 (Kim et al. 2004, Juhl 2005). In addition, flushing rates may have exceeded the doubling times of the species, which is reported for *Alexandrium* species to be generally >48 hr (Juhl 2005, Brosnahan et al. 2015), inhibiting cells from reaching high enough concentrations to form blooms (Roelke & Pierce 2011).

The results of the 2018 oyster data evaluations were similar to those of 2017. Based on modeling of 2018 data, oyster health and survival were most impacted by location factors (site and placement location), temperature, and DO. Just as in 2017, overall interval mortality was low (<12%) in 2018, especially when compared to typical mortality associated with other oyster stressors, such as the oyster parasite *P. marinus*. However, the relative differences between the different sites and treatments provide valuable information. As in 2017, oyster mortality was lower at the subtidal planting location compared to the intertidal planting location, suggesting

that intertidal planting may have incurred additional stress to oysters in 2018, in the absence of the two HABs of interest. Both interval and cumulative mortality were highest for intertidal oysters at the Ware River site in July 2018, compared to subtidal Ware River oysters and those at other depths and sites. Interval mortality at the Ware River intertidal peaked in Mid-July at just under 12%. Cumulative mortality at the Ware intertidal was significantly higher than that in other placement locations and sites beginning in Mid-July. This trend continued throughout the rest of the sampling season, and by the final sampling point in early October, cumulative mortality was >25%.

The reason for the relatively higher oyster mortality in the Ware River intertidal is unknown, although it may have been related to salinity and/or HAB species other than *M. polykrikoides* and *A. monilatum*. Salinity alone can strongly influence oyster physiology; adult oysters are typically found in salinities between 10-30, but can tolerate salinities ranging from 0-42 for limited periods of time (Gunter 1955). Physiologically, oysters function best at salinities from 15-18 and grow most efficiently at salinities from 12-28 (Newell 1985). The minimum salinity (7.2) at the 2017 sites was observed in the Ware River site compared to the other three sites (minima ranging from 9.1-11.8). Although these values fall within the range oysters can tolerate, research indicates rapid changes in salinity can cause significant effects (Hand & Stickle 1977), and the adverse impacts of low salinity may be compounded by high temperatures (La Peyre et al. 2013). A rapid decrease in salinity occurred in the Ware River in 2018, dropping from >15 to <8 in one day (**Fig. 15**). However, this sharp drop began on 7/25/18, following the mid-July increase in oyster mortality. High-frequency water quality sampling (temperature, salinity, pH, DO) next to the subtidal cage did not detect harmful water quality conditions concurrent with the start of this mortality. However, a small spike in Chl *a* occurred in early July

(**Fig. 16D**), which could indicate higher levels of phytoplankton cells. Water sampling did not detect high concentrations of the other two HAB species, *K. veneficum* and *P. minimum*, quantified using qPCR; however, it is possible that water sampling failed to capture a spike in one of these two species, both of which can be harmful to shellfish (Luckenbach et al. 1993, Stoecker et al. 2008). It is possible HAB exposure or another unknown stressor may have initiated a mortality event, and that the rapid decrease in salinity later in July may have contributed to continued oyster mortality at the reference site in 2018; however, the actual cause of the high intertidal mortality at the Ware River site is unknown.

In contrast to previous research, modeling of the 2017 and 2018 data did not indicate a significant relationship between oyster growth rate and placement location (intertidal vs. subtidal). Multiple studies have reported higher growth rates in subtidal oysters compared to intertidal oysters (Loosanoff 1932; Ingle & Dawson, Jr. 1952; Burrell, Jr. 1982; Roegner & Mann 1995; Bartol et al. 1999). The difference in growth observed in some studies may be associated with the longer feeding times of subtidal oysters compared to intertidal oysters, which spend part of each tidal cycle out of the water (Crosby et al. 1991). In addition, rapidly cycling DO, such as that experienced by intertidal animals, has been shown to temporarily retard the growth of juvenile oysters (Keppel et al. 2016). The growth of oysters may be negatively impacted by exposure to high temperatures (>30°C) (Rybovich et al. 2016), such as those experienced by oysters grown intertidally in the Chesapeake Bay in the summer. In accordance with these findings, modeling of the 2017 data indicated a significant relationship between oyster growth rate and both DO ($p<0.05$) and temperature ($p<0.01$). However, no significant relationships were found between 2018 oyster growth rates and any of the water quality parameters evaluated.

The second objective of this study was to make recommendations of culture strategies that minimize HAB impacts and maximize oyster production. The results of this study suggest neither *M. polykrikoides* nor *A. monilatum* had strong impacts on oyster health and survival in 2017; however, location factors (site and placement location) were significantly associated with metrics of oyster health and survival in both 2017 and 2018. For instance, mortality was significantly lower for oysters grown subtidally compared to those grown intertidally in both summers ($p<0.05$). Based on these findings, intertidal deployment may be more stressful to oysters in the summer. Thus, subtidal placement might be beneficial to oysters cultured during stressful environmental conditions. Recommendations cannot be made regarding oyster size class with respect to HABs, as oysters were all similar sizes at the time of bloom onset in 2017. In addition, recommendations cannot be made about bottom vs. surface deployment with regard to HAB impacts, as blooms did not occur the year surface cages were included.

More than one season of bloom data is likely necessary to characterize the relationship between cultured oysters and the HAB species *M. polykrikoides* and *A. monilatum*. Increasing the frequency of water sampling during the time of blooms would be beneficial in future studies. Higher-frequency HAB concentration data would help characterize the progression of the blooms and the length of time oysters were actually exposed to blooms. This may be particularly important at high-energy sites, such as the York River location, where the fast-flowing water promotes bloom dispersal and patchiness. From a statistical perspective, having larger sample sizes also increases the precision of parameter estimates, reduces the standard errors, and increases the likelihood of detecting a statistically significant relationship, if such a relationship exists. Thus, higher-frequency water sampling would provide more data to inform the potential relationship between the HAB species and oyster metrics of health and survival. Future studies

might also include a short-term vertical migration study of *M. polykrikoides* and *A. monilatum*, considering both species are reported to vertically migrate (Park et al. 2001, Pease 2016, Griffith et al. 2018). These data would also inform the amount of time oysters at different placement locations are exposed to *M. polykrikoides* and *A. monilatum*.

More replication in terms of placement locations and study sites would likely be informative in future studies. For instance, studies might incorporate a floating cage treatment, in addition to bottom cages, at multiple sites to evaluate the potential relationship between oysters cultured at this placement location and exposure to *M. polykrikoides* and *A. monilatum*. This project attempted to investigate the impacts of *M. polykrikoides* and *A. monilatum* at sites with and without blooms of the two species, as well as at sites with a range of energetics. In 2017, the three study sites included the Perrin River at a low-energy HAB-endemic location, the York River at high-energy HAB-endemic location, and the Ware River at an intermediate-energy location where blooms of *M. polykrikoides* and *A. monilatum* had not been reported. Although the Ware River site provided a valuable reference in terms of HAB presence/absence, future studies might incorporate both a low- and a high-energy reference site to allow the HAB variable to be isolated from the water energy variable.

In addition to exploring the potential for a lag time between HAB occurrence and oyster impacts via modeling, future studies might also monitor oyster metrics likely to respond more quickly to fluctuating HAB concentrations. For instance, oysters could be collected regularly for the quantification of GDA, the toxin produced by *A. monilatum*. Quantifying GDA would inform whether oysters bioaccumulate GDA, which is currently not well understood. Quantifying the toxin in oyster tissues would also give some indication of whether the oyster is actually feeding on the HAB cells. Considering that previous studies have reported feeding inhibition in the

presence of toxigenic algal species (Hégaret et al. 2007), including *A. monilatum* (May et al. 2010), it is important to know not only how long oysters were exposed to HAB cells, but also whether the animals actually fed on the cells. Feeding inhibition may be particularly problematic for younger, smaller oysters as they likely have smaller energy reserves. Future studies might evaluate the impacts of *M. polykrikoides* and *A. monilatum* on smaller oysters by deploying spat oysters (~5 mm) at field sites immediately prior to blooms.

Results of this study provide valuable information about the factors that influence the health and survival of oysters cultured using different methods during a summer when *M. polykrikoides* and *A. monilatum* blooms occurred, as well as a summer when blooms did not occur. Based on 2017 and 2018 data, this study suggests that factors not directly related to HABs, including site, placement location, and other water quality parameters, were more significantly related to oyster health and survival. However, more than one year of bloom data is likely necessary to fully evaluate the impacts of *M. polykrikoides* and *A. monilatum* as potential stressors to the oyster aquaculture industry, particularly in light of the fact that blooms of both species are generally expanding in the Chesapeake Bay (Marshall et al. 2008; Marshall & Egerton 2009, 2013; Dauer et al. 2010), and the distribution and severity of HABs are expected to increase with climate change (Hallegraeff 2010). In addition, the increasing temperatures, increasing ocean acidity, and other factors associated with climate change may increase oyster stress and increase their susceptibility to additional stressors, such as HABs. For all of these reasons, it is necessary to continue gathering information on the impacts of *M. polykrikoides* and *A. monilatum* to the oyster aquaculture industry.

REFERENCES

Abe, M., Inoue, D., Matsunaga, K., Ohizumi, Y., Ueda, H., Asano, T., Murakami, M. & Y. Sato. 2002. Goniodomin A, an antifungal polyether macrolide, exhibits antiangiogenic activities via inhibition of actin reorganization in endothelial cells. J. Cell. Physiol. 190:109-116.

Akaike, H. 1973. Information Theory and an Extension of the Maximum Likelihood Principle. In: Proceedings of the 2nd International Symposium on Information Theory. B. N. Petrov, & F. Csaki (Eds.). Budapest. pp. 267-281.

Aldrich, D. V., Ray, S. M. & W. B. Wilson. 1967. *Gonyaulax monilata*: population growth and development of toxicity in cultures. J. Protozoo. 14:636-639.

Anderson, D. M, Taylor, C. D., & E. V. Armbrust. 1987. The effects of darkness and anaerobiosis on dinoflagellate cyst germination. Limnol. Oceanogr. 32(2):340-351.

Anderson, D. M., Stock, C. A., Keafer, B. A., Nelson, A. B., Thompson, B., McGillicuddy, Jr., D. J., Keller, M., Matrai, P. A. & J. Martin. 2005. *Alexandrium fundyense* cyst dynamics in the Gulf of Maine. Deep-Sea Res. Pt II. 52:2522-2542.

Anderson, D. M., Alpermann, T. J., Cembella, A., Collos, Y., Masseret, E. & M. Montresor. 2012. The globally distributed genus *Alexandrium*: Multifaceted roles in marine ecosystems and impacts on human health. Harmful Algae. 14:10-35.

Backer, L. C. & D. J. McGillicuddy, Jr. 2006. Harmful algal blooms: at the interface between coastal oceanography and human health. Oceanography. 19(2):94-106.

Baird, D. & R. Ulanowicz. 1989. The seasonal dynamics of the Chesapeake Bay ecosystem. Ecol. Monogr. 59(4):329-364.

Balech, E. 1985. The genus *Alexandrium* or *Gonyaulax* of the Tamarensis group. In: Proceedings of the Third International Conference on Toxic Dinoflagellates. St. Andrews, New Brunswick, Canada. June 8-12, 1985. pp. 33-38.

Bartol, I. K., Mann, R. & M. Luckenbach. 1999. Growth and mortality of oysters (*Crassostrea virginica*) on constructed intertidal reefs: effects of tidal height and substrate level. J. Exp. Mar. Biol. Ecol. 237:157-184.

Bass, E. L. & B. W. Kuvshinoff. 1983. Evidence for a neuroactive component in the toxic extract from *Gonyaulax monilata*. Comp. Biochem. Physiol. 75C:131-134.

Bass, E. L., Pinion, J. P., & M. E. Sharif. 1983. Characteristics of a hemolysin from *Gonyaulax monilata* Howell. Aquat. Toxicol. 3:15-22.

Beck, M. W. et al. 2011. Oyster reefs at risk and recommendations for conservation, restoration, and management. Bioscience. 61:108-116.

Bishop, M. J. & C. H. Peterson. 2006. Direct effects of physical stress can be counteracted by indirect benefits: oyster growth on a tidal elevation gradient. Oecologia. 147(3):426-433.

Bricelj, V. M., Lee, J. H., Cembella, A. D. & D. M. Anderson. 1990. Uptake kinetics of paralytic shellfish toxins from the dinoflagellate *Alexandrium fundyense* in the mussel *Mytilus edulis*. Mar. Ecol. Prog. Ser. 63:177-188.

Brosnahan, M. L., Velo-Suárez, L. , Ralston, D. K., Fox, S. E., Sehein, T. R., Shalapyonok, A., Sosik, H. M., Olson, R. J. & D. M. Anderson. 2015. Rapid growth and concerted sexual transitions by a bloom of the harmful dinoflagellate *Alexandrium fundyense* (Dinophyceae). Limnol. Oceanogr. 60:2059-2078.

Burkholder, J. M., Glibert, P. M. & H. M. Skelton. 2008. Mixotrophy, a major mode of nutrition for harmful algal species in eutrophic waters, Harmful Algae. 8(1):77-93.

Burrell, Jr., V. G. 1982. Overview of the South Atlantic oyster industry. J. World Maricult. Soc. 1:125-127.

Burreson, E. M. & J. D. Andrews. 1988. Unusual intensification of Chesapeake Bay oyster diseases during recent drought conditions. Presented at OCEANS ’88: ‘A Partnership of Marine Interests.’ Baltimore, MD: IEEE. 799-802.

Carnegie, R. B. & E. M. Burreson. 2011. Declining impact of an introduced pathogen: *Haplosoridium nelsoni* in the oyster *Crassostrea virginica* in Chesapeake Bay. Mar. Ecol. Prog. Ser. 432:1-15.

Clemons, G. P., Pham, D. V. & J. P. Pinion. 1980. Insecticidal activity of *Gonyaulax* (Dinophyceae) cell powders and saxitoxin to the German cockroach. J. Phycol. 16:305-307.

Connell, C. & J. Cross. 1950. Mass mortality of fish associated with the protozoan *Gonyaulax* in the Gulf of Mexico. Science. 112:359-363.

Crosby, M. P., Roberts, C. F. & P. D. Kenny. 1991. Effects of immersion time and tidal position on in situ growth rates of naturally settled eastern oysters, *Crassostrea virginica* (Gmelin, 1791). J. of Shellfish Res. 10(1):95-103.

Dame, R. F. & S. Libes. 1993. Oyster reefs and nutrient retention in tidal creeks. J. Exp. Mar. Biol. Ecol. 17:251-258.

Dauer, D. M., Marshall, H. G., Donat, J. R., Lane, M. F., Doughten, S. C., Hoffman, F. A. & R. Kurada. 2010. Current status and long-term trends in water quality and living resources in

the Virginia tributaries and Chesapeake Bay mainstem from 1985 through 2009. Final report submitted to Chesapeake Bay Program.

Erker, E. F., Slaughter, L. J., Bass, E. L., Pinion, J. P. & J. Wutoh. 1985. Acute toxic effects in mice of an extract from the marine algae *Gonyaulax monilata*. Toxicon. 23(5):761-767.

Espiña, B., Cagide, E., Louzao, M. C., Vilariño, N., Vieytes, M. R., Takeda, Y., Sasaki, M. & L. M. Botana. 2016. Cytotoxicity of goniodomin A and B in non contractile cells. Toxicol. Lett. 250-251:10-20.

Ford, S. E., & R. Smolowitz. 2007. Infection dynamics of an oyster parasite in its newly expanded range. Mar Biol. 151:119-133.

Furukawa, K., Sakai, K., Watanabe, S., Maruyama, K., Murakami, M., Yamaguchi, K. & Y. Ohizumi. 1993. Goniodomin A induces modulation of actomyosin ATPase activity mediated through conformational change of actin. J. Biol. Chem. 268:26026-26031.

Gainey, L. F., Jr. & S. E. Shumway. 1988. A compendium of the responses of bivalve molluscs to toxic dinoflagellates. J. Shellfish Res. 7(4):623-628.

Gates, J. A. & W. B. Wilson. 1960. The toxicity of *Gonyaulax monilata* Howell to *Mugil cephalus*. Limnol. Oceanogr. 5:171-174.

Glibert, P. M, Icarus Allen, J., Artioli, Y., Beusen, A., Bouwman, L., Harle, J., Holmes, R. & J. Holt. 2014. Vulnerability of coastal ecosystems to changes in harmful algal bloom distribution in response to climate change: projections based on model analysis. Global Change Biol. 20:3845-3858.

Gobler, C. J., Berry, D. L., Anderson, O. R., Burson, A., Koch, F., Rodgers, B. S., Moore, L. K., Goleski, J. A., Allam B., Bowser, P., Tang, Y. & R. Nuzzi. 2008. Characterization, dynamics, and ecological impacts of harmful *Cochlodinium polykrikoides* blooms on eastern Long Island, NY, USA. Harmful Algae. 7:293-307.

Griffith, A., Shumway, S. & C. Gobler. 2018. Differential mortality of North Atlantic bivalve molluscs during harmful algal blooms caused by the dinoflagellate, *Margalefidinium polykrikoides*. Estuaries Coasts. 42(1):190-203.

Gunter, G. 1955. Mortality of oysters and abundance of certain associates as related to salinity. Ecology. 36:601-605.

Hallegraeff, G. M. 1993. A review of harmful algal blooms and their apparent global increase. Phycologia. 32:79-99.

Hallegraeff, G. M. 2010. Ocean climate change, phytoplankton community responses, and harmful algal blooms: a formidable predictive challenge. J. Phycol. 46:220-235.

Halstead, B. W. & E. J. Shantz. 1984. Paralytic shellfish poisoning. World Health Organ. Offset Publication. 79:1-59.

Hand, S. C. & W. B. Stickle. 1977. Effects of tidal fluctuations of salinity on pericardial fluid composition of the American oyster, *Crassostrea virginica*. Mar. Biol. 42:259-272.

Handy, S. M., Demir, E., Hutchins, D. A., Portune, K. J., Whereat, E. B., Hare, C. E., Rose, J. M., Warner, M., Farestad, M., Cary, S. C. & K. J. Coyne. 2008. Using quantitative real-time PCR to study competition and community dynamics among Delaware Inland Bays harmful algae in field and laboratory studies. Harmful Algae. 7:599-613.

Hardaway, C. S., Thomas, G. R., Zacherle, A. W. & B. K. Fowler. 1984. Vegetative Erosion Control Project: Final Report. Prepared for Virginia Division of Soil and Water, Technical Report, Virginia Institute of Marine Science, Gloucester Point, VA, 275 pp., Appendices.

Harding, J. M., Mann, R., Moeller, P. & M. S. Hsia. 2009. Mortality of the veined rapa whelk, *Rapana venosa*, in relation to a bloom of *Alexandrium monilatum* in the York River, United States. J. Shellfish Res. 28(2):363-367.

Harris, C. M., Reece, K. S., Stec, D. F., Scott, G. P., Jones, W. M., Hobbs, P. L. & T. M. Harris. In review. Goniodomin in the Caribbean: Structural analysis of an algal toxin from an ancient bloom. Harmful Algae.

Haven, D. S. & R. Morales-Alamo. 1970. Filtration of particles from suspension by the American oyster *Crassostrea virginica*. The University of Chicago Press in association with the Marine Biological Laboratory. Biol. Bull. 139(2):248-264.

Hégaret, H., Wikfors, G. H. & S. E. Shumway. 2007. Diverse feeding responses of five species of bivalve mollusc when exposed to three species of harmful algae. J. Shellfish Res. 26:549-559.

Herman, J., Shen, J. & J. Huang. 2007. Tidal flushing characteristics in Virginia's Tidal Embayments. Final report submitted to Virginia Coastal Zone Management Program and Virginia Department of Environmental Quality.

Howell, J. F. 1953. *Gonyaulax monilata*, sp. nov., the causative dinoflagellate of a red tide on the East coast of Florida in August-September, 1951. Trans. Am. Microsc. Soc. 72:153-156.

Hsia, M. H., Morton, S. L., Smith, L. L., Beauchesne, K. R., Huncik, K. M. & P. D. R. Moeller. 2006. Production of goniodomin A by the planktonic, chain-forming dinoflagellate *Alexandrium monilatum* (Howell) Balech isolated from the Gulf Coast of the United States. Harmful Algae. 5:290-299.

Hudson, K. 2018. Virginia shellfish aquaculture situation and outlook report: Results of the 2017 Virginia shellfish aquaculture crop reporting survey. VIMS marine resource report, no.

2018-9. Virginia Sea Grant Marine Extension Program, Virginia Institute of Marine Science.

Hudson, K. & T. J. Murray. 2016. Virginia shellfish aquaculture situation and outlook report: results of the 2015 Virginia shellfish aquaculture crop reporting survey. VIMS marine resource report, no. 2016-4. Virginia Sea Grant Marine Extension Program, Virginia Institute of Marine Science.

Ingle, R. M. & C. E. Dawson, Jr. 1952. Growth of the American oyster *Crassostrea virginica* (Gmelin) in Florida waters. Bulletin of Marine Science of the Gulf and Caribbean. 2:393-404.

Jeong, H. J., Du Yoo, Y., Kim, J. S., Hoon Kim, T., Kim, J. H., Seon Kang, N. & W. Yih. 2004. Mixotrophy in the phototrophic harmful alga *Cochlodinium polykrikoides* (Dinophycean): Prey species, the effects of prey concentration, and grazing impact. J. Eukaryot. Microbiol. 51:563-569.

Juhl, A. R. 2005. Growth rates and elemental composition of Alexandrium monilatum, a red-tide dinoflagellate. Harmful Algae. 4(2):287-295.

Keafer, B. A., Buesseler, K. O. & D. M. Anderson. 1992. Burial of living dinoflagellate cysts in estuarine and nearshore sediments. Mar. Micropaleontol. 20:147-161.

Keppel, A. G., Breitburg, D. L. & R. B. Burrell. 2016. Effects of co-varying diel-hypoxia and pH on growth in the juvenile Eastern oyster, *Crassostrea virginica*. PLoS ONE. 11(8):e0161088.

Kim, D., Matsuyama, Y., Nagasoe, S., Yamaguchi, M., Yoon, Y., Oshima, Y., Imada, N. & T. Honjo. 2004. Effects of temperature, salinity and irradiance on the growth of the harmful red tide dinoflagellate *Cochlodinium polykrikoides* Margalef (Dinophyceae). J. Plankton Res. 26(1):61-66.

Krock, B., Tillmann, U., Wen, Y., Hansen, P. J., Larsen, T. O. & A. J. C. Andersen. 2018. Development of a LC-MS/MS method for the quantification of goniodomins A and B and its application to *Alexandrium pseudogonyaulax* strains and plankton field samples of Danish coastal waters. Toxicon. 155:51-60.

Kudela, R. & C. J. Gobler. 2012. Harmful dinoflagellate blooms caused by *Cochlodinium* sp.: global expansion and ecological strategies facilitating bloom formation. Harmful Algae. 14:71-86.

La Peyre, M. K., Eberline, B. S., Soniat, T. M. & J. F. La Peyre. 2013. Differences in extreme low salinity timing and duration differentially affect eastern oyster (*Crassostrea virginica*) size class growth and mortality in Breton Sound, LA. Estuar. Coast Shelf Sci. 135:146e157.

Landsberg, J. H. 2002. The effects of harmful algal blooms on aquatic organisms. Rev. Fish. Sci. 10:113-390.

Li, J., Glibert, P. M. & G. Yonghui. 2015. Temporal and spatial changes in Chesapeake Bay water quality and relationships to *Prorocentrum minimum*, *Karlodinium veneficum*, and CyanoHAB events, 1991-2008. Harmful Algae. 42:1-14.

Loosanoff, V. L. 1932. Observations on propagation of oysters in James and Corrotoman Rivers and the seaside of Virginia. Virginia Commission of Fisheries. 46.

Lorenzen, C. 1967. Determination of chlorophyll and phaeopigments: spectrophotometric equations. Limnol. Oceanogr. 12:343-346.

Lubkin, S., Ross, K. & K. S. Reece. 2017. Detecting harmful algal blooms in the Chesapeake Bay using Sentinel-2 Earth observations. Oral Presentation, 9th US Symposium on Harmful Algae, Nov. 11-17, 2017, Baltimore, MD.

Luckenbach, M. W., Sellner, K. G., Shumway, S. E. & K. Greene. 1993. Effects of two bloom forming dinoflagellates, *Prorcentrum minimum* and *Gyrodinium uncatenum*, on the growth and survival of the Eastern oyster, *Crassostrea virginica* (GMELIN 1791). J. Shellfish. Res. 12:411-415.

Mackenzie, C. L. 2007. Causes underlying the historical decline in Eastern oyster (*Crassostrea virginica* Gmelin, 1791) landings. J. Shellfish Res. 26(4):927-938.

MacKiernan, G. (1968) Thesis: Seasonal distribution of dinoflagellates in the lower York River, Virginia. College of William & Mary. 104 pp.

Marshall, H. G., Egerton, T. A., Burchardt, L., Cerbin, S. & M. Kokocinski. 2005. Long term monitoring results of harmful algal populations in Chesapeake Bay and its major tributaries in Virginia, U.S.A. Oceanol. Hydrobiol. Stud. 34(Suppl. 3):35-41.

Marshall, H. G., Egerton, T. A., Johnson, R., Semcheski, M., Bowman, N. & N. Mansfield. 2008. Re-occurring harmful algal blooms in the tidal waters of Virginia, USA. Ocean Sciences Meeting; March 2-7, 2008; Orlando, Florida.

Marshall, H. G. & T. A. Egerton. 2009. Phytoplankton blooms: their occurrence and composition within Virginia tidal tributaries. VA J. Sci. 60(3):149-164.

Marshall, H. G & T. A. Egerton. 2013. Assessing seasonal relationships between chlorophyll a concentrations to phytoplankton composition, biomass, and abundance, emphasizing the bloom producing algae (HAB and others) within the James, Elizabeth, and Lafayette rivers in Virginia. Final report submitted to Virginia Department of Environmental Quality.

May, S. P., Burkholder, J. M., Shumway, S. E., Hégaret, H., Wikfors, G. H. & D. Frank. 2010.

Effects of the toxic dinoflagellate *Alexandrium monilatum* on survival, grazing and behavioral response of three ecologically important bivalve molluscs. Harmful Algae. 9:281-293.

McCullagh, P. & J. A. Nelder. 1989. Generalized Linear Models. 2nd Edition, Chapman and Hall, London. 532 pp.

Mons, M. P., Egmond, H. P. & G. J. A. Speijers. 1998. Paralytic shellfish poisoning: A review. National Institute of Public Health and the Environment. Bilthoven, The Netherlands. Rept. 38802005. 47 pp.

Morse, D. C. 1947. Some observations on seasonal variations in plankton populations, Patuxent River, Maryland, 1943-1945. Chesapeake Biol. Lab. 65:1-31.

Mulholland, M. R., Morse, R. E., Boneillo, G. E., Bernhardt, P. W., Filippino, K. C., Procise, L. A., Blanco-Garda, J. L., Marshall, H. G., Egerton, T. A., Hunley, Moore, K. A., Berry, D. L. & C. J. Gobler. 2009. Understanding causes and impacts of the dinoflagellate, *Cochlodinium polykrikoides*, blooms in the Chesapeake Bay. Estuaries Coast. 32:734-747.

Murakami, M., Makabe, K., Yamaguchi, K., Konosu, S. & M. R. Wälchli. 1988. Goniodomin a, a novel polyether macrolide from the dinoflagellate *Goniodoma pseudogoniaulax*. Tetrahedron Lett. 29:1149-1152.

Newell, R. I. E. 1985. Physiological effects of the MSX parasite *Haplospoidium nelsoni* (Haskin, Stauber and Mackin) on the American oyster *Crassostrea virginica* (Gmelin). J. Shellfish Res. 5:91-95.

Newell, R. I. E. 1988. Ecological changes in Chesapeake Bay: are they the result of overharvesting the American oyster, *Crassostrea virginica*? Understanding the estuary: advances in Chesapeake Bay research. 129:536-546.

Nordstrom, J. L., Vickery, M. C. L., Blackstone, G. M., Murray, S. L. & A. DePaola. 2007. Development of a multiplex real-time PCR assay with an internal amplification control for the detection of total and pathogenic *Vibrio parahaemolyticus* bacteria in oysters. J. Appl. Environ. Microbiol. 73(18):5840-5847.

Park, J. G., Jeong, M. K., Lee, J. A., Cho, K. & O. Kwon. (2001). Diurnal vertical migration of a harmful dinoflagellate, Cochlodinium polykrikoides (Dinophyceae), during a red tide in coastal waters of Namhae Island, Korea. Phycologia. 40:292-297.

Pease, S. K. D. (2016) Thesis: *Alexandrium monilatum* in the lower Chesapeake Bay: Sediment cyst distribution and potential health impacts to *Crassostrea virginica*. Virginia Institute of Marine Science, College of William & Mary.

Perry, H. M., Stuck, K. C. & H. D. Howse. 1979. First record of a bloom of *Gonyaulax monilata* in coastal waters of Mississippi. Gulf Res. Rep. 6:313-316.

Peterson, C. H., Grabowski, J. H. & S. P. Powers. 2003. Estimated enhancement of fish production resulting from restoring oyster reef habitat: quantitative valuation. Mar. Ecol. Prog. Ser. 264:249-26.

R Core Team (2018). R: A language and environment for statistical computing. R Foundation for Statistical Computing, Vienna, Austria. URL https://www.R-project.org/.

Rainer, J. S. & R. Mann. 1992. A comparison of methods for calculating condition index in Eastern oysters, *Crassostrea virginica* (Gmelin, 1791). J. Shellfish Res. 11(1):55-58.

Reece, K. S. 2007-2017. Enhanced surveillance of risk factors and health effects related to harmful algal blooms. Annual report submitted to Virginia Department of Health for National CDC HAB Database.

Reece, K. S., Vogelbein, W. K. & R. B. Carnegie. 2016. Strategies to minimize the impact of mid-Atlantic emerging harmful algal bloom (HAB) species on *Crassostrea virginica*. Annual report submitted to VA Sea Grant. Award #NA10OAR4170085, VASG#A/71517C.

Roegner, G. C. & R. Mann. 1995. Early recruitment and growth of the American oyster *Crassostrea virginica* (Bivalvia: Ostreidae) with respect to tidal zonation and season. Mar. Ecol. Prog. Ser. 117:91-101.

Roelke, D. L. & R. H. Pierce. 2011. Effects of inflow on harmful algal blooms: some considerations. J. Plankton Res. 33(2):205-209.

Rothschild, B. J., Ault, J. S., Goulletquer, P. & M. Héral. 1994. Decline of the Chesapeake Bay oyster population: a century of habitat destruction and overfishing. Mar. Ecology Prog. Ser. 111(1/2):29-39.

Rybovich, M., La Peyre, M., Hall, S. G. & J. F. La Peyre. 2016. Increased temperatures combined with lowered salinities differentially impact oyster size class growth and mortality. J. Shellfish Res. 35:101-113.

Schulte, D. M. 2017. History of the Virginia Oyster Fishery, Chesapeake Bay, USA. Front. Mar. Sci. 4:127.

Scott, G. P. & K. S. Reece. 2018. Emerging patterns of late summer harmful algal blooms in the lower Chesapeake Bay. Poster presented at the National Shellfisheries Association 110th Annual Meeting in Seattle, WA.

Sellner, K. G., Doucette, G. J. & G. J. Kirkpatrick. 2003. Harmful algal blooms: causes, impacts and detection. J. Ind. Microbiol. Biot. 30(7):383-406.

Sharma, G. M., Michaels, L. & P. R. Burkholder. 1968. Goniodomin, a new antibiotic from a dinoflagellate. J. Antibiot. 21(11):659-664.

Shaw, B. L. & H. I. Battle. 1957. The gross and microscopic anatomy of the digestive tract of the oyster, *Crassostrea virginica* (Gmelin). Can. J. Zool. 35: 325-347.

Shumway, S. E. 1990. A review of the effects of algal blooms on shellfish and aquaculture. J. World. Aquac. Soc. 21:65-104.

Sievers, A. M. 1969. Comparative study of *Gonyaulax monilata* and *Gymnodinium breve* to annelids, crustaceans, mollusks, and a fish. J. Protozool. 16:401-404.

Stoecker, D. K., Adolf, J. E., Place, A. R., Glibert, P. M. & D. W. Merritt. 2008. Effects of the dinoflagellates *Karlodinium veneficum* and *Prorocentrum minimum* on early life history stages of the eastern oyster (*Crassostrea virginica*). Mar. Biol. 154:81-90.

VA DEQ. 2014. Quality Assurance Project Plan (QAPP) for James River Chlorophyll-a Study: Special Study #14098.

Van Dolah, F. M. 2000. Diversity of Marine and Freshwater Algal Toxins. In: L. Botana, editor. Seafood toxicology: pharmacology, physiology and detection. New York: Marcel Dekker. pp. 19-43.

Vandersea, M. W., M. W., Kibler, S. R., Van Sant, S. B. , Tester, P. A., Sullivan, K., Eckert, G., Cammarata, C., Reece, K., Scott, G., Place, A., Holderied, K., Hondolero, D. & R. W. Litaker. 2017. qPCR assays for *Alexandrium fundyense* and *A. ostenfeldii* (Dinophyceae) identified from Alaskan waters and a review of species-specific *Alexandrium* molecular assays. Phycologia. 56(3):303-320.

Walne, P. R. & R. Mann. 1975. Growth and biochemical composition in *Ostrea edulis* and *Crassostrea gigas*. In: H. Barnes, editor. Proc. 9th Eur. Mar. Biol. Symp., Oban. Aberdeen: Aberdeen University Press. pp. 587-607.

Wang, Da-Zhi. 2008. Neurotoxins from marine dinoflagellates: A brief review. Mar. Drugs. 6(2):349-371.

Wardle, W. J., Ray, S. M. & A. S. Aldrich. 1975. Mortality of marine organisms associated with offshore summer blooms of the toxic dinoflagellate *Gonyaulax monilata* Howell at Galveston, Texas. In: V. R. LoCicero, editor. Proceedings of the First International Conference on Toxic Dinoflagellate Blooms. Wakefield: Science and Technology Foundation. pp. 257-263.

Whyte, J. N. C., Haigh, N., Ginther, N. G. & L. J. Keddy. 2001. First record of blooms of *Cochlodinium* sp (Gymnodiniales, Dinophyceae) causing mortality to aquacultured salmon on the west coast of Canada. Phycologia. 40:298-304.

Wilberg, M. J., Wiedenmann, J. R. & J. M. Robinson. 2013. Sustainable exploitation and management of autogenic ecosystem engineers: application to oysters in Chesapeake Bay. Ecol. Appl. 23(4):766-776.

Wilson-Ormond, E. A., Powell, E. N. & S. M. Ray. 1997. Short-term and small-scale variation in food availability to natural oyster populations: Food, flow and flux. Mar. Ecol. 18:1-34.

Wood, J. C. & J. D. Andrews. 1962. *Haplosporidiurn costale* (Sporozoa) associated with a disease of Virginia oysters. Science. 136:710-711.

Table 1. Physical characteristics of oyster deployment sites in the Perrin River (HAB-endemic location; blue shading), York River (HAB-endemic location; orange shading), Big Island (HAB-endemic location; purple shading), and the Ware River (reference location; grey shading). Oysters were grown at the Perrin, York, and Ware River sites in summers 2017 and 2018, and at the Big Island site in summer 2018 only.

Parameter	Perrin River	York River	Big Island	Ware River
Substrate	Mud	Sand	Mud-Sand mix	Mud-Sand mix
Relative energy condition	Low	High	Low-Moderate	Moderate
Relative flushing rate	Intermediate	Fast	Fast	Slow

Table 2. Example of a linear regression table generated for 2017 interval oyster mortality data, in which site (YR refers to the York River site, and PR refers to the Perrin River site), placement location (ST refers to subtidal), temperature, salinity, pH, and DO are evaluated as predictor variables. Parameters with $p<0.001$ are marked with ***, $p<0.01$ with **, and $p<0.05$ with *.

Conditional model:

	Estimate	Std. Error	z value	Pr(>|z|)	
(Intercept)	-2.236597	0.015636	-143.04	< 2e-16	***
siteYR	0.037633	0.024700	1.52	0.127605	
sitePR	0.039723	0.018151	2.19	0.028638	*
placementST	0.004047	0.014140	0.29	0.774714	
Temp	0.027416	0.008147	3.37	0.000765	***
Salt	0.016908	0.010443	1.62	0.105431	
pH	-0.014271	0.010036	-1.42	0.155054	
DO	0.017474	0.010304	1.70	0.089898	.

Table 3. Summary statistics of select water quality parameters at the oyster deployment sites in the Perrin River (HAB-endemic location; blue shading), York River (HAB-endemic location; orange shading), and Ware River (reference location; grey shading) in summer 2017. Water quality parameters are based on measurements quantified in 15-min intervals by a data sonde positioned adjacent to the subtidal cages at each site.

Parameter	**Perrin River**		**York River**		**Ware River**	
	IT	ST	IT	ST	IT	ST
Monitoring interval (Total days)	6/9/17 - 10/9/17 (122)		6/6/17 - 10/10/17 (126)		6/8/17 - 10/9/17 (123)	
% Time aerial exposed	21.5	0.1	20.7	0	16.8	0.4
Temperature (°C)						
Average	27.1		25.9		27.2	
Range	21.0 - 34.8		20.4 - 32.0		20.9 - 33.5	
Salinity						
Average	19.8		20.2		18.5	
Range	14.4 - 22.2		16.3 - 22.5		14.2 - 20.3	
pH						
Average	7.8		7.9		7.9	
Range	7.1 - 8.4		7.3 - 8.8		7.3 - 8.5	
DO (mg L^{-1})						
Average	6.2		7.4		6.9	
Range	2.9 - 12.2		2.0 - 22.0		3.6 - 13.1	
Chl *a* (µg L^{-1})						
Average	11.8		10.3		12.9	
Range	0.3 - 461.9		0.2 - 483.9		0.1 - 106.7	

Table 4. AIC model comparison tables for 2017 oyster data. The model with the most empirical support, i.e. the lowest ΔAIC, in each suite is bolded and was used to generate the subsequent linear regression table for each dependent oyster variable.

Model	-2log(L)	Number of Parameters	AIC	ΔAIC
Interval Mortality				
M_1	-253.9	12	-229.9	3.6
M_2	**-251.5**	**9**	**-233.5**	**0.0**
M_3	-253.2	10	-233.2	0.3
M_4	-233.2	8	-217.2	16.3
Cumulative Mortality				
M_1	-438.6	12	-414.6	4.1
M_2	**-436.7**	**9**	**-418.7**	**0.0**
M_3	-437.8	10	-417.8	0.9
M_4	-420.0	8	-404.0	14.6
Shell Height				
M_1	704.8	12	728.8	2.3
M_2	**708.4**	**9**	**726.4**	**0.0**
M_3	708.0	10	728.0	1.6
M_4	745.4	8	761.4	34.9
Growth Rate				
M_1	**-84.1**	**12**	**-60.1**	**0.0**
M_2	-72.4	9	-54.4	5.7
M_3	-73.2	10	-53.2	6.8
M_4	-67.1	8	-51.1	9.0
Condition Index				
M_1	-36.8	12	-12.8	2.1
M_2	-31.5	9	-13.5	1.4
M_3	**-34.9**	**10**	**-14.9**	**0.0**
M_4	-21.2	8	-5.2	9.7

Table 5. Linear regression tables for 2017 oyster data. Independent variables investigated included site, placement location, and water quality parameters. Sites included the Ware River reference site (represented by the Intercept), the Perrin River (PR), and the York River (YR). Placement locations included intertidal (represented by the Intercept) and subtidal (ST). Water quality parameters included standardized temperature (temp.std), salinity (salt.std), pH (pH.std), dissolved oxygen (DO.std), Chlorophyll *a* (chl.std), *Alexandrium monilatum* cell concentration (*A.monilatum*.std), and *Margalefidinium polykrikoides* cell concentration (*M.polykrikoides*.std). All independent variables determined to be significant based on the p-value are bolded. Parameters with $p<0.001$ are marked with ***, $p<0.01$ with **, and $p<0.05$ with *.

Indep. Var.	Parameter Estimate	Standard Error
Interval Mortality		
(Intercept)	-2.237***	0.016
YR	0.038	0.025
PR	**0.040***	**0.018**
ST	0.004	0.014
temp.std	**0.027*****	**0.008**
salt.std	0.017	0.010
pH.std	-0.014	0.010
DO.std	0.017	0.010
Cumulative Mortality		
(Intercept)	0.051***	0.006
YR	-0.001	0.009
PR	**0.022*****	**0.007**
ST	**-0.011***	**0.005**
temp.std	**-0.011*****	**0.003**
salt.std	0.001	0.004
pH.std	-0.001	0.004
DO.std	0.004	0.004
Shell Height		
(Intercept)	45.688***	2.883
YR	**-10.247***	**4.554**
PR	-6.279	3.347
ST	0.411	2.607
temp.std	**-8.233*****	**1.502**
salt.std	0.097	1.925
pH.std	-1.883	1.850
DO.std	1.634	1.900
Growth Rate		
(Intercept)	0.442***	0.040
YR	-0.023	0.069
PR	-0.067	0.046
ST	-0.032	0.037
temp.std	**0.068****	**0.021**
salt.std	-0.011	0.029
pH.std	0.014	0.027
DO.std	**-0.059***	**0.026**
chl.std	-0.020	0.017
A.monilatum.std	0.034	0.018
***M. polykrikoides*.std**	**0.053****	**0.017**
Condition Index		
(Intercept)	1.754***	0.075
YR	0.231	0.123
PR	-0.092	0.090
ST	-0.087	0.055
temp.std	**0.102****	**0.038**
salt.std	0.015	0.047
pH.std	0.017	0.038
DO.std	0.032	0.036
chl.std	-0.056	0.030

Table 6. Summary statistics of select water quality parameters at the oyster deployment sites in the Perrin River (HAB-endemic location; blue shading), York River (HAB-endemic location; orange shading), Big Island (HAB-endemic location; purple shading), Ware River (reference location; grey shading), in summer 2018. Water quality parameters were quantified in 15-min intervals by a data sonde positioned adjacent to the subtidal cage at each site.

Parameter	**Perrin River**		**York River**		**Big Island**		**Ware River**	
	IT	ST	IT	ST	IT	ST	IT	ST
Monitoring interval (Total days)	6/19/18 - 10/8/18 (111)		6/21/18 - 10/8/18 (109)		6/20/18 - 10/9/18 (111)		6/19/18 - 10/10/18 (113)	
% Time aerial exposed	14.1	0	18.6	0	29.1	0	21.7	0
Temperature (°C)								
Average	28.6		27.7		27.9		28.7	
Range	23.9 - 33.6		24.3 - 31.7		22.9 - 32.9		23.9 - 34.0	
Salinity								
Average	14.9		15.0		15.4		14.2	
Range	11.7 - 17.3		9.1 - 18.1		11.8 - 18.8		7.2 - 16.2	
pH								
Average	7.7		7.9		7.9		7.8	
Range	7.0 - 8.6		7.5 - 8.7		6.9 - 8.6		7.3 - 8.3	
DO (mg L^{-1})								
Average	5.9		7.2		6.8		6.8	
Range	2.0 - 11.0		4.3 - 14.7		2.8 - 11.6		1.2 - 11.3	
Chl *a* (µg L^{-1})								
Average	8.9		11.2		9.5		15.1	
Range	7.8 - 10.2		0.1 - 115.1		1.2 - 72.8		1.9 - 68.1	

Table 7. AIC model comparison tables for 2018 oyster data. The model with the most empirical support, i.e. the lowest ΔAIC, in each suite is bolded and was used to generate the subsequent linear regression table for each dependent oyster variable.

Model	-2log(L)	Number of Parameters	AIC	ΔAIC
Interval Mortality				
M_1	-95.1	11	-73.1	0.7
M_2	**-93.8**	**10**	**-73.8**	**0.0**
Cumulative Mortality				
M_1	-24.8	11	-2.8	1.5
M_2	**-24.3**	**10**	**-4.3**	**0.0**
Height				
M_1	437.2	11	459.2	1.1
M_2	**438.1**	**10**	**458.1**	**0.0**
Growth Rate				
M_1	-55.4	11	-33.4	1.7
M_2	**-55.0**	**10**	**-35.0**	**0.0**

Table 8. Linear regression tables for 2018 oyster data. Independent variables investigated included site, placement location, and water quality parameters. Sites included the Ware River reference site (represented by the Intercept), the Big Island site (BI), the Perrin River (PR), and the York River (YR). Placement locations included intertidal (represented by the Intercept) and subtidal (ST). Water quality parameters included standardized temperature (temp.std), salinity (salt.std), pH (pH.std), dissolved oxygen (DO.std), and Chlorophyll *a* (chl.std). All independent variables determined to be significant based on the p-value are bolded. Parameters with $p<0.001$ are marked with ***, $p<0.01$ with **, and $p<0.05$ with *.

Indep. Var.	Parameter Estimate	Standard Error
Interval Mortality		
(Intercept)	-2.076***	0.034
BI	**-0.088***	**0.043**
YR	-0.048	0.046
PR	**-0.133****	**0.043**
ST	**-0.084****	**0.030**
temp.std	0.021	0.017
salt.std	0.018	0.017
pH.std	0.029	0.021
DO.std	**-0.063****	**0.021**
Cumulative Mortality		
(Intercept)	-1.444***	0.061
BI	**-0.236****	**0.077**
YR	**-0.301*****	**0.082**
PR	**-0.345*****	**0.076**
ST	**-0.290*****	**0.053**
temp.std	**-0.074***	**0.029**
salt.std	0.021	0.029
pH.std	-0.016	0.038
DO.std	0.038	0.038
Height		
(Intercept)	40.773***	2.657
BI	-2.552	3.388
YR	**-7.353***	**3.610**
PR	0.061	3.360
ST	3.613	2.346
temp.std	**-5.304*****	**1.291**
salt.std	1.951	1.291
pH.std	-3.201	1.673
DO.std	**7.297*****	**1.667**
Growth Rate		
(Intercept)	0.332	0.059
BI	-0.016	0.072
YR	0.070	0.078
PR	-0.011	0.068
ST	-0.005	0.045
temp.std	0.045	0.024
salt.std	0.025	0.029
pH.std	-0.008	0.036
DO.std	-0.042	0.037

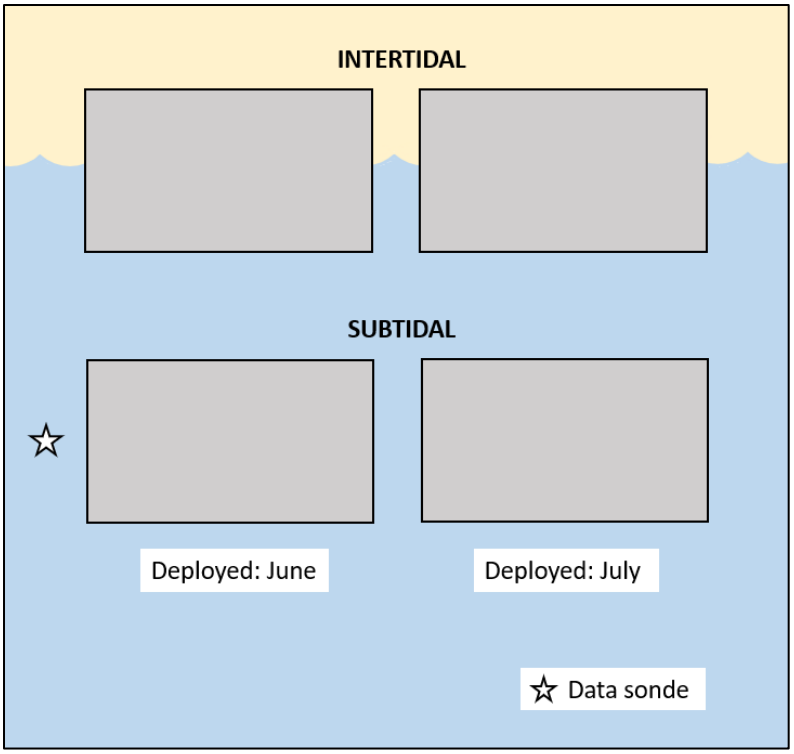

Figure 1. Oyster cage (grey rectangles) deployment at each of the three sites, the Perrin River, York River, and Ware River, in summer 2017. Each cage contained oysters in three pseudo-replicate bags. Cages were deployed intertidally and subtidally twice, between 6/1/17-6/2/17 and between 7/5/17-7/6/17. A sonde (white star) was deployed alongside all subtidal cages.

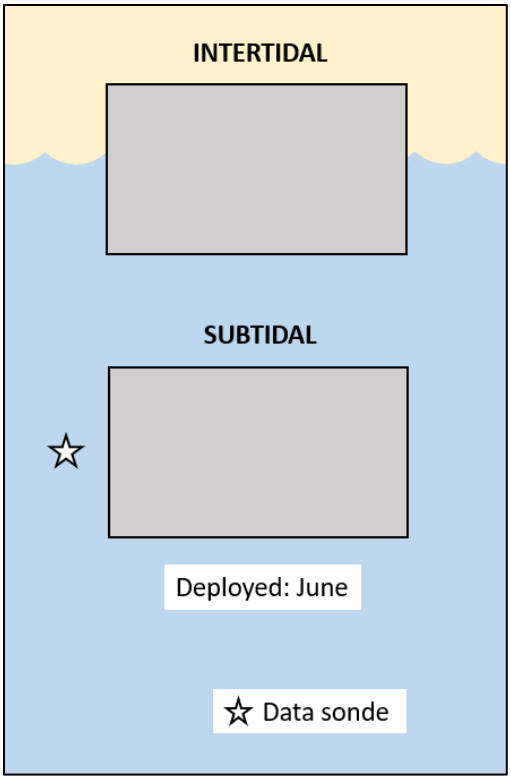

Figure 2. Oyster cage (grey rectangles) deployment at each of the four sites, the Perrin River, York River, Big Island, and Ware River, in summer 2018. Each cage contained oysters in three pseudo-replicate bags. At all sites, cages were deployed intertidally and subtidally between 6/20/18-6/21/18. A sonde (white star) was deployed alongside all subtidal cages.

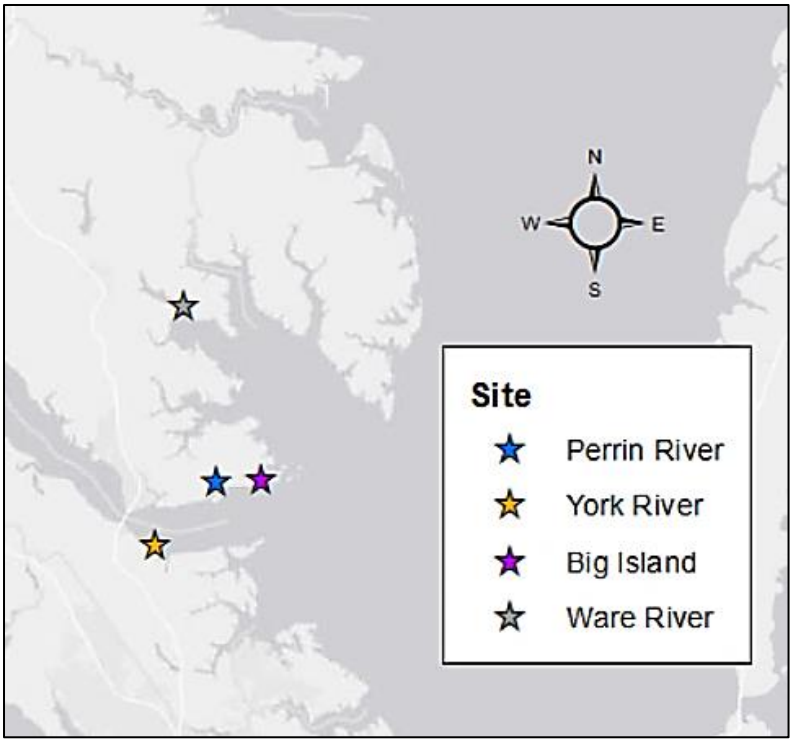

Figure 3. Map of the four sites of oyster deployment in the lower Chesapeake Bay in summers 2017 and 2018. The low-energy Perrin River site (blue star), high-energy York River site (orange star), and intermediate-energy Big Island site (purple star) represent HAB-endemic locations, while blooms of *Alexandrium monilatum* and *Margalefidinium polykrikoides* do not typically occur at the intermediate-energy Ware River site (grey star). Note: oysters were deployed at Big Island in summer 2018 only.

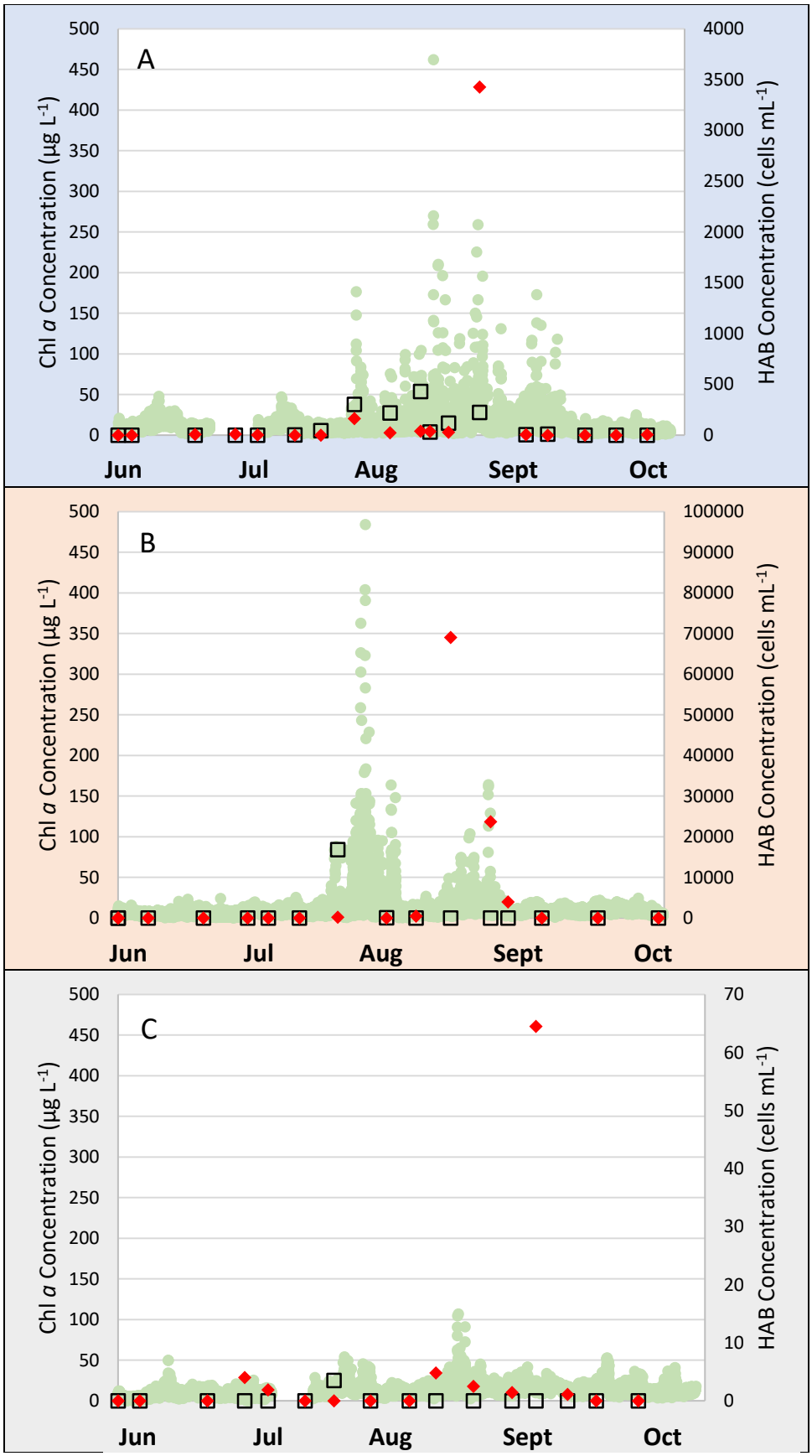
A
B
C
Chl a Concentration (µg L-1)
HAB Concentration (cells mL-1)
Jun
Jul
Aug
Sept
Oct

Figure 4. Cell concentrations of harmful algal bloom (HAB) species *Margalefidinium polykrikoides* (black squares) and *Alexandrium monilatum* (red diamonds) sampled next to the subtidal cages at the Perrin River (HAB-endemic location; **A**), York River (HAB-endemic location; **B**), and Ware River (reference location; **C**) sites in 2017. HAB cell concentrations were determined using qPCR. Chlorophyll *a* (Chl *a*; pale green) was measured every 15 min via a data sonde next to the subtidal cages at all sites.

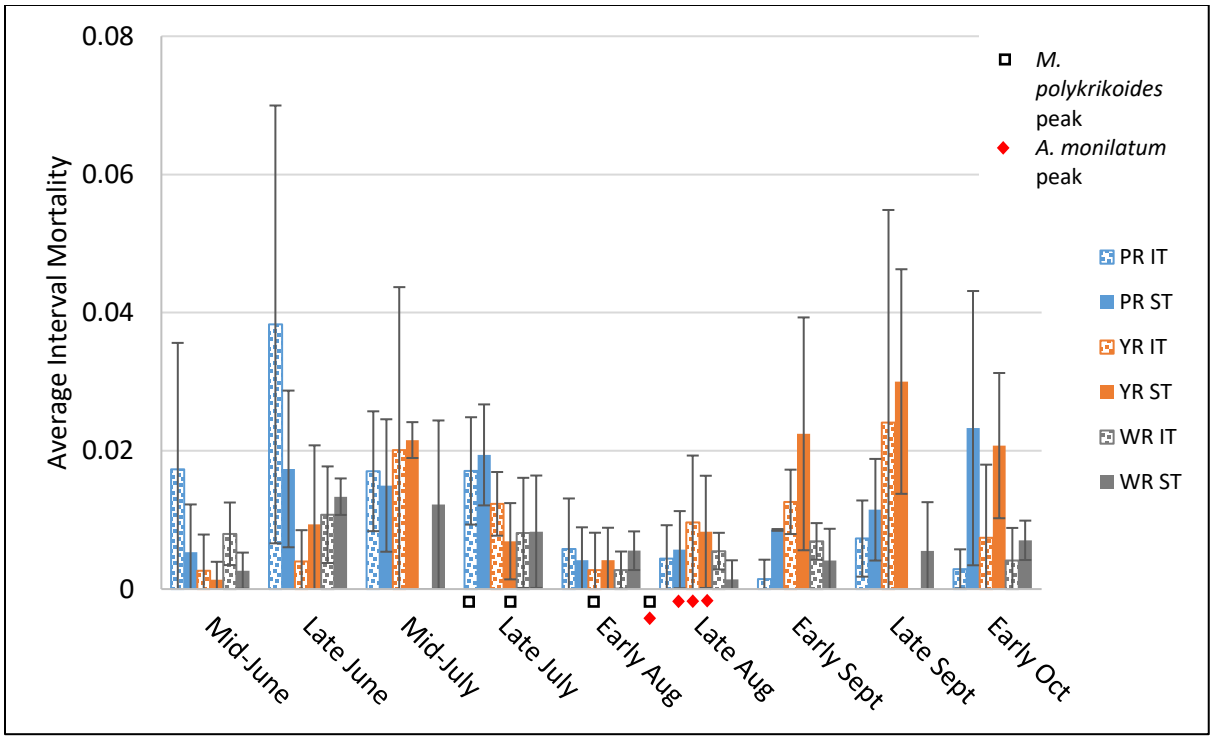

Figure 5. Average interval mortality of oysters deployed in June 2017. Oysters were deployed at the Perrin River (PR) site intertidally (IT; dotted blue) and subtidally (ST; solid blue), the York River (YR) site intertidally (dotted orange) and subtidally (solid orange), and the Ware River (WR) site intertidally (dotted grey) and subtidally (solid grey). Error bars represent the 95% confidence intervals. The approximate time of the peak cell concentration of *M. polykrikoides* (black square) and *A. monilatum* (red diamond) at each depth at the PR and YR sites is noted below the appropriate bar. The peak concentrations of *M. polykrikoides* at the ST at the PR site, and *A. monilatum* at the IT at the PR site, occurred in mid-August, and are thus marked between the early and late August sampling points.

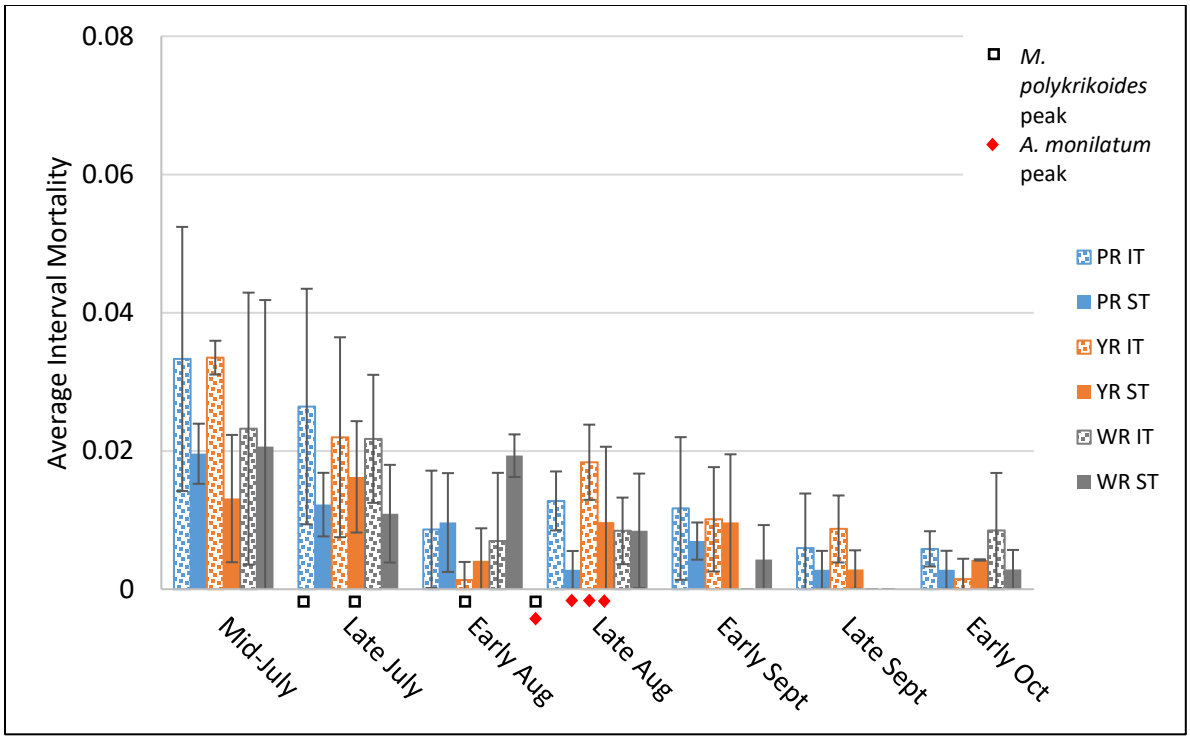

Figure 6. Average interval mortality of oysters deployed in July 2017. Oysters were deployed at the Perrin River (PR) site intertidally (IT; dotted blue) and subtidally (ST; solid blue), the York River (YR) site intertidally (dotted orange) and subtidally (solid orange), and the Ware River (WR) site intertidally (dotted grey) and subtidally (solid grey). Error bars represent the 95% confidence intervals. The approximate time of the peak cell concentration of *M. polykrikoides* (black square) and *A. monilatum* (red diamond) at each depth at the PR and YR sites is noted below the appropriate bar. The peak concentrations of *M. polykrikoides* at the ST at the PR site, and *A. monilatum* at the IT at the PR site, occurred in mid-August, and are thus marked between the early and late August sampling points.

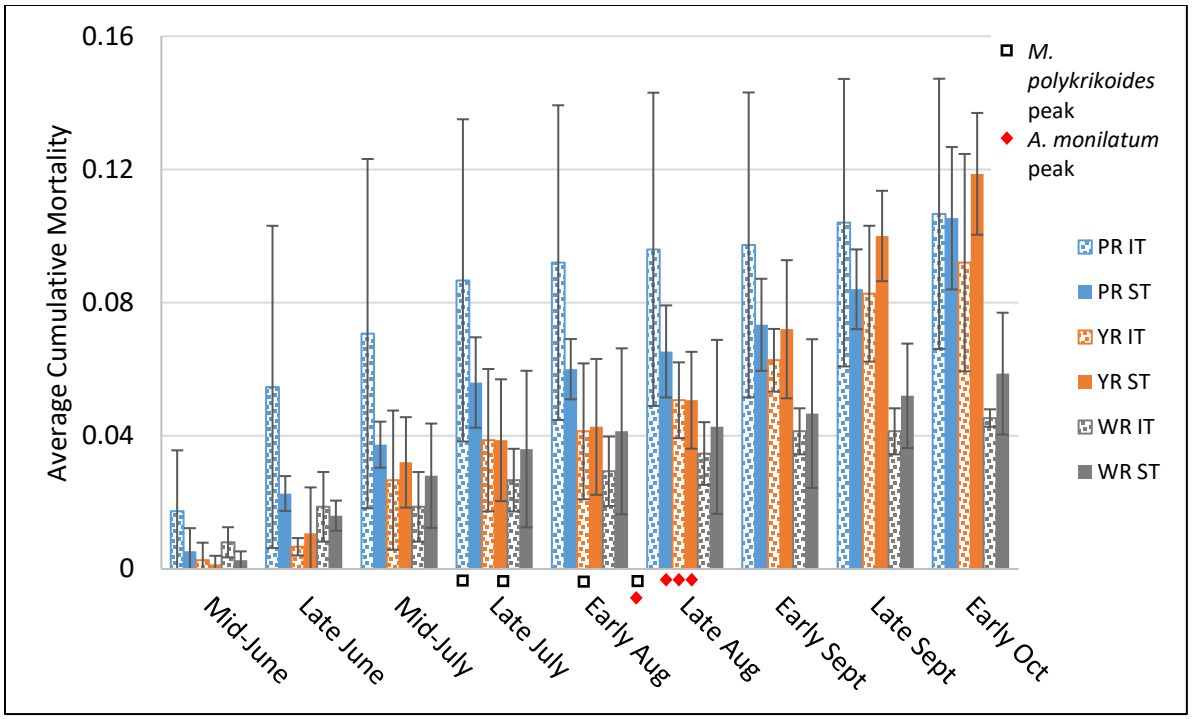

Figure 7. Average cumulative mortality of oysters deployed in June 2017. Oysters were deployed at the Perrin River (PR) site intertidally (IT; dotted blue) and subtidally (ST; solid blue), the York River (YR) site intertidally (dotted orange) and subtidally (solid orange), and the Ware River (WR) site intertidally (dotted grey) and subtidally (solid grey). Error bars represent the 95% confidence intervals. The approximate time of the peak cell concentration of *M. polykrikoides* (black square) and *A. monilatum* (red diamond) at each depth at the PR and YR sites is noted below the appropriate bar. The peak concentrations of *M. polykrikoides* at the ST at the PR site, and *A. monilatum* at the IT at the PR site, occurred in mid-August, and are thus marked between the early and late August sampling points.

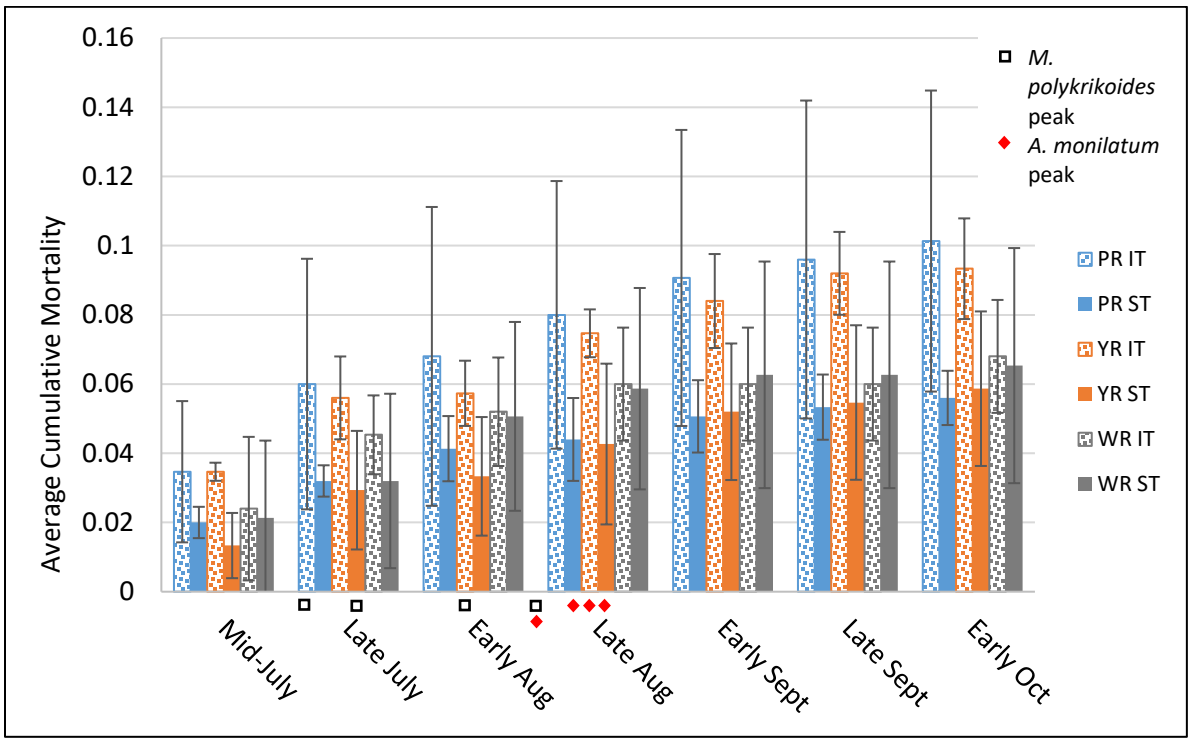

Figure 8. Average cumulative mortality of oysters deployed in July 2017. Oysters were deployed at the Perrin River (PR) site intertidally (IT; dotted blue) and subtidally (ST; solid blue), the York River (YR) site intertidally (dotted orange) and subtidally (solid orange), and the Ware River (WR) site intertidally (dotted grey) and subtidally (solid grey). Error bars represent the 95% confidence intervals. The approximate time of the peak cell concentration of *M. polykrikoides* (black square) and *A. monilatum* (red diamond) at each depth at the PR and YR sites is noted below the appropriate bar. The peak concentrations of *M. polykrikoides* at the ST at the PR site, and *A. monilatum* at the IT at the PR site, occurred in mid-August, and are thus marked between the early and late August sampling points.

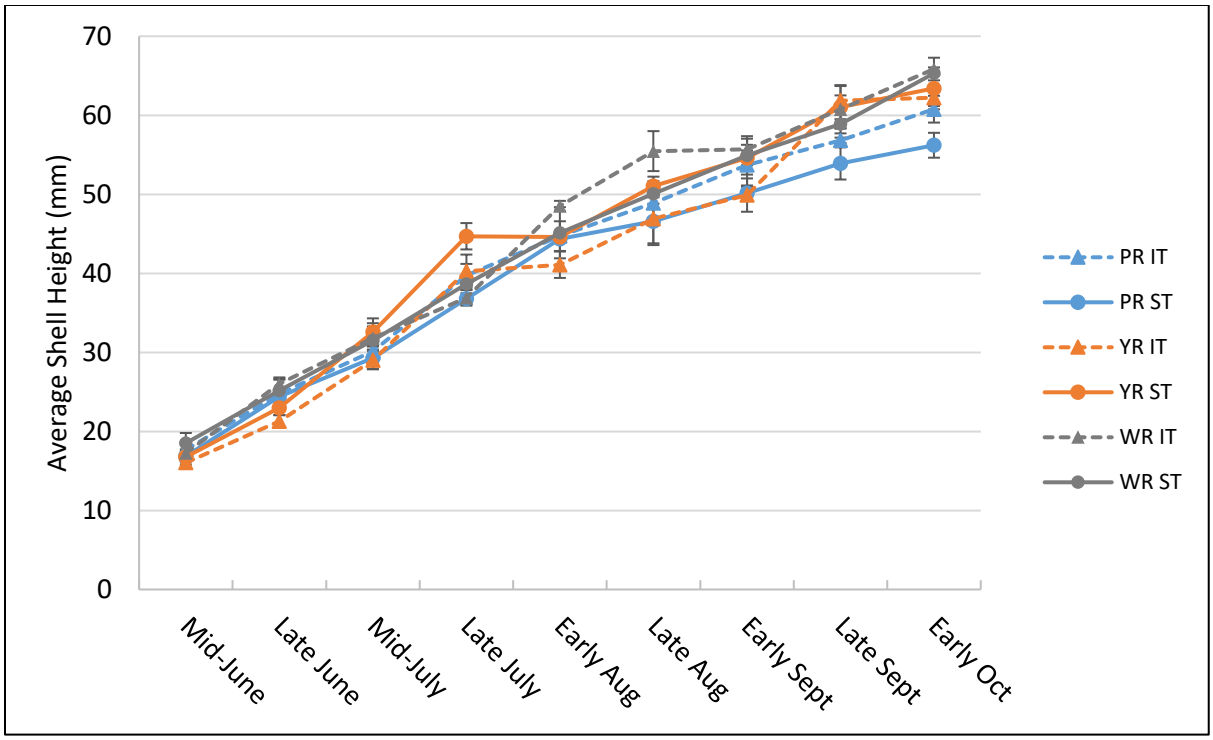

Figure 9. Average shell height (mm) of oysters deployed in June 2017. Oysters were deployed at the Perrin River (PR) site intertidally (IT; blue triangle and dashed line) and subtidally (ST; blue circle and solid line), the York River (YR) site intertidally (orange triangle and dashed line) and subtidally (orange circle and solid line), and the Ware River (WR) site intertidally (grey triangle and dashed line) and subtidally (grey circle and solid line). Error bars represent the 95% confidence intervals.

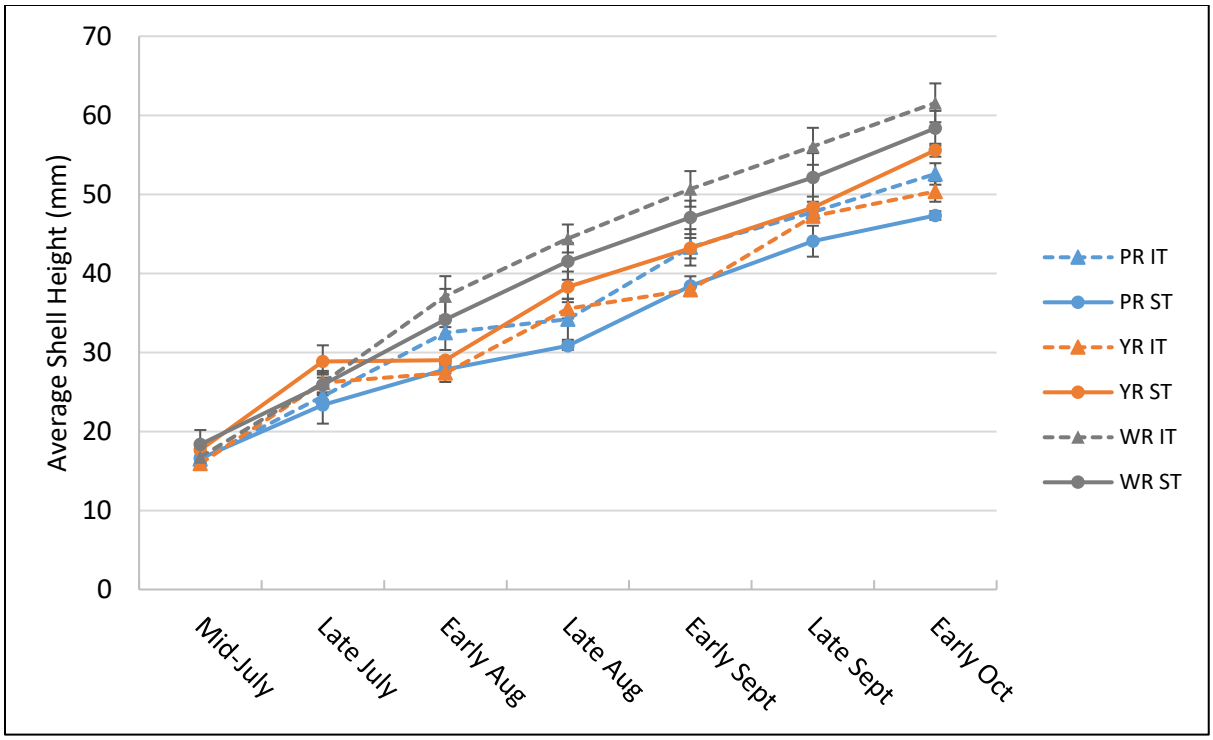

Figure 10. Average shell height (mm) of oysters deployed in July 2017. Oysters were deployed at the Perrin River (PR) site intertidally (IT; blue triangle and dashed line) and subtidally (ST; blue circle and solid line), the York River (YR) site intertidally (orange triangle and dashed line) and subtidally (orange circle and solid line), and the Ware River (WR) site intertidally (grey triangle and dashed line) and subtidally (grey circle and solid line). Error bars represent the 95% confidence intervals.

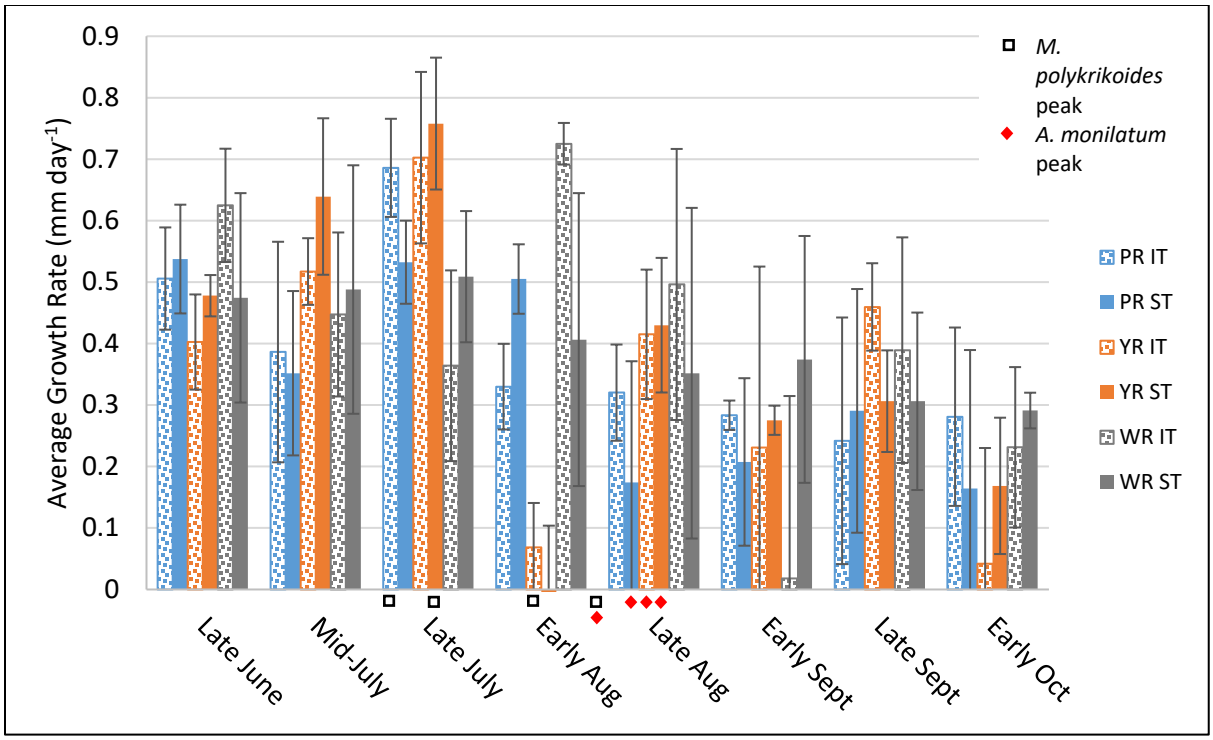

Figure 11. Average growth rate (mm day^{-1}) of oysters deployed in June 2017. Oysters were deployed at the Perrin River (PR) site intertidally (IT; dotted blue) and subtidally (ST; solid blue), the York River (YR) site intertidally (dotted orange) and subtidally (solid orange), and the Ware River (WR) site intertidally (dotted grey) and subtidally (solid grey). Error bars represent the 95% confidence intervals. The approximate time of the peak cell concentration of *M. polykrikoides* (black square) and *A. monilatum* (red diamond) at each depth at the PR and YR sites is noted below the appropriate bar. The peak concentrations of *M. polykrikoides* at the ST at the PR site, and *A. monilatum* at the IT at the PR site, occurred in mid-August, and are thus marked between the early and late August sampling points.

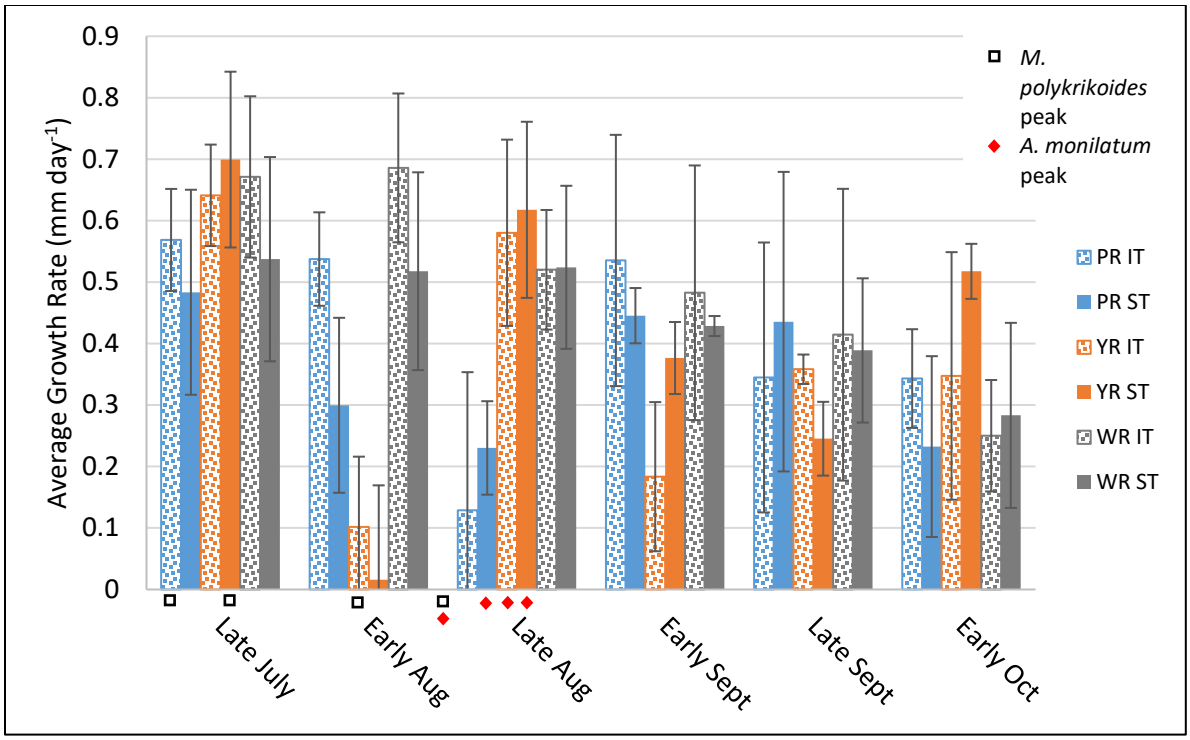

Figure 12. Average growth rate (mm day^{-1}) of oysters deployed in July 2017. Oysters were deployed at the Perrin River (PR) site intertidally (IT; dotted blue) and subtidally (ST; solid blue), the York River (YR) site intertidally (dotted orange) and subtidally (solid orange), and the Ware River (WR) site intertidally (dotted grey) and subtidally (solid grey). Error bars represent the 95% confidence intervals. The approximate time of the peak cell concentration of *M. polykrikoides* (black square) and *A. monilatum* (red diamond) at each depth at the PR and YR sites is noted below the appropriate bar. The peak concentrations of *M. polykrikoides* at the ST at the PR site, and *A. monilatum* at the IT at the PR site, occurred in mid-August, and are thus marked between the early and late August sampling points.

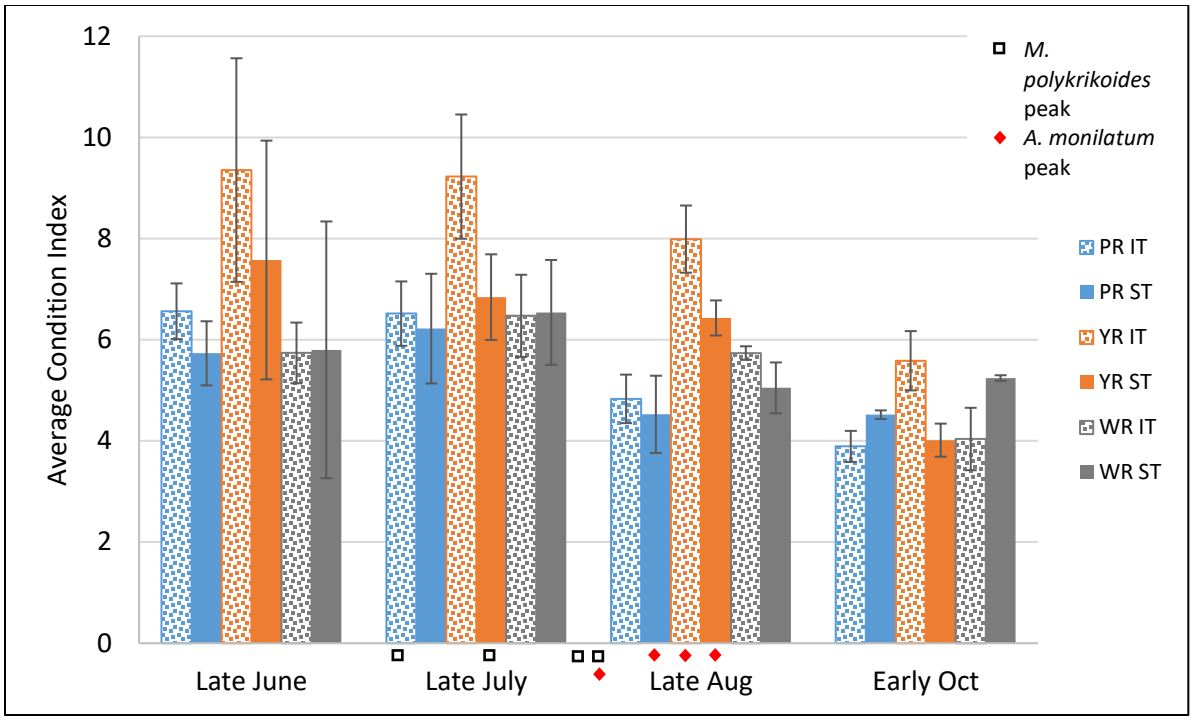

Figure 13. Average condition index (CI) of oysters deployed in June 2017. Oysters were deployed at the Perrin River (PR) site intertidally (IT; dotted blue) and subtidally (ST; solid blue), the York River (YR) site intertidally (dotted orange) and subtidally (solid orange), and the Ware River (WR) site intertidally (dotted grey) and subtidally (solid grey). CI was calculated according to Rainer & Mann 1992. Error bars represent the 95% confidence intervals. The approximate time of the peak cell concentration of *M. polykrikoides* (black square) and *A. monilatum* (red diamond) at each depth at the PR and YR sites is noted below the appropriate bar. The peak concentration of *M. polykrikoides* occurred at the IT at the YR site in early August and is marked immediately to the right of the late July sampling. The peak concentrations of *M. polykrikoides* at the ST at the PR site, and *A. monilatum* at the IT at the PR site, occurred in mid-August, and are thus marked immediately to the left of the late August sampling point.

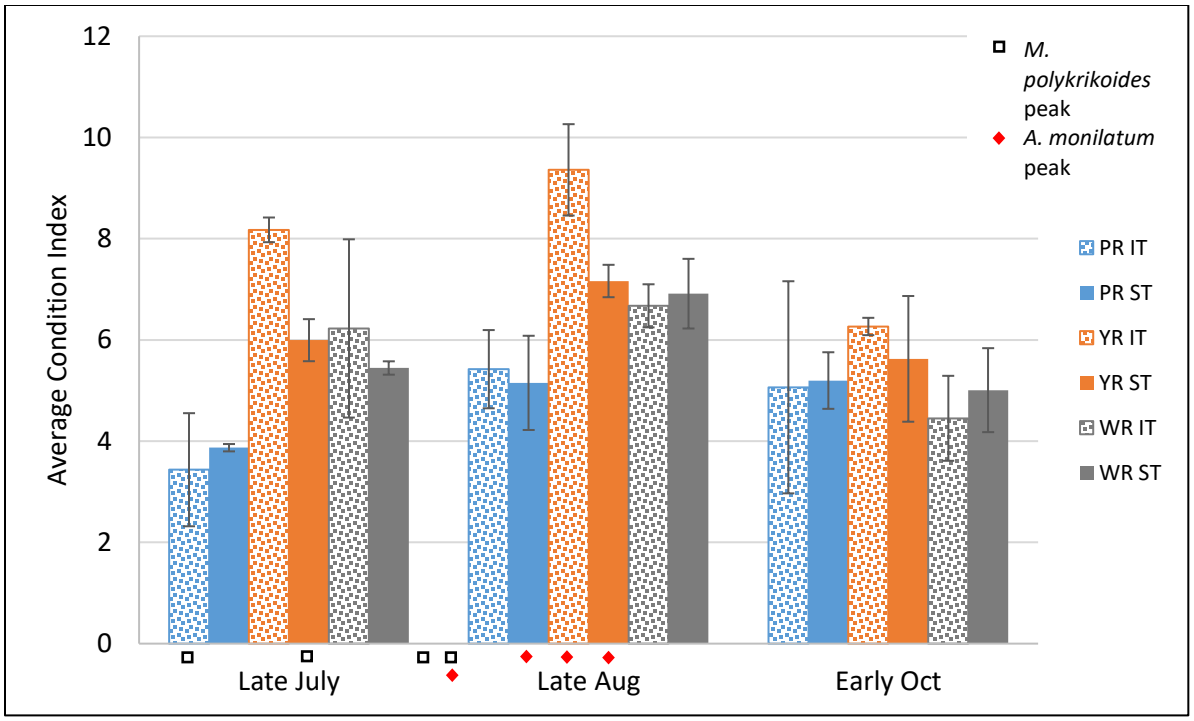

Figure 14. Average condition index (CI) of oysters deployed in July 2017. Oysters were deployed at the Perrin River (PR) site intertidally (IT; dotted blue) and subtidally (ST; solid blue), the York River (YR) site intertidally (dotted orange) and subtidally (solid orange), and the Ware River (WR) site intertidally (dotted grey) and subtidally (solid grey). CI was calculated according to Rainer & Mann 1992. Error bars represent the 95% confidence intervals. The approximate time of the peak cell concentration of *M. polykrikoides* (black square) and *A. monilatum* (red diamond) at each depth at the PR and YR sites is noted below the appropriate bar. The peak concentration of *M. polykrikoides* occurred at the IT at the YR site in early August and is marked immediately to the right of the late July sampling. The peak concentrations of *M. polykrikoides* at the ST at the PR site, and *A. monilatum* at the IT at the PR site, occurred in mid-August, and are thus marked immediately to the left of the late August sampling point.

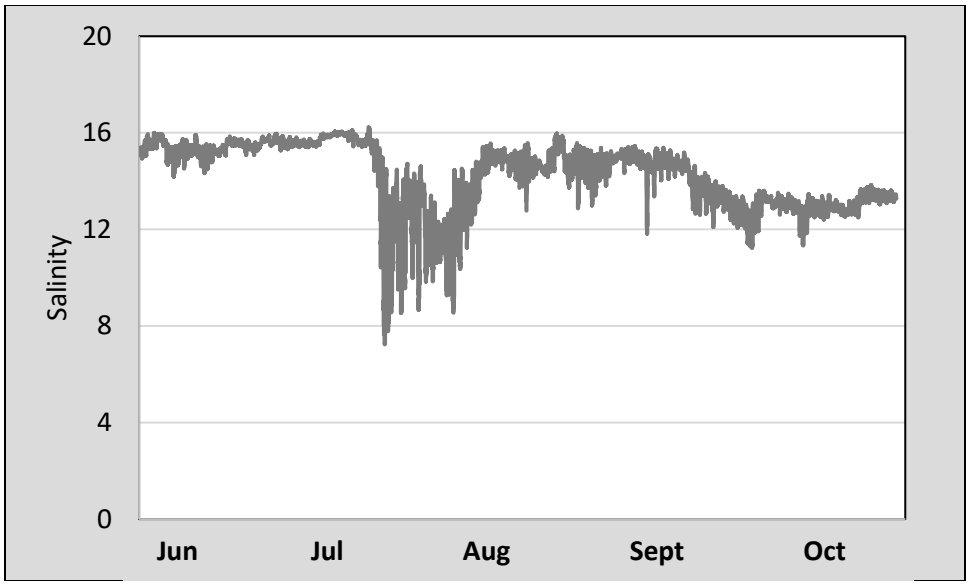

Figure 15. Salinity data collected every 15 min next to the subtidal cage in the Ware River in 2018. Salinity values decreased from >15 to <8 on 7/25/18.

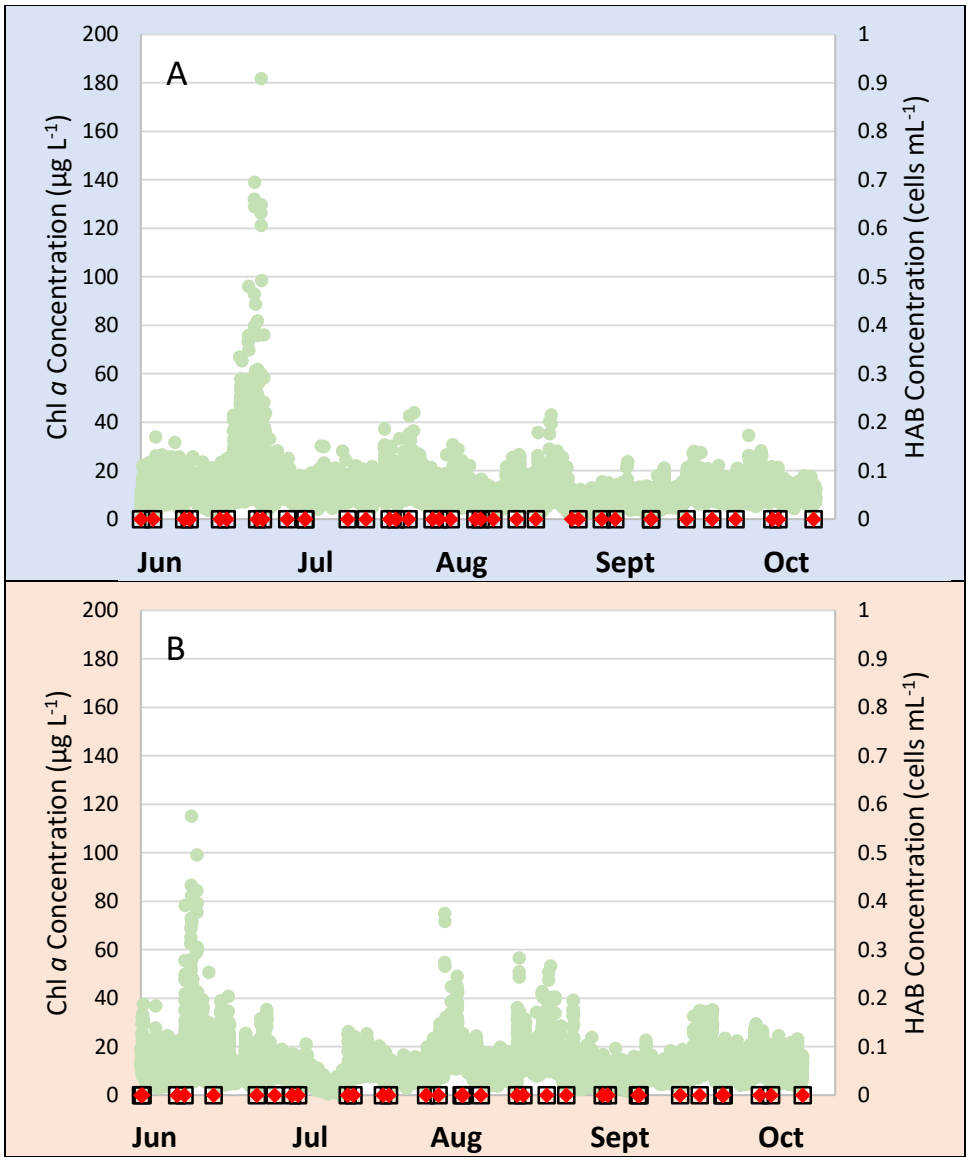
A
B
Chl a Concentration (µg L-1)
HAB Concentration (cells mL-1)
200
180
160
140
120
100
80
60
40
20
0
1
0.9
0.8
0.7
0.6
0.5
0.4
0.3
0.2
0.1
0
Jun
Jul
Aug
Sept
Oct

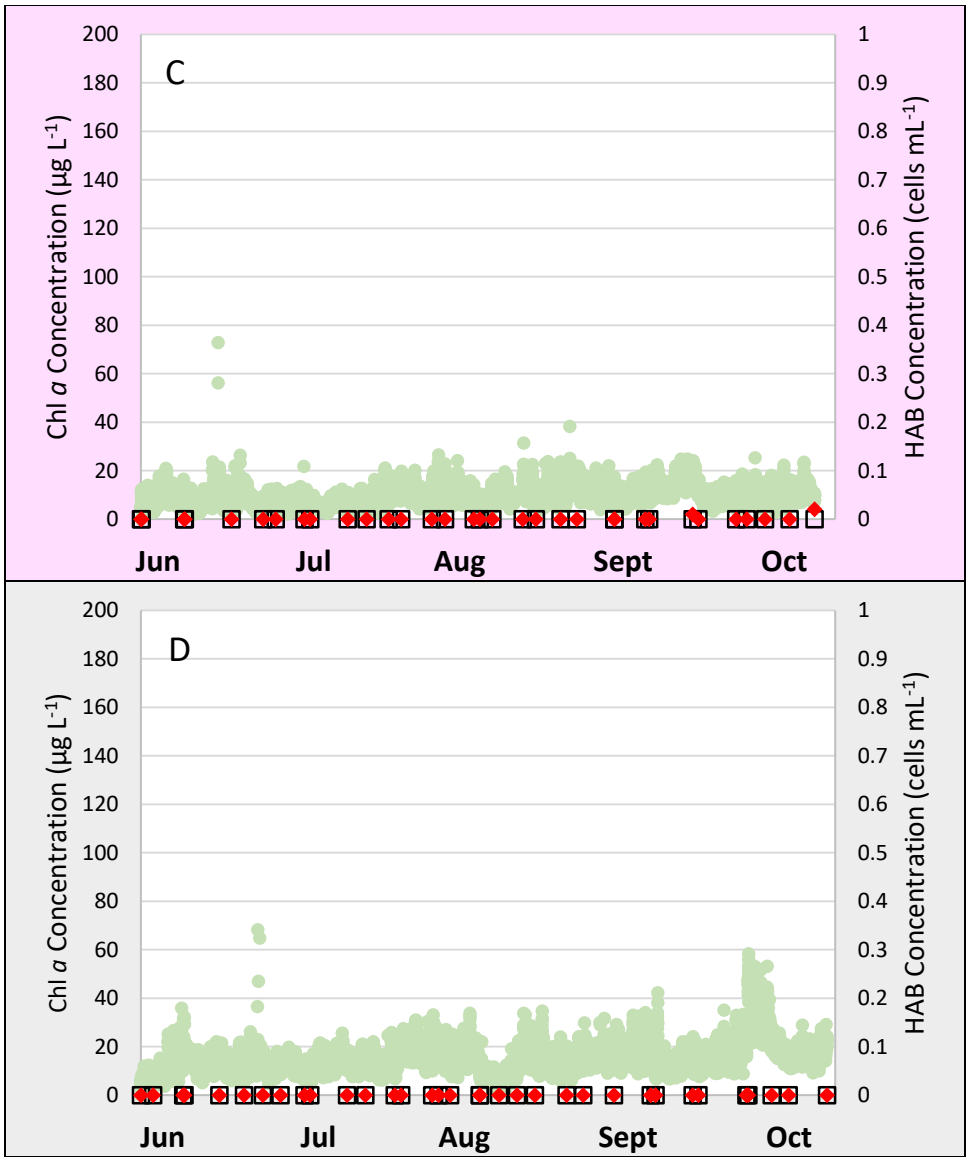

Figure 16. Cell concentrations of harmful algal bloom (HAB) species *Margalefidinium polykrikoides* (black squares) and *Alexandrium monilatum* (red diamonds) sampled next to the subtidal cages at the Perrin River (HAB-endemic location; **A**), York River (HAB-endemic location; **B**), Big Island (HAB-endemic location; **C**), and Ware River (reference location; **D**) sites in 2018. HAB cell concentrations were determined using qPCR. Chlorophyll *a* (Chl *a*; pale green) was measured every 15 min via a data sonde next to the subtidal cages at all sites.

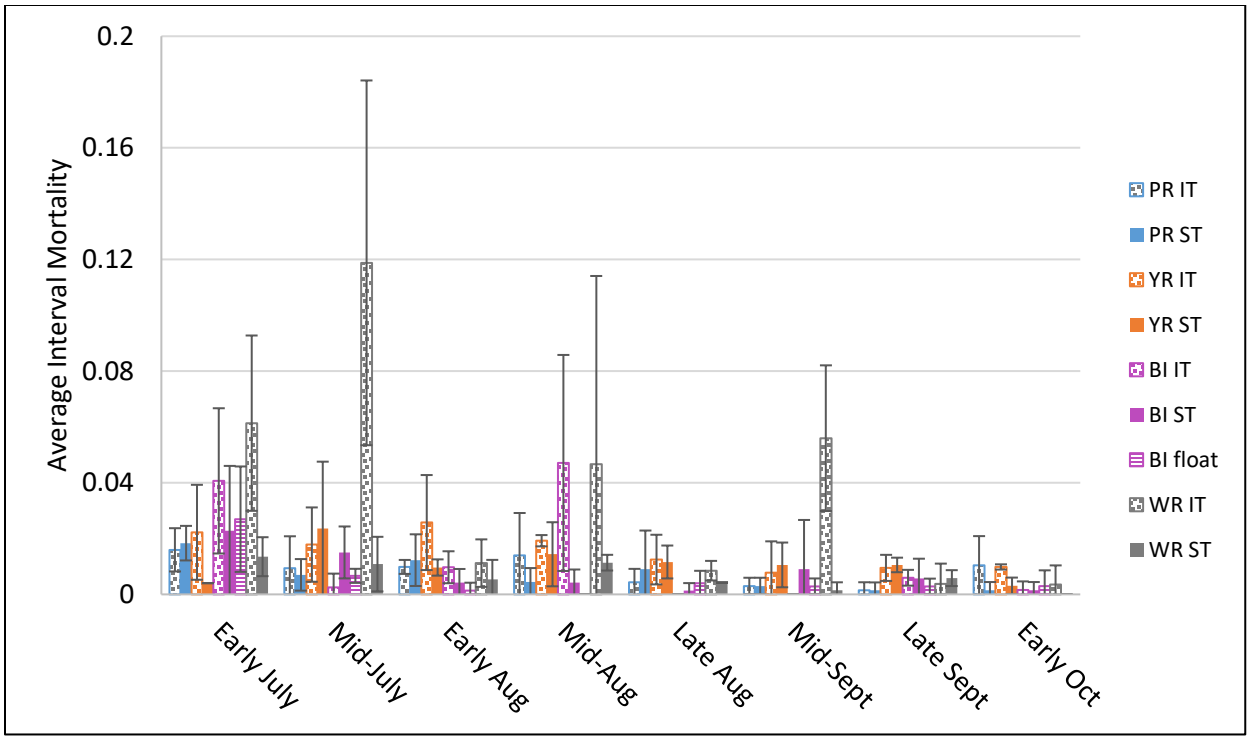

Figure 17. Average interval mortality of oysters deployed in July 2018. Oysters were deployed at the Perrin River (PR) site intertidally (IT; dotted blue) and subtidally (ST; solid blue), the York River (YR) site intertidally (dotted orange) and subtidally (solid orange), the Big Island (BI) site intertidally (dotted purple) and subtidally (solid purple) and at the surface (horizontal purple lines), and the Ware River (WR) site intertidally (dotted grey) and subtidally (solid grey). Error bars represent the 95% confidence intervals.

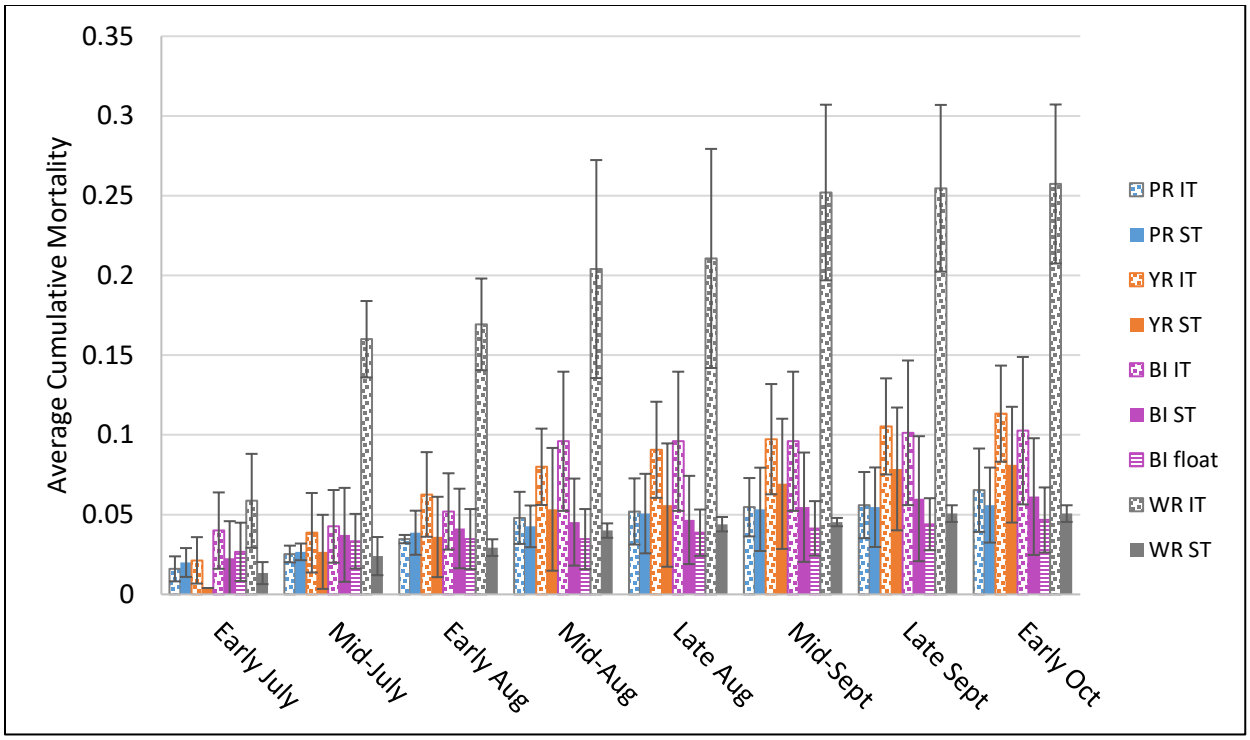

Figure 18. Average cumulative mortality of oysters deployed in July 2018. Oysters were deployed at the Perrin River (PR) site intertidally (IT; dotted blue) and subtidally (ST; solid blue), the York River (YR) site intertidally (dotted orange) and subtidally (solid orange), the Big Island (BI) site intertidally (dotted purple) and subtidally (solid purple) and at the surface (horizontal purple lines), and the Ware River (WR) site intertidally (dotted grey) and subtidally (solid grey). Error bars represent the 95% confidence intervals.

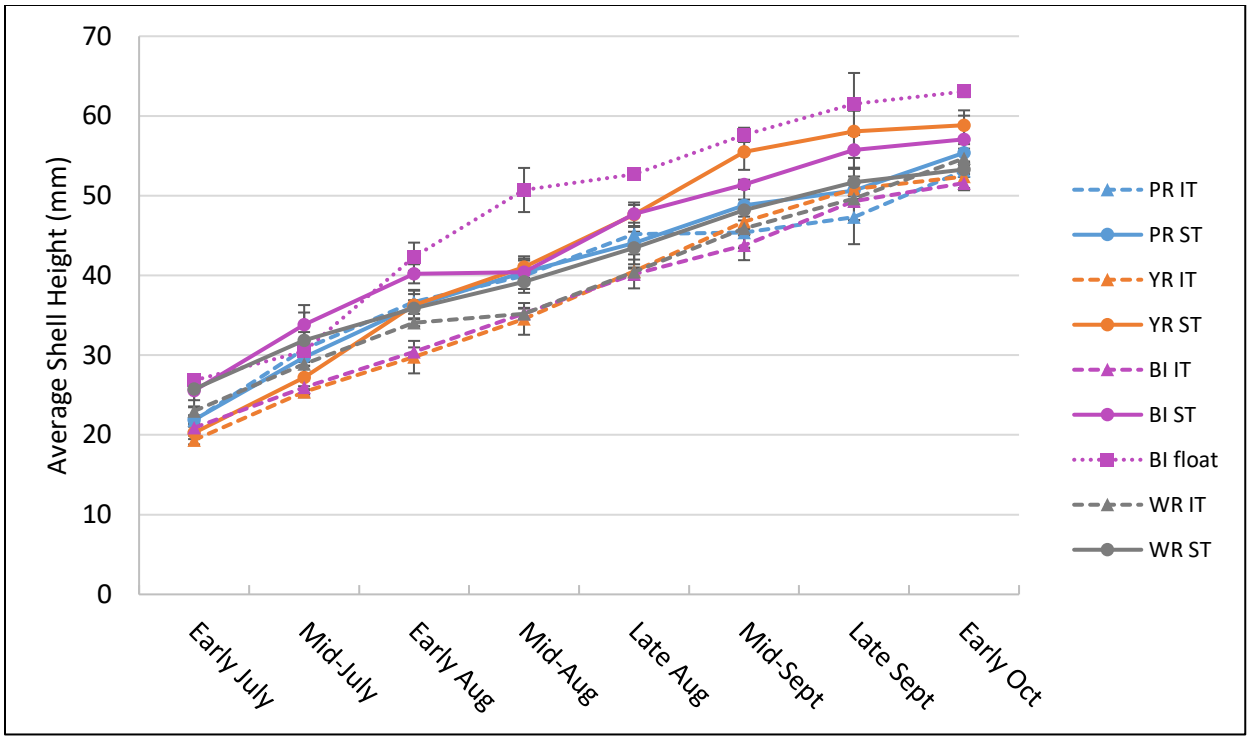

Figure 19. Average shell height (mm) of oysters deployed in July 2018. Oysters were deployed at the Perrin River (PR) site intertidally (IT; blue triangle and dashed line) and subtidally (ST blue circle and solid line), the York River (YR) site intertidally (orange triangle and dashed line) and subtidally (orange circle and solid line), the Big Island (BI) site intertidally (purple triangle and dashed line) and subtidally (purple circle and solid line) and at the surface (purple square and dotted line), and the Ware River (WR) site intertidally (grey triangle and dashed line) and subtidally (grey circle and solid line). Error bars represent the 95% confidence intervals.

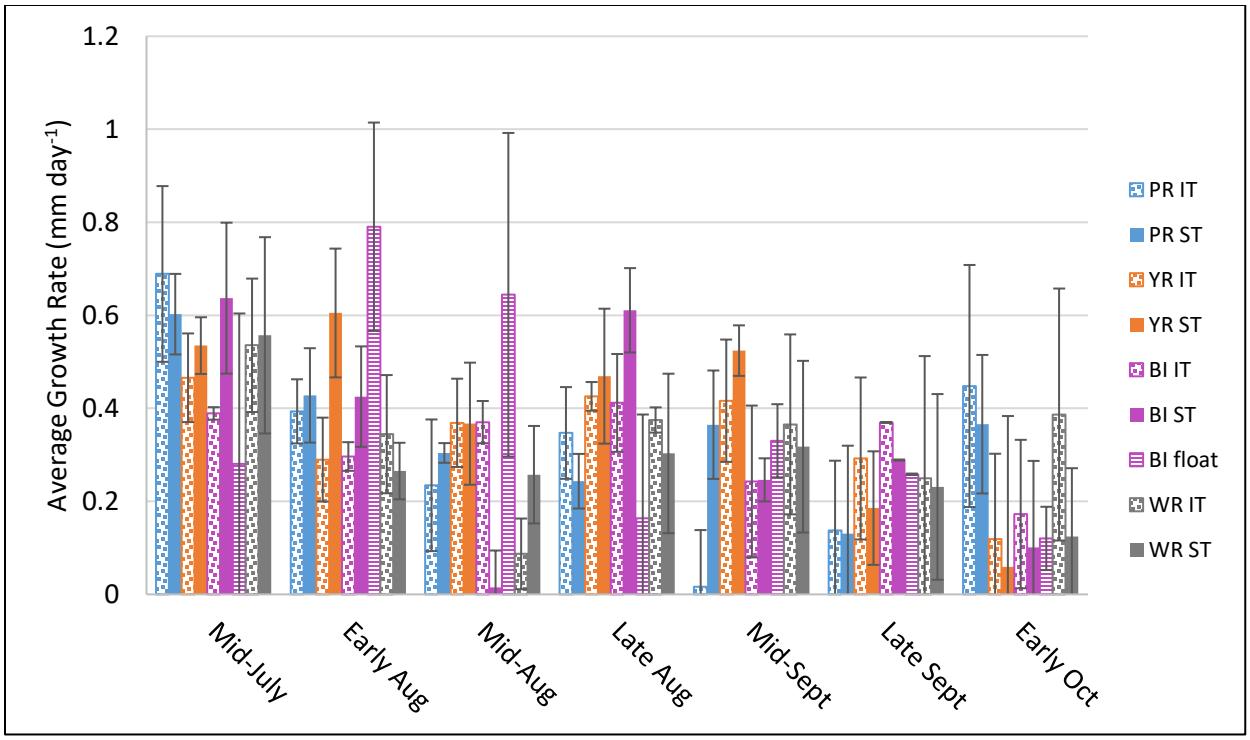

Figure 20. Average growth rate (mm day^{-1}) of oysters deployed in July 2018. Oysters were deployed at the Perrin River (PR) site intertidally (IT; dotted blue) and subtidally (ST; solid blue), the York River (YR) site intertidally (dotted orange) and subtidally (solid orange), the Big Island (BI) site intertidally (dotted purple) and subtidally (solid purple) and at the surface (horizontal purple lines), and the Ware River (WR) site intertidally (dotted grey) and subtidally (solid grey). Error bars represent the 95% confidence intervals.

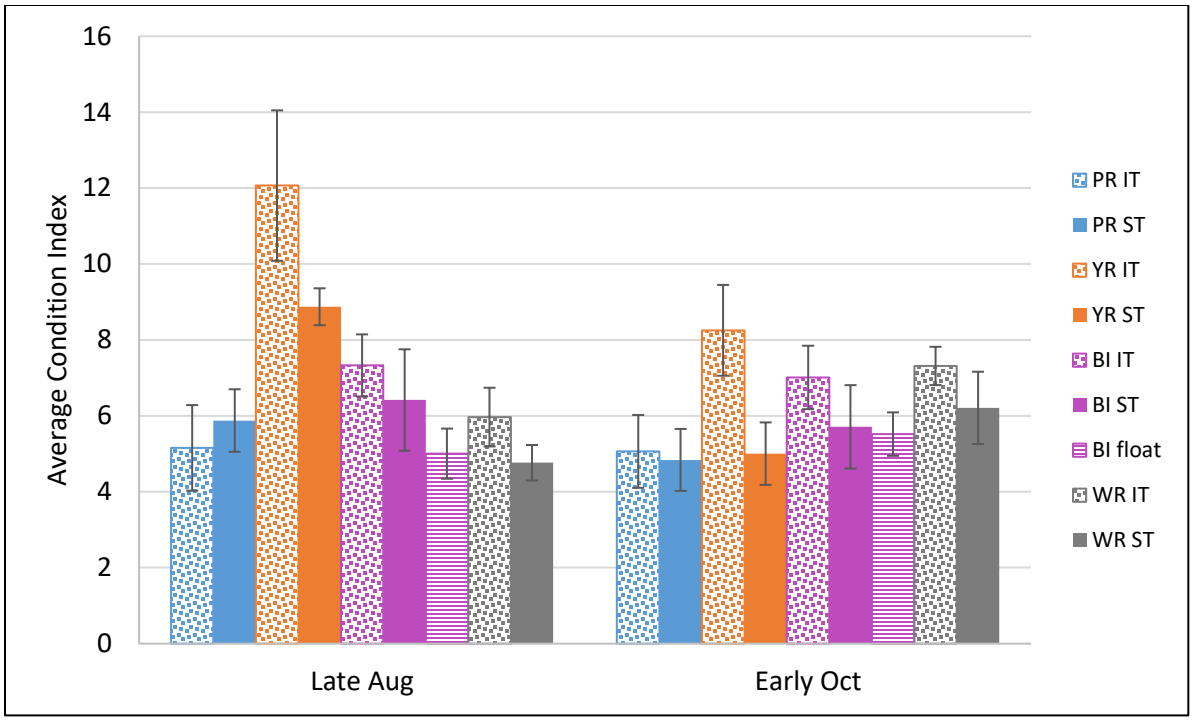

Figure 21. Average condition index (CI) of oysters deployed in July 2018. Oysters were deployed at the Perrin River (PR) site intertidally (IT; dotted blue) and subtidally (ST; solid blue), the York River (YR) site intertidally (dotted orange) and subtidally (solid orange), the Big Island (BI) site intertidally (dotted purple) and subtidally (solid purple) and at the surface (horizontal purple lines), and the Ware River (WR) site intertidally (dotted grey) and subtidally (solid grey). Error bars represent the 95% confidence intervals.